

Influential role of cell - ECM interactions in leukemogenesis

Vu Thi Thu Thao

2012

Vu, T. T. T. (2012). Influential role of cell - ECM interactions in leukemogenesis. Master' s thesis, Nanyang Technological University, Singapore.

<https://hdl.handle.net/10356/50500>

<https://doi.org/10.32657/10356/50500>



**NANYANG
TECHNOLOGICAL
UNIVERSITY**

**INFLUENTIAL ROLE OF CELL – ECM
INTERACTIONS IN LEUKEMOGENESIS**

VU THI THU THAO

SCHOOL OF CHEMICAL AND BIOMEDICAL

ENGINEERING

2012

INFLUENTIAL ROLE OF CELL – ECM INTERACTIONS IN LEUKEMOGENESIS

VU THI THU THAO

School of Chemical and Biomedical Engineering

A thesis submitted to the Nanyang Technological University in partial
fulfilment of the requirement for the degree of Master of Engineering

2012

Abstract

Cellular interaction with the extracellular matrix (ECM) inside the bone marrow is an important component in the regulation and progression of leukemia. In this inaugural work, we were able to entrap whole ECM proteins in an intricate microporous matrix that enabled us to study the effects of three-dimensional (3D) cell-ECM interactions in a controlled *in vitro* system. The Ca-alginate hydrogel was first examined for its physical properties, with respect to matrix topography, stiffness and constitutive components of the alginate. It was then investigated for its ability to support myeloleukemia cell proliferation and differentiation both in the presence and absence of supporting ECM proteins such as fibronectin, laminin and collagen-I. We used the erythroleukemic cell line K562 as a model for chronic myeloid leukemia.

Our results show that 3D Ca-alginate hydrogel provided superior support in proliferation and was able to induce spontaneous multi-lineage differentiation of K562 cells *in vitro*. In the presence of fibronectin and laminin, enhanced cell proliferation was achieved in 3D hydrogels but not observed in 2D cultures. In addition, we discovered that protein-incorporated hydrogels were able to create hematopoietic inductive microenvironments for lineage-specific cell differentiation, not achieved in 2D cultures. The manipulation of biophysical and biochemical properties in the Ca-alginate hydrogel system provides a tool for recreating aspects of the bone marrow and allows us to move away from conventional models performed on 2D tissue culture systems that are deemed inadequate, as they often misrepresent molecular cues present in the intricate 3D bone marrow environment. In conclusion, the Ca-alginate hydrogel provides a robust engineering platform for studying hematopoiesis and leukemia *in vitro*.

Acknowledgement

This thesis is dedicated to all my loved ones, who in one way or another, giving constant support during my entire Master study. It has been a tough pathway, to be honest, no roses or else but with unconditional love, support and encouragement, the dream has materialized. For all of what you did, I am deeply grateful.

To my direct supervisor, my very first boss as well, A/P Mayasari Lim. I learnt a lot under her guidance, her open sharing and her profound experience. I learnt the way she taught me do research, so thoughtful and meticulous that freaked me out some time. But then I got amazing result than ever imagine. I have grown, under her attentive supervising, to a more experienced “professional”, a more confident communicator and a better English writer. I guess I will hardly find any professor that carefully amends my wording in manuscripts as she does.

To my love, Pham Xuan Hoa, for being there, just for me, whenever I need. Every stage of my life in university, every corner that I hid during ups and downs, always got his presence. Without him, I would never complete my study that smoothly and productively.

To my labmates, Cao Xue and Teo Ailing, for being understanding, friendly and helpful. We had chit chat during boring times in lab, we had fun going training or conferences together, and we helped each other in lab work. I will always remember Cao Xue smiling face “Go back write your thesis, I can do the experiment. Don’t worry!!!”

To my FYP students and interns that I had a chance to meet. You are the very first mentee of mine and you filled my work life with exciting training times, intriguing questions and

fresh ideas too. Special thanks to Harpreet Kaur and Carine Lim for great contribution to my project.

To Noor Haslinda, the lab executive for helping us put through all lab orders and stuffs, so that we did not need to worry much on lab maintenance, such things as topping up of CO₂ tank etc.

To Dr Ong Teng Teng, Dr Yu Shucong, Dr Fang Ning and Xiaojia, the lab technicians for the trainings on equipment usage. Thanks so much for your helpfulness that facilitate the effectiveness of my experiments.

To my fellow friends in Bioengineering division Averil Chen, Lau Ting Ting, Low Weiching, Bernice Oh, Ng Shu Rui. I will always remember the birthday parties we had together, the cookies we shared whenever somebody came back from overseas. The support you gave, the cheer you made. Thank you for all.

To my father, Vu Huu Hieu, for absolute trust in me. He always said “No worries about her!” whenever someone asked him about my study.

To my mother, Ngo Thi Thu Thuy, for her endless love. “Thank you” would never be enough for all her sleepless nights, her worries, caress and efforts as well. I just would like to shout out to her first “I did it, finally”.

And last but not least, all my closed friends here and there somewhere in the world. They might not be physically by my side, but always follow every step that I made. Thank you for being a second shoulder to me, anytime.

List of published work

TTT. Vu, H. Kaur, M. Lim (2011) Toward a bone marrow niche: Culture of hematopoietic cells in two-dimensional versus three-dimensional microenvironments. *First International Symposium on Biomedical Engineering*, eds Chua C, Lee M, Guan Y, Chen J, Luo K, Lai C, Kwoh C, Lee J, Chian K, & Wu S (Research Publishing), pp 314-322.

Table of Contents

List of abbreviation.....	xv
List of figures	xvii
List of tables	xix
Chapter 1	1
Introduction.....	1
1.1 Objectives & Scope.....	4
1.2 Thesis outline	5
Chapter 2	7
Background & Literature review	7
2.1 Hematopoiesis	7
2.2 Leukemogenesis	13
2.3 The bone marrow microenvironment	15
2.3.1 <i>Stromal cells</i>	16
2.3.2 <i>Growth factors</i>	18
2.3.3 <i>The extracellular matrix (ECM)</i>	19
2.4 Role of specific cell-ECM interactions	22
2.4.1 <i>In normal hematopoiesis</i>	22

2.4.2	<i>In leukemogenesis</i>	24
2.5	Three-dimensional scaffolds for <i>in vitro</i> hematopoiesis	27
2.5.1	<i>Macro-porous scaffolds</i>	28
2.5.2	<i>Micro-porous scaffolds</i>	31
2.5.3	<i>Nano-structured scaffolds</i>	32
2.5.4	<i>Scaffolds for studying leukemogenesis</i>	33
Chapter 3	35
Characterization of Ca-alginate hydrogel	35
3.1	Introduction.....	36
3.2	Materials and methods.....	37
3.2.1	<i>Materials</i>	37
3.2.2	<i>Generation of gel block</i>	38
3.2.3	<i>Mechanical characterization</i>	39
3.2.4	<i>Scanning electron microscopy</i>	39
3.2.5	<i>High-performance liquid chromatography(HPLC)</i>	39
3.3	Results	40
3.3.1	<i>Mechanical properties of alginate hydrogel (HV vs LV)</i>	40
3.3.2	<i>SEM imaging</i>	44
3.3.3	<i>M:G ratio (HV vs LV)</i>	47
3.4	Discussion.....	48

3.5	Conclusion	51
Chapter 4	53
Cell-matrix interactions in 3D Ca-alginate culture	53
4.1	Introduction.....	54
4.2	Materials and methods.....	55
4.2.1	<i>Materials</i>	55
4.2.2	<i>Cell encapsulation</i>	55
4.2.3	<i>Cell culture</i>	56
4.2.4	<i>Cell proliferation assay</i>	57
4.2.5	<i>Cell viability and morphology</i>	57
4.2.6	<i>Flow cytometry</i>	58
4.3	Results	59
4.3.1	<i>Cell proliferation and viability</i>	59
4.3.2	<i>Spontaneous differentiation of K562 cells in 3D hydrogel</i>	63
4.3.3	<i>Optimization of alginate hydrogel size</i>	65
4.3.4	<i>Effects of low viscosity (LV) alginate</i>	67
4.4	Discussion	69
4.5	Conclusion	72
Chapter 5	75
Role of cell-ECM interactions	75

5.1	Introduction.....	75
5.2	Materials and Methods	77
5.2.1	<i>Experimental design</i>	77
5.2.2	<i>Materials</i>	77
5.2.3	<i>Cell encapsulation</i>	78
5.2.4	<i>Cell culture</i>	79
5.2.5	<i>Cell proliferation assay</i>	79
5.2.6	<i>Cell morphology</i>	79
5.2.7	<i>Flow cytometry</i>	80
5.3	Results	80
5.3.1	<i>Enhanced proliferation of cells cultured in 3D with fibronectin and laminin</i>	80
5.3.2	<i>Cell-ECM interactions exhibit a dose-response relationship</i>	82
5.3.3	<i>Effects of ECM proteins on cell maturation</i>	84
5.4	Discussion	90
5.5	Conclusion	92
Chapter 6	95
Conclusions	95
6.1	Mechanical properties of Ca-alginate hydrogel	95
6.2	Three-dimensional Ca-alginate as a platform for cell development	96
6.3	Study of cell-ECM interactions.....	96

6.4	Limitation.....	97
6.5	Future work.....	98
6.6	Final Conclusions	98
References.....		101

List of abbreviation

2D	two-dimensional
3D	three-dimensional
AML	acute myelogenous leukemia
BFU-E	burst-forming unit
BM	bone marrow
CFU	colony-forming unit
CFU-E	erythroid colony-forming unit
CFU-GEMM unit	granulocyte/erythroid/macrophage/megakaryocyte colony-forming
CLP	common lymphoid progenitor
CML	chronic myelogenous leukemia
CMP	common myeloid progenitor
Col	collagen
ECM	extracellular matrix
FACS	fluorescence-activated cell-sorting analysis
FN	fibronectin
G	guluronic acid
HLA	human leukocyte antigen

HPLC	high-performance liquid chromatography
HPC	hematopoietic progenitor cell
HSC	hematopoietic stem cell
HV	high viscosity
LN	laminin
LT-HSC	long-term hematopoietic stem cell
LT-BMC	long-term bone marrow culture
LTC-IC	long-term culture-initiating cell
LV	low viscosity
M	mannuronic acid
MMP	multipotent progenitor
MW	molecular weight
SCF	stem cell factor
SEM	scanning electron microscopy
ST-HSC	short-term hematopoietic stem cell
TCP	tissue culture polystyrene

List of figures

Figure 2-1 Hierarchic development of HSCs in the presence of supporting cytokines	9
Figure 2-2 Model of leukemia transformation	14
Figure 3-1 Molecular structure of alginate polymer	38
Figure 3-2 Preparation of gel blocks	38
Figure 3-3 Mechanical properties of Ca-alginate hydrogels.....	41
Figure 3-4 Morphology of alginate beads made from HV and LV alginates.	43
Figure 3-5 Cross-section structure of alginate hydrogels.	45
Figure 3-6 SEM images of Ca-alginate hydrogel surface.....	46
Figure 3-7 HPLC results of two different alginates.	47
Figure 4-1 Process of making alginate hydrogel.....	56
Figure 4-2 Micrographs of K562 cells in 2D vs 3D culture.	60
Figure 4-3 Cell proliferation in 2D TCP vs 3D alginate hydrogel cultures as measured by WST assay at different initial seeding density from 1-5E5 cells/ml.....	61
Figure 4-4 Viability of K562 cells in 2D TCP and 3D Ca-alginate hydrogel cultures as manually counted using trypan blue exclusion dye and in live/dead fluorescence cell staining.....	62
Figure 4-5 Micrographs of Wright-giemsa stained cells cultured in 2D & 3D at day 7.	64
Figure 4-6 Effect of bead size and alginate concentration on cell expansion.	66
Figure 4-7 Morphology of K562 culture in alginate hydrogel at day 3 & 7.....	67
Figure 4-8 Viability and proliferation of K562 cells in different alginate hydrogels.	68
Figure 5-1 Process of making alginate hydrogel.....	78

Figure 5-2 Cell proliferation in 2D TCP vs 3D alginate hydrogel cultures as measured by WST assay.	81
Figure 5-3 Metabolic rate of K562 cells in different ECM cultures: fibronectin, laminin & collagen.....	83
Figure 5-4 Results of Fluorescence-Activated Cell-Sorting analysis of lineage-specific marker expression.....	87
Figure 5-5 K562 expression of $\beta 1$ integrins over time as analyzed by FACS.....	88
Figure 5-6 Micrographs of Wright-giemsa stained K562 cells cultured with different ECM proteins.....	89

List of tables

Table 2-1 Morphology and characteristics of Wright-stained blood cells of myeloid lineage.....	10
Table 2-2 Summary of major ECM proteins within the femoral bone marrow.....	21
Table 2-3 Integrins and their ligands on HPCs	26
Table 2-4 Summary of biomaterials usedforhematopoiesis	29
Table 4-1 Average population doubling time (PDT) of K562 in 2D vs 3D culture over the first 4 days of culture.	60
Table 4-2 Expression of CD34, CD38 markers in K562 cells in different culture systems	63

Chapter 1

Introduction

Hematopoietic stem cell (HSC) represents one of the most well-studied and widely used somatic stem cells for therapeutic applications over the past few decades. Since its discovery in 1960s, HSC has offered a promising tool in treatment of numerous hematological disorders and cancers. Allogeneic HSC-rich bone marrow and later, umbilical cord blood transplantations have been successful in reconstituting the hematopoietic system in children with leukemia, Fanconi's anemia, and α thalassemia [1-7]. Successes in clinical applications of HSCs owe to their extensive proliferative capacity and their ability toward multi-lineage differentiation [8]. This is because HSCs are multipotent; they have an ability to produce at least 10 distinct lineages of mature cells that effectively replace/replenish myeloablative blood cells, including erythrocytes, leukocytes and platelets [8]. The proliferation capacity of progenitor cells is greatly dependent on their ontogenic origin: HSCs found in fetal liver are generally more proliferative than those found in cord blood than those in the bone marrow.

Under pathological circumstances, the high capacity of self-renewal and differentiation makes HSCs most vulnerable as targets for tumorigenesis. With the machinery for self-renewal and long-term persistency within bone marrow niches, it gives them a greater opportunity to accumulate mutations over more mature short-lived cell types [9]. Leukemia is therefore typically initiated within the bone marrow where an abnormal outgrowth of immature hematopoietic blasts is detected; leukemic cells become arrested at various stages of differentiation disrupting normal hematopoiesis. In the chronic phase of such diseases, immature leukemic cells find their way to the vasculature and metastasize into other tissues such as the spleen or liver. The progression of leukemia depends not only on the severity of genetic aberration but is often controlled by cellular interactions in the bone marrow. It has been understood that specific niches found at the site of hematopoiesis provide vital cues that are critical in maintaining homeostasis of normal hematopoiesis. Alterations in the bone marrow niches will therefore impact normal cellular behaviors, however, even within healthy bone marrows, leukemic cells are still able to find niches for their survival. The profound relationship in cellular behaviors with components inside the bone marrow is therefore imperative toward the understanding of disease initiation, progression and termination in leukemia.

Role of extracellular matrix (ECM) on hematopoiesis

Over the past few decades, much effort has been made to unveil molecular cues in hematopoiesis. Many intrinsic and extrinsic growth factors involved were identified [10-12], but less attention has been paid to the role of the surrounding extra-cellular matrix (ECM) and researchers have not yet been successful in recreating the bone marrow microenvironment. Matrix components not only serve structural functions, but play an

active role in controlling different cellular behaviors, including cell adhesion, proliferation and migration in both normal hematopoiesis and pathological circumstances [13]. Communication between cells and matrix components via binding of integrins can trigger signaling pathways that facilitate leukemic cell development; such observations have been evident in certain leukemias within specific niches. These niches support leukemic cell proliferation, direct migration of cells from one niche to another during their developmental stages, and early release into the blood stream [14]. Growing evidences today continually suggest the regulatory role of ECM in progressive disorders of the hematopoietic system; the understanding of cell-ECM interaction can therefore enlighten us in the control of leukemia.

Significance of 2D versus 3D microenvironment

In vitro studies on hematopoiesis were conventionally performed on two-dimensional (2D) tissue culture polystyrene (TCP), which was believed to misinterpret molecular cues presented in the *in vivo* bone marrow environment. Although HSCs are suspension cells, they exist in the bone marrow in a three-dimensional (3D) environment establishing close interactions with its surrounding matrix. Within its natural environment, the cell receives biochemical and mechanical signals from a complex interplay of cells, soluble and insoluble proteins, and matrix architecture. It is thus postulated that a 3D reconstruction of bone marrow mimicry is necessary for the proper study of normal and abnormal hematopoiesis *in vitro*.

The purpose of this project is to study cell-ECM interactions in a controlled 3D *in vitro* microenvironment and understand the impact of 3D representations on leukemic cell

development. Through a unique approach, we attempt to recapitulate 3D cell-matrix interactions within a microporous architecture provided by the Ca-alginate hydrogel system, which is proposed to better render mechanical cues essential for ‘normal’ hematopoiesis. By tuning the chemical constituents of the matrix elements, we aim to reconstruct cell-ECM interactions in its most natural context resembling the bone marrow environment. Our motivation is to provide a tunable 3D culture platform for engineering specific cellular niches to study hematopoietic and leukemic cell behaviors. We hope that this work will bring us closer to discoveries in leukemia biology.

1.1 Objectives & Scope

The focus of this project is to engineer a realistic *in vitro* microenvironment for studying the effects of 3D cell-ECM interactions in regulating leukemic cell behaviors. In particular, we are interested in understanding its influences on cell proliferation and differentiation. Cell development towards myeloid lineage is of interest for myeloid leukemia while other differentiation pathways as well as HSCs plasticity will not be covered.

Specific aims of this project are:

- (i) To characterize physical and mechanical properties of the Ca-alginate hydrogel as a 3D microporous construct for cell culture
- (ii) To study the effect of a 3D microporous construct on leukemic cell proliferation and differentiation for chronic myeloid leukemia

(iii) To study the effect of ECM proteins on leukemic cell proliferation and differentiation in chronic myeloid leukemia

1.2 Thesis outline

This thesis will begin with a background discussion on topics related to hematopoiesis and *in vitro* expansion of hematopoietic cells for research as well as clinical applications. Natural hematopoiesis and leukemogenesis are reviewed and detailed descriptions on the characteristics of common hematopoietic cells will be given. Components of the bone marrow niche will be then examined, uncovering the complex environment where hematopoietic cells reside and develop. The last two sections will be devoted to deliberate latest findings on cell-ECM interactions and the expansion of hematopoietic and leukemic cells using different *in vitro* models.

The following three chapters report the three main studies in this project, namely characterization of Ca-alginate hydrogel, cell-matrix interactions in 3D Ca-alginate and specific roles of cell-ECM interactions. In chapter 3, the examination of important mechanical properties of our Ca-alginate hydrogel was conducted, including morphological characterization by light and scanning electron microscopy, quantification of matrix stiffness and determination of M:G ratio in the alginates used. This will form a reference to support later studies on cell behaviors. Chapter 4 highlights the capability of Ca-alginate in maintaining erythroleukemic cell growth as compared to traditional tissue culture flask system. The cell proliferation rate, viability, and differentiation status were investigated. Optimization of various components in the Ca-alginate hydrogel was also performed to determine desired properties of the hydrogel matrix. The next chapter

(chapter 5) reports the specific influences of cell-ECM interactions in abnormal hematopoiesis, using the developed Ca-alginate model. We studied cell proliferation and differentiation capacity of erythroleukemic cell K562 in the presence of three commonly found proteins including fibronectin, laminin and collagen-I. The last chapter summarizes key findings from this project and closes with general thoughts toward future directions in the study of cell-ECM interactions for hematopoiesis.

Chapter 2

Background & Literature review

This chapter provides relevant background on the important components constituting and regulating hematopoiesis. These include ordered cell development in normal hematopoiesis, potential pathways in leukemogenesis and general role of the native bone marrow environment. The review provides a thorough examination of pioneering works and latest advances in the field specifically in the role of cell and extracellular matrix interactions in both normal and abnormal hematopoiesis. In the context of 3D microenvironments, efforts toward its recreation *in vitro* are extensively discussed. This review serves as a reference for our method and approach toward engineering a 3D *in vitro* system for leukemia.

2.1 Hematopoiesis

Hematopoiesis represents a highly regulated process whereby balanced production and replenishment of a spectrum of blood cells are controlled daily over a lifetime. In

hematopoiesis, the central component is the hematopoietic stem cell (HSC) which is located sequentially in yolk sac (embryo), liver, spleen, umbilical cord blood and finally in adult bone marrow [15-17]. HSC has high self-renewal capacity to provide sufficient primitive cells to sustain hematopoiesis, while generating mature cells through differentiation. Today, it is generally agreed that Lin⁻Thy1.1^{lo}Sca-1⁺ HSCs, found within the “LSK” (Lin⁻Sca-1⁺c-kit⁺) fraction, is the prevailing definition for murine HSCs [18-20]. Within the LSK fraction, several criteria have been used to identify the most primitive self-renewing HSCs with long-term reconstituting activities (LT-HSCs). LT-HSCs was found present in the CD34⁻, CD38⁺, or Thy1.1^{lo} fraction of the LSK population [19, 20]. In contrast, the LSK population with CD34⁺, CD38⁻, or Thy1.1⁻ phenotype is capable of only transient reconstitution, thereby containing short-term HSCs (ST-HSCs) or multipotent progenitors (MMPs) [20, 21]. Mature blood cells are categorized into two separate lineages: lymphoid and myeloid with their respective precursors - common lymphoid progenitor (CLP) and common myeloid progenitor (CMP). These committed progenitors undergo further differentiation before they terminally transform to mature blood elements.

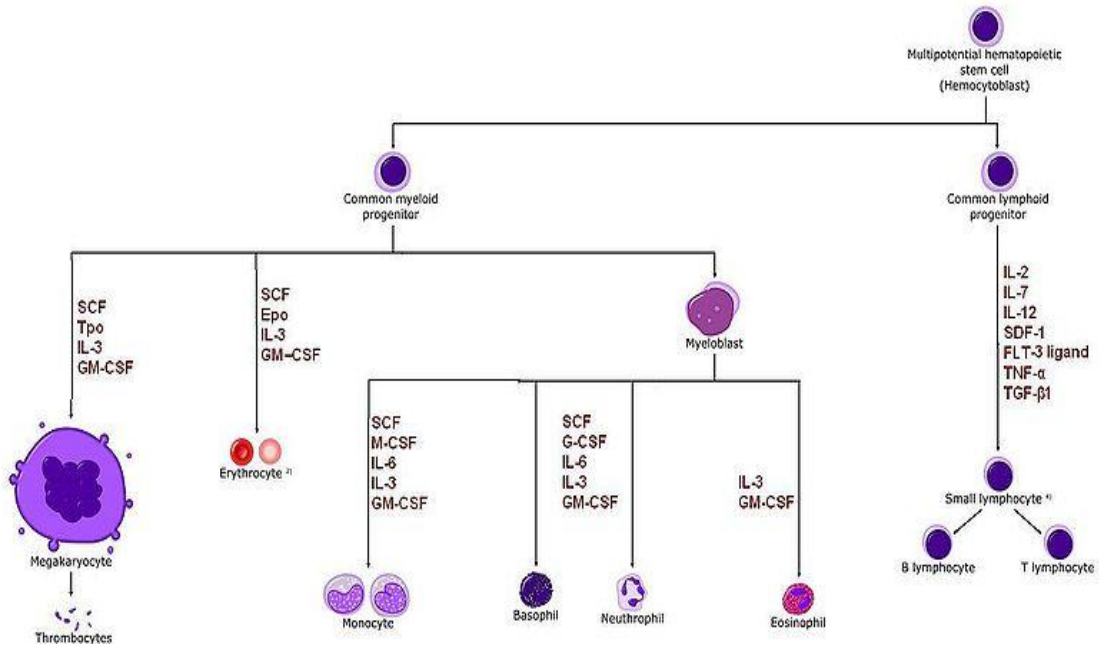


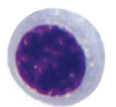


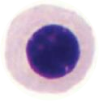


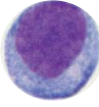
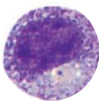
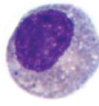
Figure 2-1 Hierarchic development of HSCs in the presence of supporting cytokines [22]. SCF-stem cell factor, G-CSF - granulocyte colony stimulating factor, GM-CSF – granulocyte-macrophage CSF, ILs – interleukins.

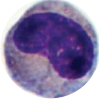

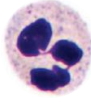
To specify the type of progenitors, the term colony-forming unit (CFU), together with a lineage suffix, is often used to define the differentiating ability of HSCs to form distinct colonies of mature cells in semisolid agar or methylcellulose. CMP cells are known as granulocyte/erythrocyte/macrophage/megakaryocyte colony-forming units (CFU-GEMM) while their downstream committed products are granulocyte/macrophage colony-forming units (CFU-GM) and erythrocyte colony-forming units (CFU-E). Erythrocyte burst-forming units (BFU-E) are the more commonly measured precursor of the CFU-E. Hierarchic development and morphology of different blood cell types are represented in Figure 2-1 and Table 2-1. Briefly, cells undergoing erythrocytic differentiation appear smaller and having more condensed nucleus. Upon maturation, extrusion of nucleus occurs producing anucleated reticulocytes. At the final stage, cells

attain their biconcave morphology to become mature erythrocytes. Granulocytic cells are characterized by great amount of granules in their cytoplasm and an indented nucleus. The number of indentation increases with cell maturation stage and clear granules are formed as the cells further differentiate to three mature types of granulocytes (basophilic, neutrophilic and eosinophilic). Megakaryocytes exhibit multiple nucleoli and giant morphology, which later give rise to thrombocytes budding from their surface.

Table 2-1 Morphology & characteristics of Wright-stained blood cells of myeloid lineage.

Erythroblasts	Proerythroblast		~20 mm, largest erythroid precursor Fine, uniform chromatin with one or more nucleoli A granular basophilic cytoplasm
	Basophilic erythroblast		10-18mm BN I - Intensely staining, slightly coarse nuclear chromatin, deeply basophilic cytoplasm BN II - Condensed, spoke-like nuclear chromatin
	Polychromatic normoblast		10 - 15 mm, relatively coarse, intensely staining chromatin Active hemoglobin formation Polychromatophilic cytoplasm

	Orthochromatic erythroblast		10-15 mm, incapable of cell division Small, dense nucleus, pinkish cytoplasm Extrusion of nucleus produces reticulocyte
	Reticulocyte		10-15 mm, released into peripheral blood Contain mitochondria, ribosomes, Golgi body remnants Hemoglobin synthesis continues (20-30%)
	Erythrocyte		6-8 mm, biconcave shape Incapable of hemoglobin synthesis Life span of 120 days
Granulocytic cells	Myeloblast		12-20 mm, moderately basophilic cytoplasm, few granules Diffuse chromatin, several nucleoli Capable of cell division
	Promyelocyte		15-25 mm, basophilic cytoplasm, reddish-purple granules Slightly indented nucleus, nucleolus, Golgi zone Capable of cell division
	Myelocyte		10-20 mm slightly basophilic cytoplasm, no nucleolus Specific neutrophilic, eosinophilic, or basophilic granules

		<p>Partial chromatin condensation, no nucleoli</p> <p>Two generations, early forms capable of cell division</p>
Metamyelocyte		<p>10-12 mm, neutrophilic, eosinophilic, or basophilic granules</p> <p>Indented or U-shaped nucleus</p> <p>Incapable of cell division</p>
Bands		<p>15-25 mm, basophilic cytoplasm, reddish-purple granules</p> <p>Slightly indented nucleus, nucleolus, Golgi zone</p> <p>Capable of cell division</p>
Mature neutrophil		<p>10-20 mm, slightly basophilic cytoplasm, no nucleolus</p> <p>Specific neutrophilic, eosinophilic, or basophilic granules</p> <p>Partial chromatin condensation, no nucleoli</p> <p>Two generations, early forms capable of cell division</p>

2.2 Leukemogenesis

Many hematologic diseases, such as leukemia, are proven to originate from different pathogenic events that lead to leukemogenesis. In chronic myelogenous leukemia (CML), chromosomal translocation (Philadelphia chromosome) results in the oncogenic fusion of bcr-abl gene which in turn activates a continuous cell division and causes further genomic instability. Though bcr-abl was found to be the central cause of CML as well as in other leukemia, recent studies have revealed that the surrounding bone marrow environment play an equal role to the leukemogenesis and its progression. Direct contact of leukemic cells with other stroma or with components of the extracellular matrix (ECM) may protect them from drug-induced apoptosis [23]. On the other hand, malignant cells of a severe combined immunodeficiency (SCID) mouse xenograft model of acute lymphoblastic leukemia was found to alter the bone marrow niche that sequestered transplanted human CD34⁺ cells [24]. In this manner, leukemic blasts and their surrounding microenvironment mutually affect each other in supporting leukemic outgrowth, suppressing normal hematopoiesis and promoting malignant transformation. Currently, two hypotheses have been proposed to explain the advent of leukemogenesis – 1) the abnormality in the bone marrow environment instructs aberrant behaviors of the encapsulated hematopoietic cells or 2) the aggression of leukemic cells that destroys the bone marrow niche and progressively tampers normal hematopoiesis

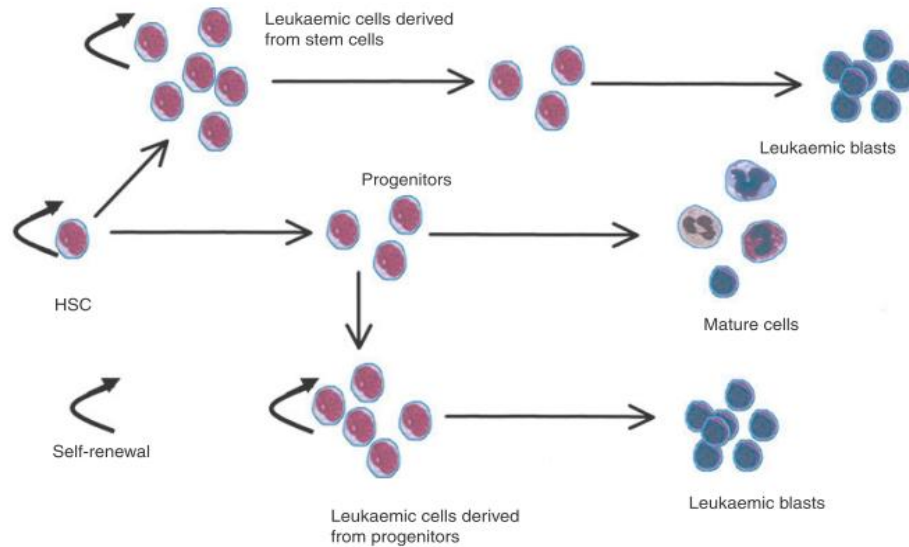


Figure 2-2 Model of leukemia transformation [9]

In any case, normal HSCs escape from regular growth control, behave differently and embark in malignant outgrowth [25, 26]. Emerging evidence proposed that cancer cells might contain some cancer stem cells, which are rare cells with indefinite self-renewal potential [27-29]. Studies on the origin of leukemic stem cells (LSCs) lean toward the belief that normal HSCs themselves are the target for leukemic transformation (Figure 2-2). This is due to the fact that HSCs have the machinery for self-renewal already activated and the long persistence time gives HSCs a greater opportunity to accumulate mutations than more mature short-lived cell type [9]. Furthermore, LSCs appear to share similar cell surface markers previously identified for normal HSCs, such as CD34, CD38, HLA-DR and CD71, while exhibiting similar heterogeneity found in their normal compartment.

K562 cell line

The oldest and most well-characterized leukemic cell line is K562, which was plural effused from the bone marrow of a patient suffering from chronic myelogenous leukemia (CML) in blast crisis. The cell line was first developed by the Lozzios in 1971 [30] and was initially assumed to be granulocytic. Later on, untreated K562 cells were found to have antigens characteristics of all four lineages including erythroid, granulocyte, monocyte, and megakaryocyte [31-36]. The expression level of these antigens is partially dependent on specific inducers which may influence antigens of different lineages in opposite directions [33]. Several physical as well as chemical inducers for K562 differentiation have been identified, such as hyperthermia, retinoid, Vitamin D, and hemin that shift the cells toward the erythroid lineage differentiation [37-39] while butyrate derivatives and tumor promoter 12-*O*-tetradecanoyl-phorbol-13acetate (TPA) driving cells to the megakaryocytic lineage [40, 41]. Little is known about the impact of ECM to the proliferation and differentiation capacity of the leukemic K562 cells. Despite its malignant origin, the cell retains some capacity for expression of alternative programs of differentiation, a characteristic of the normal multipotent HSC. Knowledge of K562 behaviors is therefore useful in the study of leukemia as well as normal hematopoiesis.

2.3 The bone marrow microenvironment

Inside the bone marrow, there are specific microenvironments or “niches” whereby HSCs reside and activated [42]. Today it is generally agreed that, those hematopoietic sites lie in the cords or wedges between highly permeable capillary-venous sinuses. Recently, researchers have found two distinct niches that give rise to different fates in HSCs: the

vascular niche - characterized by high flow, oxygen and nutrient – to support cell migration and differentiation [43] and the osteoblastic niche – a hypoxic environment with high content of Ca^{2+} for the retention of quiescent HSC pool for reproduction [44]. The capillary-venous sinus, which serves as a barrier between the bone marrow and the vasculature, encompasses fenestrated endothelial cells, basement membrane and adventitial (stromal) cells. Stromal cells are believed to produce essential growth factors (cytokines) and ECM components that directly/indirectly control cell differentiation [45-48]. Concentration gradients of growth factors within ECM created by these cells are crucial for forming distinct niches that sequentially regulate cell behaviors.

2.3.1 *Stromal cells*

The four types of marrow stromal cells are the endothelial cell, adventitial reticular cell, macrophage, and adipocyte. Direct contact with stromal cells is believed to facilitate hematopoietic cell survival, growth, and development, both *in vivo* and *in vitro* [49, 50]. The beneficial effect of the stroma is greatly exerted through the secretion of cytokines or receptor presentation on the cell surface.

Endothelial cells have been proven responsible for the production of G-CSF and GM-CSF *in vitro* [22]. In addition, matured blood cells must pass through the endothelial cell lining of the sinus wall to enter the vasculature. However, this egression occurs through transient migration ports just near the junctions of endothelial cells [51]. Endothelial cells are also responsible for transporting of plasma-derived substances into the hematopoietic space via endocytosis [52].

Adventitial reticular cells are fibroblastic cells which form an extensive network of fine cytoplasmic processes that surround the hematopoietic cells. They cover the highest proportion in the stroma accounting for approximately 65% of the endothelial surface. This surface coverage is however versatile, which can decrease significantly in response to hematopoietic stress, thereby believed to make way for hematopoietic cell egression by exposing more area for transportation [53]. Adventitial cells synthesize a wide range of important bone marrow soluble components, including M-CSF, G-CSF, GM-CSF, IL-1 and IL-6 *in vitro* [54-56]. Adventitial cells are able to transform to adipocytes, taking up fat when exposed to hydrocortisone *in vitro* [57].

Macrophage has been postulated as an indispensable cell for the control of hematopoiesis due to its wide distribution throughout the body, which allows it to sustain homeostasis. Although this role of macrophage is still highly controversial, the cells are definitely critical in regulating erythropoiesis, which take place in isolated islets around an associated macrophage nurse cell. In addition, macrophages are considered to be a major source of cytokines under steady state conditions, and can induce other cells to produce cytokines under times of hematopoietic stress. Macrophages produce GM-CSF, IL-1, EPO, and a multitude of other secretory products, including inhibitory substances such as TNF- α and IFN- γ [58]. Interestingly, performance of macrophages *in vitro* was found varying significantly with oxygen tension and pH fluctuation, and might respond to changes in shear stress *in vivo* [58].

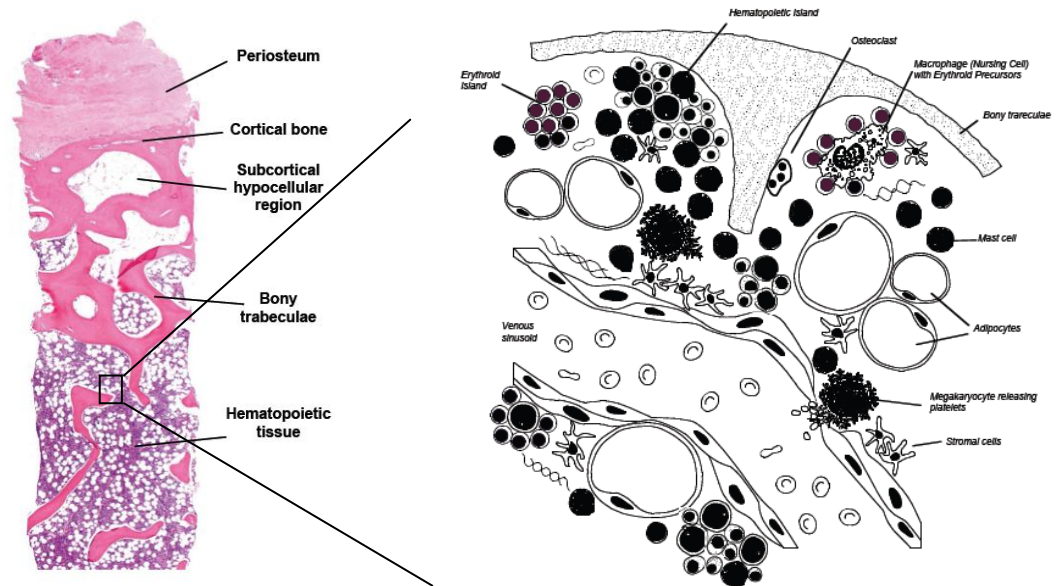


Figure 2-3 The bone marrow microenvironment [59]

Bone marrow adipocytes are believed to have different origin from other organs. It was shown that they were most probably derived from adventitial cells, which take up fat and transform into fat tissue in the presence of corticosteroids. *In vivo*, large amount of fat cells in marrow (yellow marrow) often means low hematopoietic activity while hematopoiesis-active sites contain fewer adipocytes (red marrow). In contrast, most investigators reported that the formation of adipocytes *in vitro* is required in a stroma to support hematopoiesis, whereas only a few reported that adipocytes are not important in long-term bone marrow cultures (LTBMC). Finally, it has been suggested that adipocytes may inactivate cytokines in LTBMC when present in very large numbers.

2.3.2 Growth factors

Within a specific niche, hematopoiesis is regulated partly by growth factors (cytokines), in particular interleukins (ILs) and colony-stimulating factors (CSFs), which overlap in

their effects on cells [60]. However, their impact on the proliferation and differentiation of primitive progenitors in stroma-dependent LTBMCM appear controversial. Combination of low levels of growth factors may result in enhanced primitive hematopoietic progenitors activities, with respect to proliferation and differentiation [61, 62]. Alternatively, adhered rather than soluble growth factors may be critical for hematopoiesis. Heparan-sulfate proteoglycans present in the ECM of adherent stromal layers bind and concentrate GM-CSF, IL3, and b-FGF [63-65]. In addition to positive growth regulatory molecules, several diffusible molecules can inhibit the proliferative status of the mainly quiescent stem cell, including macrophage inflammatory protein-1 α (MIP-1 α), and transforming growth factor- β (TGF- β) [66-69]. Since hematopoietic cells can get into contact with specific ECM proteins, they would co-localize with these growth factors, creating the hypothetical “stem cell niche”.

2.3.3 *The extracellular matrix (ECM)*

Structure of the ECM inside the bone marrow shows the same composition to those found in other tissue, i.e. the presence of collagen type I and III (produced by fibroblast), type IV (produced by endothelial cells), proteoglycans and glycoproteins such as fibronectin were detected. Among them, major identified ECM components at the endosteal surface where HSCs home to include fibronectin (FN), collagen I (Col I), and laminin (LN) [70]. Each protein occupies specific localization in large amounts within the bone marrow (Table 2-2) and is believed to play distinct roles in the regulation of hematopoiesis.

Fibronectin is a large fibril-forming glycoprotein (450 kDa) composed of two similar subunits (2500 amino-acid residues long) joined by a pair of disulfide bonds at

their carboxyl termini and folded in a series of globular domains separated by regions of flexible polypeptide chains (Figure 2-4). At least two regions in this protein have been identified as cell adhesion sites: a cell binding domain (75 – 120 kDa) and a heparin binding domain (33/66 kDa). The cell binding domain, with RGD as the sequence of minimal recognition site, provides an adhesion site for most cells via the $\alpha 5 \beta 1$ integrin receptor and to a lesser degree through the $\alpha v \beta 3$ or GpIIb-IIIa receptors. The heparin binding domain, containing CS1, FN-C/H I and FN-C/H II peptides, promotes cell-ECM interactions through the $\alpha 4 \beta 1$ integrin or proteoglycans. Bone marrow endothelial cells and fibroblasts can produce FN containing all three cell adhesion sites in the alternatively spliced heparin binding domain.

Collagen is found abundantly as a fibrous protein in the extracellular space of the bone marrow microenvironment. The most common types are type I, II, III and IV. Col I-III, assembled as collagen fibers, constitute the structural backbone of the extracellular space. Among these three types, Col I is the major protein in bone, comprising approximately 90 percent of its protein. Col IV, in contrast, is assembled into a sheet-like mesh work that constitutes a major part of basal membrane.

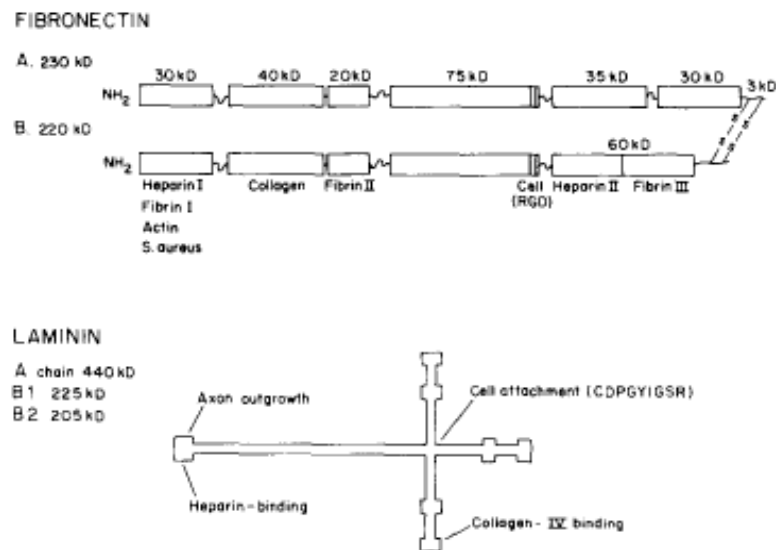


Figure 2-4 Domain structures of fibronectin and laminin [71]

Laminin is an 850 kDa complex of three very long polypeptide chains α , β and γ arranged in the shape of a cross held together by disulfide bond (Figure 2-4). So far, 5 α (α 1-5), 3 β (β 1-3), and 3 γ (γ 1-3) chain variants have been recognized, and 15 different heterotrimers have been proposed in the regulation of cell adhesion. Major cell-binding domains of LN lie in the carboxy terminus of α chain. Hence, the adhesion of cells to LN is mainly determined by the α chain. Several integrins (α 1 β 1, α 2 β 1, α 3 β 1, α 6 β 1, α 6 β 4, α 7 β 1, α 9 β 1, α v β 3) bind to LN at different affinities. Researchers showed the presence of LN-2 (α 2 β 1 γ 1), LN-8 (α 4 β 1 γ 1) and LN-10 (α 5 β 1 γ 1) but none of the other LN α chains in the bone marrow [72].

Table 2-2 Summary of major ECM proteins within the femoral bone marrow^a [70]

	Bone: compact and/or trabeculae	Endosteal surface/ endosteal marrow	Periosteal surface	Central marrow	Marrow sinuses and/or arteries	vessels:
Fibronectin	+++	+++	+++	++	-	
Collagen I	+++	+++ ^b	-	-	-	
Collagen II	-	-	++	-	-	
Collagen IV	+	++ ^b	++	-	++	
Laminin	+	-	+++	+	+++	

^a+++ : bright expression; ++ : moderate expression; + : faint expression; - : absent

^bExpression of these proteins was discontinuous. Grading is for the positive areas

Other ECM components include negatively charge polysaccharide chains called *glycosaminoglycans (GAGs)*, which includes *hemonectin* - a 60 kDa ECM protein recognized in the bone marrow microenvironment only and *thrombospondin* - a 450 kDa subunits cross-linked by disulfide bonds produced by platelets, endothelial cells and fibroblasts. It is believed that these proteins also take part in the modulation of hematopoieic cell development, including the maturation and release of granulocytic cells from the bone marrow microenvironment. However, their molecular architecture and the corresponding surface receptors have not yet been identified.

2.4 Role of specific cell-ECM interactions

2.4.1 In normal hematopoiesis

The roles of ECM in normal hematopoiesis include localization of the primitive stem cell, maintaining cell quiescence in the osteoblastic niche, and signaling for cell proliferation,

differentiation and cell egression upon stressful condition. Cell-ECM interactions were found specific to the proteins that the cells adhere to. A summary of the regulatory interactions with three common proteins is given below.

Fibronectin. Adhesion to FN has long been known crucial to the regulated maturation of erythroid progenitors [73-75]. The effect of ECM proteins on HSCs/HPCs however depends on the maturation stage of the cells. Recent studies found that in primitive progenitors, elevated adhesion to FN leads to enhanced expansion of CFU and long-term culture-initiating cells (LTC-IC), and to a lesser extent CD34⁺ cells, specifically through CS1 motif binding [76, 77]. Analysis of cell surface markers revealed fair expression of CD13, CD14, CD15 on expanded cells, implying that the interaction with CS1-FN might skew differentiation of HPCs to the myeloid lineage [77]. At least two integrins $\alpha 4\beta 1$ and $\alpha 5\beta 1$ are found to be involved in the HSC-FN interactions [78-83]; the interchangeable role of these integrins is still debatable. Recently, Huygen *et al* found that $\alpha 4\beta 1$ and $\alpha 5\beta 1$ function fluctuate reversibly during cell cycle transit. The topmost adhesion, occurs during S phase transit, was predominantly dependent on $\alpha 5$ integrin in lieu of the normal preferential $\alpha 4$ integrin-dependent adhesion manner [84, 85].

Laminin. It was noted that HSC adhesion to FN is the strongest (45-50%), while HSC-ECM adhesion appears at a lesser extent to LN (35-40%) and insignificant to Col I [78, 86]. The adhesive interaction of hematopoietic cells with LN is isoform-specific. Almost all primitive and committed progenitors as well as more differentiated cells of myelomonocytic and erythroid lineage are found to have strong adhesion to LN-10/11 but not to LN-8 and LN-1 [86]. LN-10/11 and HSC interactions leads to migration and strong mitogenic response of CD34⁺ cells; this interaction was found to be mediated by $\alpha 6$ and

$\beta 1$ integrins, especially $\alpha 3\beta 1$, $\alpha 6\beta 1$ and $\alpha 6\beta 4$ [86-88]. Recently, Hong Qian showed that $\alpha 6$ integrin acts as a homing receptor during fetal liver progenitor cell homing to bone marrow, whereas homing and engraftment of multi lineage repopulating HSCs were mediated by $\alpha 4$ receptor, indicating distinct roles for each integrin during fetal hematopoiesis [89].

Collagen. Studies on the effects of collagen on hematopoiesis are less established. Fetal liver, umbilical cord blood and bone marrow CD34⁺ cells showed no adhesion to Col-I, although the major Col-I binding integrin receptor $\alpha 2\beta 1$ is expressed on HPCs [90]. In contrast, committed myeloid and erythroid progenitor cells CFU-GM and BFU-E demonstrated significant specific binding to Col-I [91]. However, this Col binding was suggested being not mediated by the $\beta 1$ integrin class of adhesion proteins [91]. No Col-induced enhancement of proliferation was observed. More studies need to be conducted to investigate the effect of this Col binding to the activities of hematopoietic cells.

2.4.2 *In leukemogenesis*

As opposed to normal HSC, the adhesion of erythroleukemic cells to FN resulted in cell quiescence with/without inducing apoptosis [76, 92, 93]. The extent to which leukemic cells adhere to FN appears controversial. In fact, the discrepancies might originate from the different time points of recording and/or the cell cycle status of these cultured cells. Most studies showed deficient adhesion of CML cells to FN compared to hematopoietic progenitors at similar stages of differentiation [76, 94-97], which were reported at day 6 - 7 of culture. On the contrary, Molla and Marc revealed strong adhesion to FN was actually seen during the first hour of incubation, but the cells were released from the

matrix afterwards [92]. Thomas further confirmed this short-term preferential adhesion to FN to LN and Col within the first 60-min of culture [98]. The observation suggests that CML cells may possess a mechanism to help them escape from natural growth inhibition mechanisms of the stroma FN. The abnormal adhesive behaviors of CML cells to FN however were found to be unassociated with the expression of cell surface VLA-molecules. This suggests that VLA-molecules may be present but are in a non-functional state, especially on more primitive progenitors [99]. A study indicated that the defect is based on an impaired $\beta 1$ integrin function, which could be restored by treatment with interferon α [100]. All these observations suggest that FN matrix provided a permissive microenvironment within which erythroid-induced erythroleukemia cells attach and differentiate, but these cells finally lose the surface fibronectin receptor and preferential adhesion upon maturation to reticulocytes [73-75].

For collagen (Col) and laminin (LN) interactions, a fraction of bone marrow CML cells do express low levels of the $\alpha 2\beta 1$ and $\alpha 6\beta 1$ integrins, which is absent in its normal counterpart. In fact, Col receptor $\alpha 2\beta 1$ is up-regulated while $\alpha 4\beta 1$ and $\alpha 5\beta 1$ are down-regulated during the phorbol 12-myristate 13-acetate (PMA) - induced maturation of erythromegakaryocytic cells to megakaryocytic lineage [101]. Subsequently, primitive CML progenitors exhibited abnormal trafficking behaviors towards the basement membrane components LN and Col [94, 102]. Different from normal HSC, the interaction of leukemic cells to LN is specific to laminin-8 and laminin-10 only, with the regulation of $\alpha 3\beta 1$ and $\alpha 6\beta 1$ [102]. The abnormal trafficking of leukemic cells may explain for their release to the circulation through interacting with basal membrane components LN and Col [95, 103-105]. Interestingly, besides mediating cell adhesion to LN, LN receptor was

found to be associated with the cell differentiation to monocytic lineage in acute myelogenous leukemia (AML) [106].

Table 2-3 Integrins and their ligands on HPCs [99]

	Expressed on progenitors	Ligand
β 1 family [CD29]	Yes	ECM/VCAM/MadCAM
α 1 [CD49a]	No	Laminin/collagens
α 2 [CD49b]	No	Laminin/collagens
α 3 [CD49c]	No	Fibronectin/laminin/collagens
α 4 [CD49d]	Yes	CS1 domain of fibronectin/VCAM/MadCAM
α 5 [CD49e]	Yes	RGD domain of fibronectin
α 6 [CD49f]	No	Laminin/collagens
β 2 family [CD18]	Yes	ICAM 1, ICAM 2
LFA-1 [CD11a]	Yes	ICAM 1, ICAM 3
Mac1 [CD11b]	Yes	
CD11c	No	
β 3 family		
α v β 3 [GpIIb-IIIa]	No	Vitronectin, thrombospondin

Complex cell-ECM interaction may also occur in a bi-directional manner, for example adhesion of murine HSCs to purified FN, LN and Col was found to conversely enhance $\beta 1$ integrins expression [107]. Additionally, hematopoietic cells could also release molecules which in turn influence the interactions of these cells within the matrix [108, 109]. For example, erythro-megakaryocytic cells were found to synthesize LN-8 [109]. Bidirectional signaling may be one of the reasons that will explain the creation of abnormal leukemic “niches” favoring the survival, proliferation and differentiation of leukemic cells.

2.5 Three-dimensional scaffolds for *in vitro* hematopoiesis

In vitro systems have become invaluable tools for studies of hematopoiesis at different cellular and molecular levels. With a better understanding of biochemical cues in the native bone marrow, a representative *in vitro* model can provide a well-defined platform for hematopoietic research in contrast to a complex *in vivo* host environment. While biochemical factors are easily controlled in most state-of-the-art bioreactors, physical factors such as scaffolding remain a challenge in *ex* and *in vitro* hematopoietic systems. Current trends are moving toward the development of 3D scaffold as a platform for hematopoietic cell culture for a better mimicry of the native environment. More importantly, 3D constructs are believed to circumvent the problem of cell asymmetric polarity in traditional two-dimensional (2D) tissue culture plastic (TCP) and the lack of cell-cell/cell-matrix interactions in suspension culture observed in spinning flasks or bioreactors.

2.5.1 Macro-porous scaffolds

In the past few years, 3D scaffolds used for *ex vivo* expansion employed several long-established biomaterials in tissue engineering i.e. bioceramics (such as hydroxyapatite HA) [110-112], polyethylene terephthalate (PET) [113, 114], polylactic-*co*-glycolic acid (PLGA) [115], or natural collagen [116-118]. These scaffolds, either of natural or artificial polymers, essentially form a 3D macro-porous (50 - 500µm) architecture that mimics the spongy bone structure on which HSCs attach and proliferate *in vivo*. Recently, the identification of two specialized niches (the osteoblastic and vascular niches) within the native bone marrow has led to several attempts to customize scaffold surfaces for better resemblance of these microenvironments (Table 2-4). Serum coated bioceramics tricalcium phosphate (TCP) scaffolds (50 - 85%) significantly enhanced adhesion of CD34+ cells by 30% compared to the similarly-treated 2D cultures (5%) [119]. This type of system was modeled as an anchorage structure, when incorporated with essential supporting cells or growth factors, they have an ability to localize HSCs in specific 'niche' demanding for HSC expansion *in vitro*. In other studies, polymeric materials such as PET coated with fibronectin alone were proven to enhance the expansion of CD34+ and LTC-IC; these expanded cells appeared to be of erythroid lineage with increased BFU-E but decreased CFU-GM *in vitro* [110, 114]. Collagen did not present any similar effects in the same situations. The mechanism underlying these cell-matrix interactions remains unclear; nevertheless the observation suggested that covalently conjugated extracellular proteins on scaffold surfaces might provide a functioning substrate that mediates several crucial cellular events at different level

Table 2-4 Summary of biomaterials used for hematopoiesis

	Materials	Surface modified	Culture condition	Effects on hematopoietic cells	References
<i>In vitro</i>	PET	FN immobilized		Enhanced expansion of CD34+ & LTC-IC	Leong 2006
	Chitosan	Heparinized	Perfusion bioreactor (CB CD34+)	Enhanced CD34+ expansion	Matthew 2007
	Collagen microspheres		Packed-bed bioreactor, with EPO (BM MNCs)	Support extensive erythropoiesis	Mantalaris 2008
	Collagen	Heparinized to trap SDF1 α		Increased recruitment of CD45+ cells	Torensma 2008
	Bone-derived (cancellous &	Coated with MSCs induced	MyeloCult® H5100 (CB	Increased expansion of CD34+ & CD34+/CD38- with decreased	Liu 2009

	cortex)	to osteoblasts	CD34+ or MNC), long term	CD34+/CD38+ population. More CFU progenitors, mainly BFU-E & CFU-GEMM compared to CFU-GM in TCP	
	Polyvinyl formal (PVF)		Coculture with stromal cells, hypoxic condition	Expansion of HPC & erythroid cells	Miyoshi 2010
	Tricalcium phosphate (TCP)	Coated with human serum	Serum free DMEM (CB CD34+)	Increased cell adhesion (30-35%) compared to TCP (5%)	Mishra 2010
<i>In vivo</i>	PLGA	SDF1 α incorporated		Local recruitment of HSCs	Tang 2009
	Hydroxyapatite (HA)	Coated with BM stromal		Supporting HSCs and delivering HSCs to native BM <i>in vivo</i>	Takashi 2010

2.5.2 *Micro-porous scaffolds*

In contrast to macro-porous systems where HSCs would attach on scaffold surfaces in a pseudo 3D manner, micro-porous scaffolds - with pore sizes ranging from 5-20 μm within the dimensional range of a single cell –act as a true 3D cell encapsulation. Similar to natural ECM, these scaffolds embed cells without entrapping them. Cells are still able to expand, undergo morphological changes, migrate and remain in contact with other cells while vital nutrients diffuse freely throughout the matrix. The true advantage of this culture system is that HSCs are exposed to external forces from all directions. Therefore, micro-porous systems (i.e hydrogels) appear to be of more beneficial in recapitulating the native densely-packed bone marrow microenvironments. In one study, 3D reconstituted collagen I fibrillar gel was shown to support HSC expansion while HSCs retain their undifferentiated state *in vitro* [120]. An increased frequency of myeloid colony-forming units CFU-C and an upregulation of growth factors and cytokines expression were observed. Although, the expansion factor was not significantly affected as compared to control suspension cultures, it is not conclusive whether these cell characteristics arose from the cell-collagen interactions or from the spatial restriction of microscale architecture. Recently, cell confinement in small cavities has also showed to have great impact on HSC fate decision. Tilo *et al* revealed that the proliferation and differentiation of HSCs decreased when they were supported by small fibronectin-coated cavities of 15 μm [121]. Interestingly, these cells showed lower DNA synthesis and higher expression of HSC markers than those cultured in bigger cavities (20 - 80 μm), suggesting that confining HSCs in small room may help retain their stemness. This feature, if validated

would be of great importance in the techniques for *ex vivo* expansion where artificial scaffolds come closer to the native bone marrow environment. In another *in vivo* study, Mao and his colleagues combined both macro- and micro-porous systems in a hydrogel-filled calcium phosphate mesenchymal stromal cell (MSC) and HSC co-culture. The system was successfully transplanted subcutaneously in the dorsum of immune compromised mice and improved the regeneration of its vascular dependent tissues [122]. Clearly, culture of HSCs in micro-porous scaffolds poses many intriguing questions to the study of hematopoiesis; is this truly how micro ‘niches’ regulate cell proliferation and differentiation while maintaining a pool of immature HSCs *in vivo*? Micro-porous scaffolds present a promising opportunity to be exploited for different HSC applications.

2.5.3 Nano-structured scaffolds

Recent advances in the *ex vivo* expansion of hematopoietic cells emphasize on crucial role of topographical and biochemical cues on HSCs’ adhesive behaviors, thereby controlling their homing, self-renewal and lineage commitment. By developing structured nanoscale topographies in synthetic materials, novel scaffolds, microdevices, and implant coatings can be fabricated to mimic the native bone marrow environment and improve the integration of such artificial constructs. The simple and most commonly used method to create designed nanostructured scaffolds to date is electrospinning, which was shown effective to a wide range of biomaterials compatible for hematopoietic cells. These include polyethersulfone (PES) [123], poly(DL-lactide-*co*-glycolide) [124], poly(acrylic acid) [125], or with native collagen fibers [123]. This topographical cue alone was shown able to enhance the capture efficiency of HSCs onto the scaffold surface and cell

expansion capacity, while maintaining higher CFU potential than film structure made from the same material [123]. Surface-modified nanofibers with conjugated amino groups or coated E-selectin also gave favorable effects to the expansion of CD34⁺CD45⁺ cells [123-125]. However, this effect was suppressed by the absence of growth factors, which suggests the supporting role of growth factors in the regulation of hematopoietic cell proliferation and differentiation [123, 126].

2.5.4 Scaffolds for studying leukemogenesis

In contrast to normal hematopoietic cells, development of scaffolds for leukemia studies has been rather limited and only began to receive attention in the last few years. Previous studies on leukemia mostly performed on 2D flask culture provided some basic understanding of leukemic cell behaviors *in vitro*. However, growing evidences support the idea that leukemic cells behave differently in 2D and 3D construct, implying that their development is dependent on the state of the environment just as normal hematopoietic cells. Carlos *et al* recently showed a higher amplification of lymphoma cells on stroma-coated polystyrene than its comparable 2D co-culture system [127]. Likewise, mesenchymal stem cell-coated polyurethane scaffolds showed enhanced engraftment of primary acute leukemic cells when implant subcutaneously in NOD/SCID mice [128]. Different porous polymeric scaffolds were assessed by Mantalaris's group for their capability of support leukemic cells *in vitro*; all of which were superior to 2D controls and the most effective scaffold material was polyurethane [129]. There is undoubtedly a discrepancy of leukemic cells behaviors in *in vivo* and *in vitro* constructs, thereby developing 3D scaffolds for study of leukemia is vital in closing this gap. More materials

are needed to explore before we can come up with the best model for leukemogenesis *in vitro*.

Chapter 3

Characterization of Ca-alginate hydrogel

Success in recapitulating aspects of the bone marrow depends on our ability to mimic both physical and chemical characteristics of the natural leukemia environment. As one class of natural hydrogels, Ca-alginate provides a biocompatible hydrated structure that play not only a role in scaffolding but also introduce important mechanical signal similar to that from the soft tissues of the bone marrow. Culture of leukemia cells in alginate hydrogels provide 3D cellular interactions that is not present in 2D tissue flask culture. Although it is not possible/practical for us to completely recreate the bone marrow ECM due to the complexity and multiplexity of ECM components, the alginate hydrogel enables us to recapitulate aspects of the bone marrow ECM microenvironment and tailor it to study specific cell-ECM interactions. In addition, ECM proteins, when entrapped in the Ca-alginate in their most natural forms, would expose more binding sites for cell interactions than the modified/conjugated protein segments found in some other studies. By that way, Ca-alginate hydrogel with encapsulated ECM proteins provides an effective tool for recreating aspects of the *in vivo* bone marrow microenvironment. This chapter will define mechanical properties of the Ca-alginate hydrogel while chapter 4 and 5 will address the

ability to manipulate its characteristics to recreate the physical and mechanical signals present in the bone marrow. The study in this chapter will focus on the microscopic observation, morphological analysis, quantification of mechanical properties, and evaluation of overall structural integrity of the gel as a soft encapsulating system for hematopoietic cells.

3.1 Introduction

In realizing a true 3D encapsulation system effective for hematopoiesis, we examine and highlight the potentials of Ca-alginate hydrogels in mimicking different aspects of the bone marrow environment. Firstly, Ca-alginate is known for its non-toxicity, biocompatibility and simple handling procedure. These excellent features make it a useful material in tissue engineering including scaffolding for endothelial cells [130], embryonic stem cells [131, 132], and mesenchymal stem cells [133]. However, so far to our knowledge, it has not been employed for hematopoietic cell applications.

Although HSCs are suspension cells, they still require a bone marrow mimetic scaffold in supporting their normal *in vivo* behaviors. Such scaffold should resemble the intense network within the bone marrow microenvironment as the hydrated fibrous Ca-alginate hydrogel, and its stiffness should resemble those of soft tissues (1-100 KPa). Conformational properties of the Ca-alginate hydrogel are strongly dependent on the ratio of the component monomers as well as their overall distribution. Polyguluronate blocks (GG) are stiffer than the polymanuronate (MM), while the heteropolymeric blocks (MG) are the most flexible. The possibility of tuning structural and biochemical properties by

simply adjusting its monomer composition allows the manipulation of Ca-alginate in resemblance different ‘niches’ within the bone marrow - whether it is the basal muscle tissue near epiphysis or the space-filling fatty marrow in the diaphysis.

Diffusion profiles within the Ca-alginate hydrogel are also beneficial to the encapsulated cell. For Ca-alginate beads of 1.5%, it was calculated that the diffusion coefficients of small solutes (O₂ and glucose) were in the range of $6 - 14 \times 10^{-6} \text{ cm}^2/\text{s}$ [134], which is favorable to solute-waste exchange necessary in cell culture. Variations in the chemical constituents can also be used to control various physical properties of the hydrogel [135-137]. Biofunctionalization by the conjugation of a specific protein peptide or ligand [128] can be tailored to enhance specific interactions [138] thus creating a designer-specific 3D bio-synthetic *in vitro* microenvironment.

Given the flexibility and tunable physical properties of the Ca-alginate hydrogel system, we believe that cell encapsulation in Ca-alginate hydrogels can provide a realistic 3D *in vitro* model for studying leukemogenesis. We hypothesize that matrix presentation performed in a 3D microenvironment will be more representative of *in vivo* interactions and result in alterations of cellular interactions and functions from those observed in TCP.

3.2 Materials and methods

3.2.1 Materials

Sodium-alginate, CaCl₂ and phosphate buffered salt (PBS) powder were all purchased from Sigma Aldrich. A 0.10 M CaCl₂ solution was prepared by dissolving CaCl₂ powder in ultrapure water with 0.01% Tween-20 and 10mM HEPES. Alginate solutions were

prepared by dissolving 1.1% Na-alginate in PBS and then adding 2% gelatin solution (Sigma Aldrich) at ratio 19:1 to obtain mixture of 1% alginate and 0.1% gelatin.

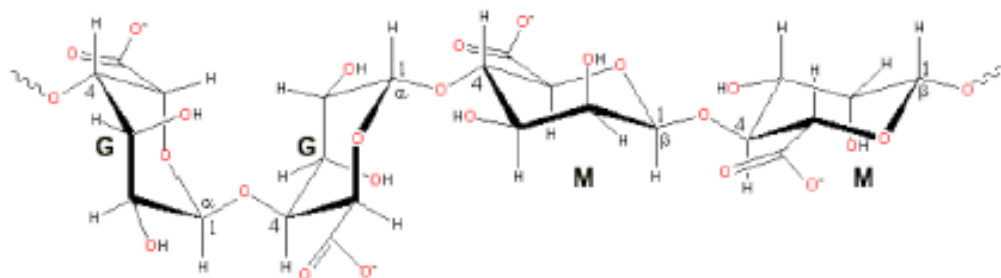


Figure 3-1 Molecular structure of alginate polymer

3.2.2 *Generation of gel block*

Alginate solution was poured into a mold with tiny pores and placed in a cubic container. 50ml of CaCl₂ solution was then added to initiate gelation. Gelation of Ca-alginate hydrogels occurs due to cross-linking action of Ca²⁺ ions with carboxylic groups in the G-blocks. To ensure a homogeneous reaction, the cubic container was capped and placed on the orbital shaker for 24hours. This allows a slow and homogenous diffusion of Ca²⁺ into the alginate solution during the gelation process and will result in a homogenous block of Ca-alginate hydrogel.



Figure 3-2 Preparation of gel blocks

3.2.3 Mechanical characterization

Compressive stress test was done on an Instron mechanical testing machine, at a rate of 0.0001mm/s. Briefly, the cylindrical block of Ca-alginate was placed on the stand, immersed in the respective CaCl_2 solution. Data collected was plotted as in stress-strain curve and elastic modulus (E) was calculated from the slope in the linear viscoelastic range. Network crosslink density, ρ_x and the average mesh size, ξ , of the polymeric were calculated by Flory's theory [127] and the equivalent network theory [129]:

$$\rho_x = E/3RT$$

$$\xi = \sqrt[3]{(6/\pi\rho_x N_A)}$$

where R is the universal gas constant, T is the absolute temperature and N_A is the Avogadro constant.

3.2.4 Scanning electron microscopy

Selected hydrogel samples were gently rinsed with PBS, fixed with 3% glutaraldehyde, and post-fixed with 1% osmium tetroxide. Samples were dehydrated using a graded series of ethanol followed by hexamethyldisilazane drying. Finally, samples were gold sputter-coated before viewing under field emission scanning electron microscope (SEM; FEI Company, Hillsboro, OR, USA) for surface and cross-section morphology scanning. Images were taken at x4000, x4500 and x5000 magnification.

3.2.5 High-performance liquid chromatography(HPLC)

HPLC on Zorbax 5 μ m column (Eclips ZDB-C18, Agilent) was performed using Agilent HPLC instrument to determine the M:G ratio of the commercial alginate used. Mobile phase contained 2mM potassium diphosphate KH_2PO_4 + methanol 5% in ultrapure water. Flow rate was set at 1.5ml/min and UV wavelength was 210nm.

3.3 Results

3.3.1 Mechanical properties of alginate hydrogel (HV vs LV)

In this study, we utilized two types of commercial alginate namely high viscosity (~250cP, HV) and low viscosity (~20cP, LV) to investigate various characteristics of the hydrogel model. Different molecular weights of each constituent polymer gave different mechanical characteristics of the resulting gel. In general, LV alginate creates 2-3 times softer gels than those made from HV alginate in the presence of the same amounts of Ca^{2+} ions. The stiffness of the HV alginate hydrogel in 150 mM of Ca^{2+} solution was found to be at 13 KPa compared to 6 KPa of gels composed from LV alginate. As we lower the concentration of Ca^{2+} ions, gel stiffness from HV alginate was measured as 11KPa while those of LV alginate was 4.5KPa in 40 mM Ca^{2+} solution.

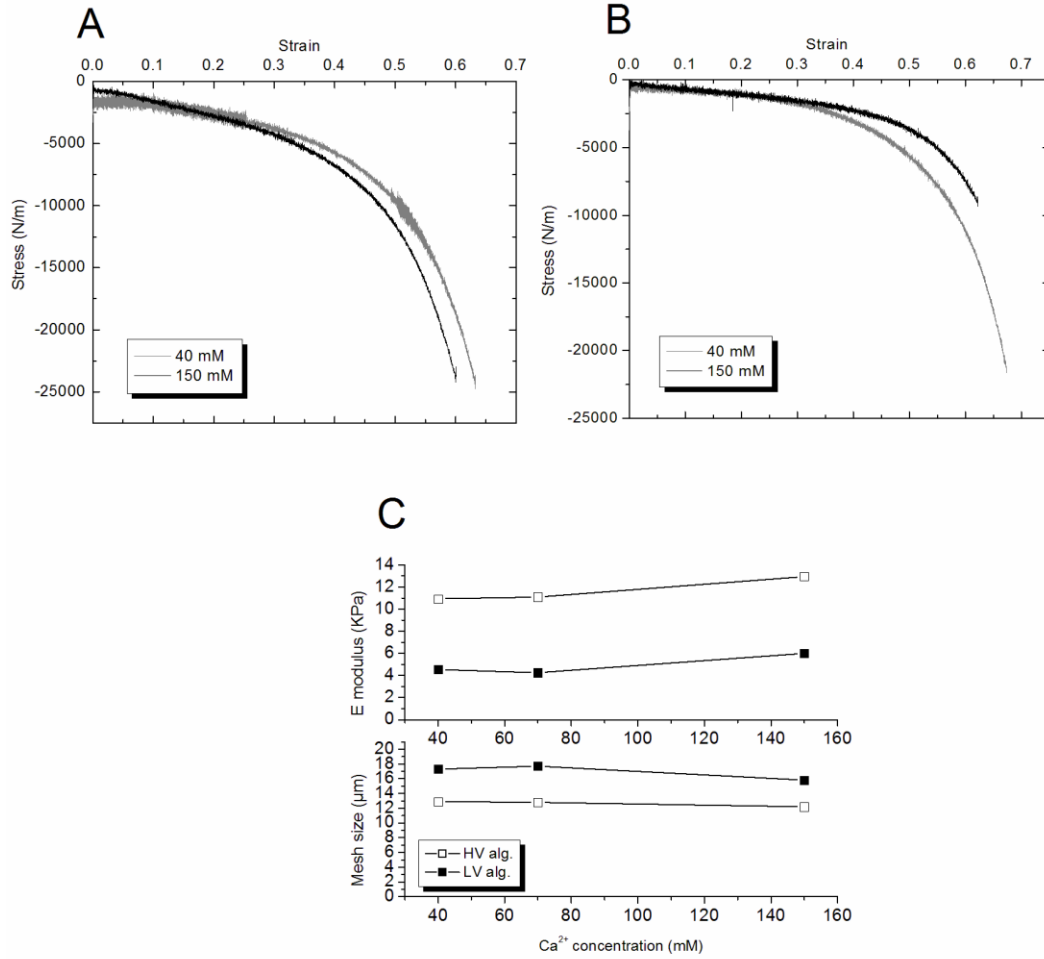


Figure 3-3 Mechanical properties of Ca-alginate hydrogels.(a) and (b) Stress-strain curve of HV and LV alginate hydrogels made from 40-150 mM Ca²⁺ concentrations. (c) Calculated E modulus and mesh size of HV and LV alginate hydrogels in different Ca²⁺ concentration

Figure 3-3 shows the stress-strain curve of alginate hydrogels made from two different types of material. In both HV and LV alginates, hydrogels exhibit high elasticity; able to withstand the maximum stress of around 10^4 N/m and a deformation up to 50% before losing their integrity. Stiffness of the matrix was found in a small range of 11-13 KPa for HV (Figure 3-3a) and 6-7 KPa for LV alginates (Figure 3-3b) (40-150 mM

concentration of Ca^{2+}). Data from matrix stiffness were found close to those of the muscular (HV alginate) and adipose (LV alginate) tissues. LV alginate, despite lower matrix stiffness, appeared more resilient to stress (higher elastic limit) than HV alginate did.

Calculated mesh size of the system ranges from 12-13 nm for HV and 16-18 nm for LV alginate. This data gives an approximate internal pore size of the hydrogel, which is also roughly 100 times smaller than a single cell; the average size of a hematopoietic cell being 20 μm . Thus the alginate hydrogel provides a truly microporous environment which encapsulates cells within the confines of its matrix.

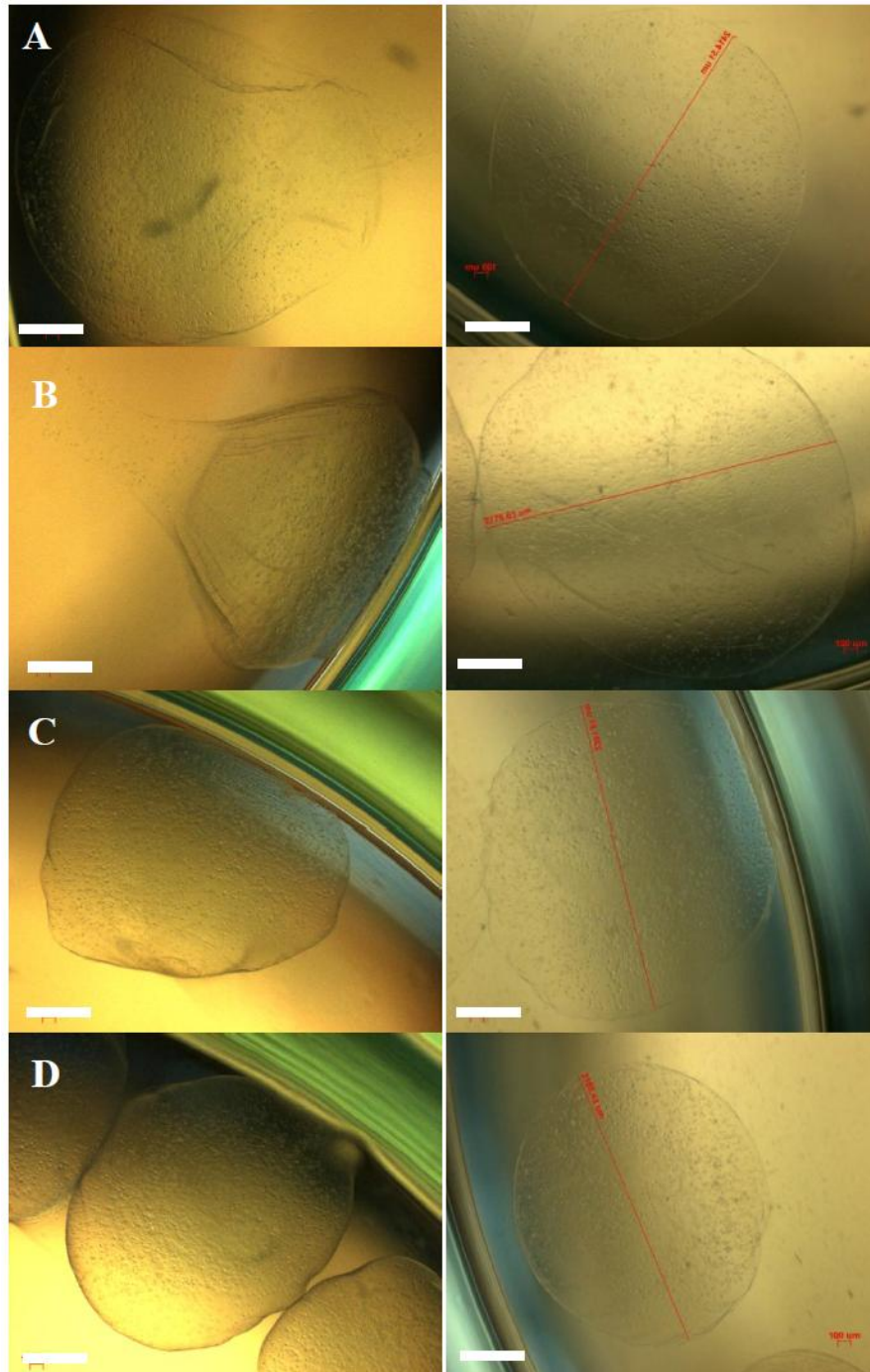


Figure 3-4 Morphology of alginate beads made from HV (left column) and LV (right column) alginates. (a) (b) (c) and (d) represent various Ca^{2+} concentration of 27mM, 40mM, 70mM and 100mM respectively. Scale bar 500 μm

Figure 3-4 shows the overall shape and morphology of alginate beads at different Ca^{2+} crosslinking concentrations. It was observed that LV alginate maintains its spherical shape regardless of the Ca^{2+} concentration (27-100 mM). On the other hand, the integrity of hydrogel beads made from HV alginate is highly affected by the amount of Ca^{2+} ions available for crosslinking. Concentrations of Ca^{2+} below 100 mM were insufficient for the gel to form a nice spherical shape. This phenomenon may be explained by reasoning that high MW polymers in HV alginate would require more Ca^{2+} ions for holding the long chain polymers together to form tight structure in the hydrogel. Insufficient crosslinking may result in slack and irregular gel architecture. Bead sizes range from 2.4 – 2.7 mm for both HV and LV alginates.

3.3.2 SEM imaging

SEM images of our Ca-alginate hydrogels revealed a highly fenestrated surface and pore-like structures of $<5\mu\text{m}$ (Figure 3-5) on their exterior surfaces. The fenestrated surfaces and fine textures along the surfaces of the alginate hydrogel provide a high surface area, which is beneficial to nutrient, ion and oxygen transport. The internal structure of the Ca-alginate is densely-packed (Figure 3-6) which resembles the condensed environment in the bone marrow.

HV and LV alginates exhibited distinct architecture with respect to Ca^{2+} concentrations (Figure 3-8). Increasing Ca^{2+} crosslinking density made polymer bundles in HV alginate thinner, exhibiting more kinks, resulting in a concave appearance on the surface. Exterior surface of the bead with lowest Ca^{2+} concentration of 27.57mM contains fewer folds and the distance between two folds is greater, leading to larger pore sizes ($5\mu\text{m}$). These pores facilitate the entry and subsequent diffusion of nutrients and oxygen

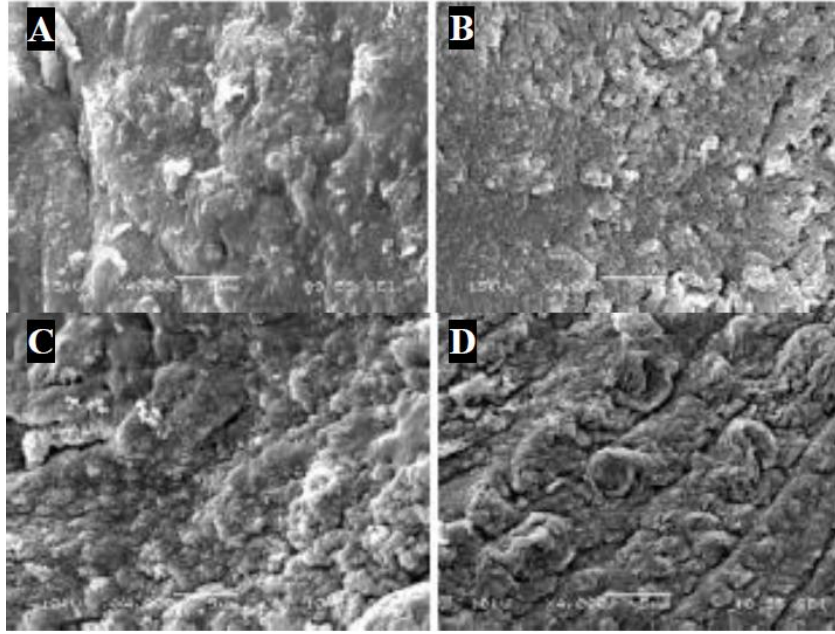


Figure 3-5 Cross-section architecture of alginate hydrogels. (left column) HV alginate, (right column) LV alginate; (a) (b) Crosslinked with 70mM and (c) (d) 100mM of Ca^{2+} concentration. Scale bar 5 μm .

to the encapsulated cells. With increasing Ca^{2+} concentration, the number of folds increased, shortening the distance between two folds and hence resulting in smaller but higher density of pore. The surface of Ca-alginate bead with the highest Ca^{2+} of 100mM has the greatest density of folds and pores, the size of which is $<1\ \mu\text{m}$. On the other hand, LV alginate appeared smoother with less polymer folds as more Ca^{2+} crosslinking are present. Pores were hardly observed in saturated Ca^{2+} crosslinked LV alginate (100-150mM). We predict that alginate hydrogel made from LV alginate crosslinked with Ca^{2+} concentration of $> 100\text{mM}$ would likely be unfavorable for cell culture. In examining the cross-section morphology of the inner gel architecture, we observed more texture and ridges created by polymer folding in both HV and LV alginate crosslinked in higher concentration of Ca^{2+} ions (Figure 3-7).

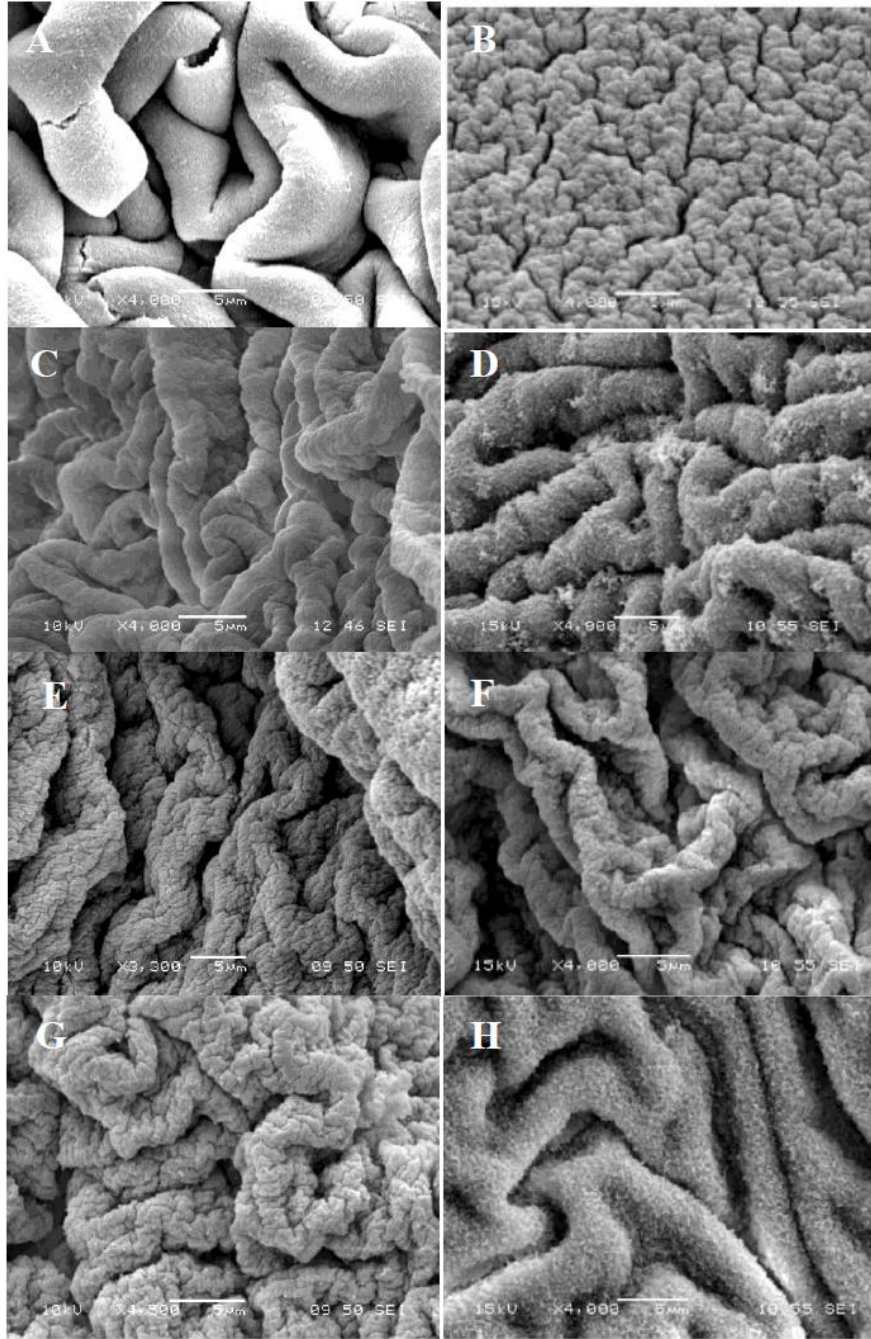


Figure 3-6 SEM images of Ca-alginate hydrogel surface. (left) HV, (right) LV; (a) (b) 27mM, (c) (d) 40mM, (e) (f) 70mM and (g) (h) 100mM of Ca^{2+} concentration. Scale bar 5 μm .

3.3.3 *M:G ratio (HV vs LV)*

Figure 3-4 shows the HPLC profile of two sodium alginate salts constitutive of the hydrogel structure. Two major peaks corresponding to the G and M acid blocks respectively. It was calculated from the chromatograph that M:G ratio of HV alginate was 0.49 and that of LV alginate was 1.78. The HV alginate has a higher number of G-blocks than LV alginate. This data is in agreement with the mechanical characterization of our HV and LV alginates: alginate with low M:G ratio i.e. high content of GG blocks tend to give stiffer matrix.

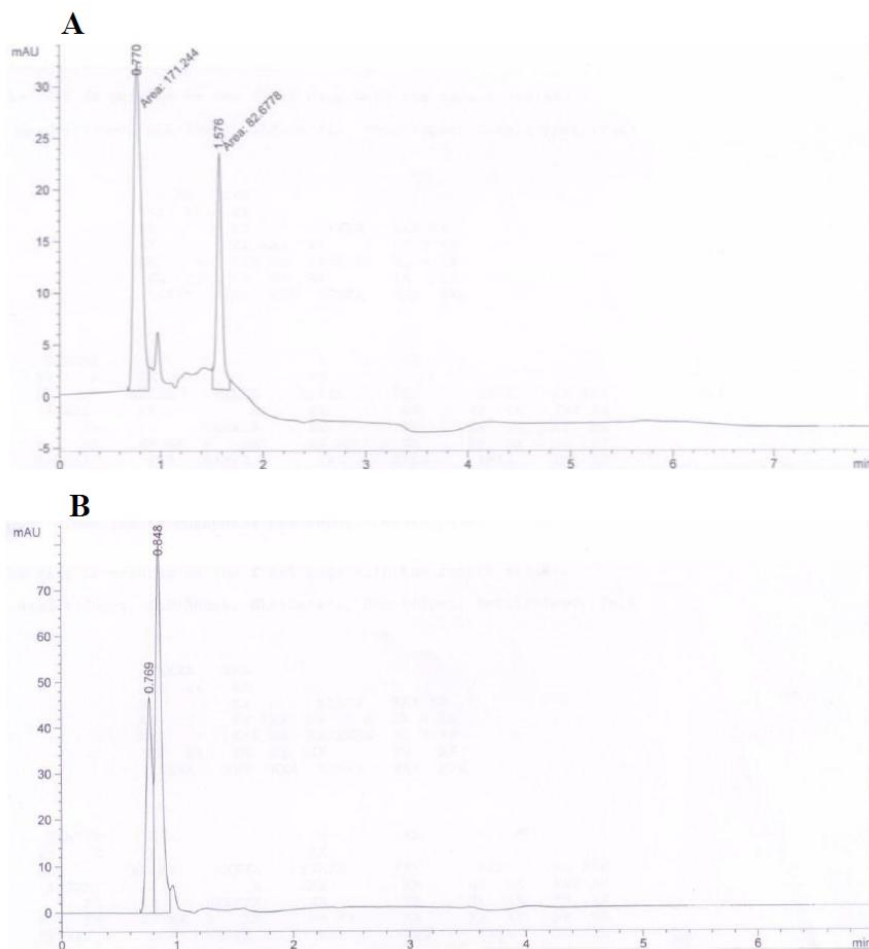


Figure 3-7 HPLC results of two different alginates. (a) HV, (b) LV

3.4 Discussion

This study examined three important properties of Ca-alginate hydrogel including matrix architecture via morphological analysis, stiffness of matrices and the M:G ratio of each alginate material, which will help in understanding the capability of such materials in hematopoietic cell culture applications. Gel morphology and the analysis of surface-to-volume ratio will give us an idea of transport properties within the highly dense hydrogel matrix; high fold density would be more beneficial to the distribution of proteins and nutrients within the matrix thus supporting better cell growth. Matrix stiffness was examined and variation in the chemical constituents will give us some ideas on how the gel can resemble that of the natural tissues while the M:G ratio will provide information on the polymer constituents and its crosslinking capacity in tuning mechanical strength of the matrix.

From the study, elastic modulus of LV alginate hydrogels was generally lower than HV alginate. A low elastic modulus may not be suitable for the fabrication of scaffolds in culturing cells that require moderate mechanical strength and support for their optimal growth. The yellow marrow within the medullary cavity of cancellous bone consists mainly of adipose tissue which has Young's modulus of 3-4KPa [139] while the main hematopoietic site – red marrow – consisting of a network of fibers would have higher stiffness measurement. In other studies, elastic modulus of soft tissue in general was found to range between 25-300KPa [140] while those of natural collagen fibers and elastin proteins were 1 GPa and 0.6 MPa respectively [141]. Hence, HV alginate is

believed to better resemble the intricate natural hematopoietic microenvironment and it will be used as our standard material in the latter cell studies.

The extent of ionic crosslinking affects the shape and overall integrity of alginate hydrogels, especially in the case of HV alginate. Beads made from HV alginate can only achieve uniform shape at 100mM concentration of Ca^{2+} ion, lower crosslinking density leads to more irregular shapes formed using the gel-drop method. The mechanical characteristics of HV alginate can be slightly altered by changing the crosslinking divalent ion (such as Ba^{2+} , Sr^{2+}) and its concentration. Replacing Ca^{2+} with Ba^{2+} or Sr^{2+} generally produces stronger beads but reduces the gel permeability in high-G alginate [142, 143].

The SEM images revealed that micro-scale topography of HV and LV alginate gels might be different. Recall that alginate gelation process is achieved by the exchange of Na^+ ions from the guluronic acids with the divalent Ca^{2+} cations, conformation of the hydrogel is therefore highly dependent on the composition of both Ca^{2+} and availability of GG blocks of the alginate. In HV alginate, which has a higher proportion of G monomers, has more GG blocks. Thus increasing Ca^{2+} concentration results in higher crosslinking density, greater degree of polymerization and microtexturing of the polymers. However, due to the likelihood of longer chain polymers in HV alginate, we hypothesize that the organization of crosslinked chains will only begin to improve in the presence of high Ca^{2+} ion concentrations, thus at 40 mM Ca^{2+} microtextures of alginate hydrogels have not yet formed. Contrary to HV alginate, LV alginate made from low MW polymers has less GG constituents and is more likely to have short GG polymer chains. At very low concentration of Ca^{2+} , polymerized short chain GG polymers in LV alginate can readily arrange themselves randomly, resulting in finer structure and textured surface. When more

Ca^{2+} ions are present, longer chains of GG- Ca^{2+} -GG crosslinking can form and the stacking of crosslinked GG groups into an egg-box structure can result, leading to thicker bundles of polymer. This stacking of crosslinked short chain polymers may establish elongated bundles, and has a conformation similar to that seen in HV alginate with long polymer chains. We argue that the density of fenestrated surface in LV alginate hydrogels decreases with increasing Ca^{2+} concentration as the high cross-linking density result in blocks of crosslinked GG polymers.

While increasing Ca^{2+} crosslinking density improves mechanical properties of the gel, shrinkage of pore size in high Ca^{2+} crosslinked alginate is expected, especially in LV alginate as revealed by SEM surface scan. This may lead to increased mechanical stress on encapsulated cells affecting the cell viability during the gelation process and a limitation in transportation within the matrix. The choice of making alginate would therefore depend on the specific application. Gels made from LV alginate can be crosslinked with low Ca^{2+} concentration (40-70 mM). However, if we were to choose the stiff scaffold to introduce certain mechanical signals as in our latter cell studies, HV alginate and Ca^{2+} of 100 mM is needed to maintain the gel integrity and minimize the compromising of the nutrient transportation.

The M:G ratio obtained from HPLC data is valuable in understanding the mechanical properties and crosslinking capability of alginate salts. Low M:G ratio meaning high content of GG blocks explain for the stronger matrix and highly textured surfaces in HV alginate. While Ca^{2+} crosslinking density of 100mM is almost 'saturated' in LV alginate with highly compact surface, HV alginate can still accommodate more crosslinking and

stacking of polymer bundles. The M:G ratio is therefore useful in predicting crosslinking patterns and behaviors of an alginate hydrogel for better control of matrix characteristics.

3.5 Conclusion

Alginate hydrogel was investigated as a highly hydrated network of polymers which is close to the native fibrous structure within the bone marrow. Stiffness of HV alginate was found in the range of 11-13 KPa while that of LV alginate was 6-7 KPa. Calculated mesh size of the system is approximated 100 times smaller than the size of a single cell. Varying Ca^{2+} concentration proved to have little impact on gel stiffness, but the integrity and micro-structure of the resulting hydrogels is affected. Macroscale gel architecture determines gel durability in long-term cell culture while the microscale topography may have greater direct impact on the cells themselves. In fact, culturing hematopoietic cells in confined spaces (15 μm) has proven to retain stemness of HSCs, as reducing the cell proliferation and differentiation while expressing higher stem cell markers [121]. Microscale topography is therefore an important consideration in reconstructing the bone marrow environment. Another advantage of the alginate system is the simple handling procedure and well-manipulated beads that make Ca-alginate hydrogel a power tool in hematopoietic cell applications.

Chapter 4

Cell-matrix interactions in 3D Ca-alginate culture

The Ca-alginate hydrogel is predicted to provide a true 3D encapsulation that support cell-cell and cell-matrix interactions. Results from chapter 3 suggest the use of HV alginate to create an inductive scaffold that replicate the physical properties of the bone marrow structure. The Ca^{2+} concentration of 100mM is the lowest concentration necessary to maintain the bead integrity, especially for long-term culture while predicted not compromising the nutrient transportation for leukemic cell culture. Hence, it was used as our standard method in constructing the 3D Ca-alginate culture system. In this chapter, we investigate the capability of Ca-alginate hydrogel in facilitating leukemic cell proliferation and differentiation. The possibility of adjusting its properties for increased cell growth will be explored while differences in both 2D and 3D context are highlighted for better insights into *in vitro* cell behaviors.

4.1 Introduction

Cell-matrix interactions exhibited different characteristics in 2D and 3D context. It was once proven that 2D culture system projects tangential cell-ECM interactions compared to the *in vivo* state, and hence resulting in unnatural cellular binding and altered mechanotransduction [144]. These changes would influence subtle cellular processes such as global histone acetylation [145], proliferation, apoptosis [146], differentiation, and gene expression [147], and as a result lead to the misinterpretation of molecular cues of hematopoietic cells in their natural 3D environment.

Tuning mechanical characteristics of the matrix is therefore capable of directing cell behaviors. For example, increasing crosslink concentration would reduce pore sizes, reducing the transportation within the matrix while exerting more stresses on the encapsulated cells. The harsh environment might therefore turn off proliferation and trigger apoptosis or differentiation.

This chapter highlights the differences found in the cell proliferation and differentiation cultured in 2D and 3D context. Cell viability and morphology are also assessed in tuning various alginate components, including the componential alginate and Ca^{2+} crosslinking used, and the sizes of hydrogel beads in an attempt to optimize conditions for hematopoietic cell culture *in vitro*.

4.2 Materials and methods

4.2.1 *Materials*

Sodium-alginate, CaCl_2 and phosphate buffered salt (PBS) powder were all purchased from Sigma Aldrich. A 0.10 M CaCl_2 solution was prepared by dissolving CaCl_2 powder in ultrapure water with 0.01% Tween-20 and 10mM HEPES. Alginate solutions were prepared by dissolving 1.1% Na-alginate in PBS and then adding 2% gelatin solution (Sigma Aldrich) at ratio 19:1 to obtain mixture of 1% alginate and 0.1% gelatin.

4.2.2 *Cell encapsulation*

Cells were resuspended in 1 ml of alginate-gelatin mixture at concentrations of $1-5 \times 10^5$ cells/ml. Assays of 96-well plates were prepared by adding 100 μl CaCl_2 solution to each well and the cell-alginate mixture was dropped from the height of 3 cm through a 25G needle into wells containing CaCl_2 solution. Cell-encapsulated gels were solidified within 5 mins after contact with CaCl_2 forming spherical beads of 2.1 mm in diameter, one bead per well. The cell-encapsulated beads were then carefully washed thrice with sterile PBS before cell culture. All the above reagents were sterilized by autoclaving and/or filtering through 0.2 μm membrane prior to use.

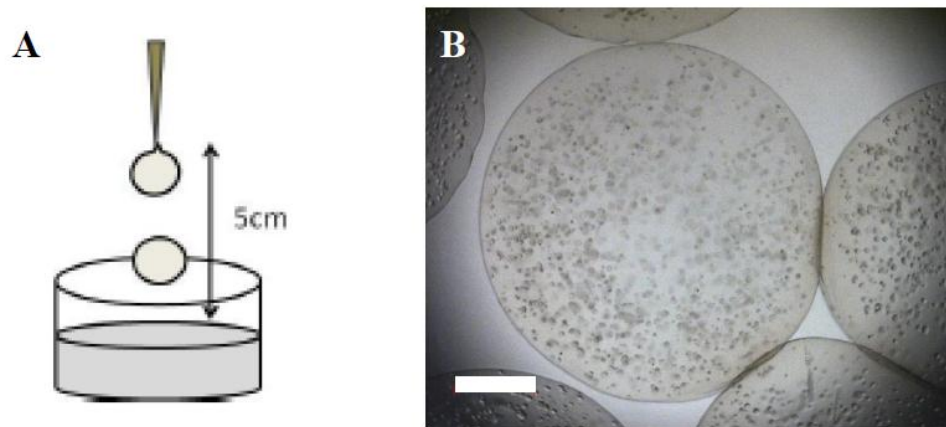


Figure 4-1 Process of making alginate hydrogel. (a) Cell-suspended alginate solution was dropped from the height from 5cm to the CaCl₂ bath in the preparation of Ca-alginate hydrogel, (b) micrograph of a hydrogel bead. Scale bar 500μm.

4.2.3 Cell culture

Human leukemic K562 cells (ATCC) were cultured in a 75 cm² tissue culture polystyrene (TCP) with Iscove's Modified Dulbecco's Medium (IMDM; Invitrogen) supplemented with 10% fetal bovine serum (FBS; Hyclone) and 1.5g/l sodium bicarbonate (Sigma Aldrich) according to ATCC formulation. Encapsulated cells for the 3D culture were cultured in 96-well plates containing the same media as stated for the 2D TCP culture. Cells were cultivated at 37°C in a fully humidified 5% CO₂ incubator for up to 2 weeks. Cell cultures were monitored daily on the light microscope and a change of media was performed every two days.

4.2.4 Cell proliferation assay

Assays were performed in 96-well plates, containing K562 cells cultured either in 2D plates or 3D hydrogels. Cell proliferation was quantitatively assessed by a highly stable WST assay (Cell Counting Kit-8; Dojindo), which uses tetrazolium salt WST-8 (2-(2-methoxy-4-nitrophenyl)-3-(4-nitrophenyl)-5-(2,3-disulfophenyl)-2H-tetrazolium, monosodium salt). WST-8 is bio-reduced by cellular dehydrogenases to an orange formazan product that is soluble in tissue culture medium. The procedure is described in Figure. In short, assay plates were incubated for 2h at 37°C and 5% CO₂. Absorbance was measured at 450 nm. A standard curve was constructed by plotting absorbance of known cell numbers for calculating the number of viable cells in assay. Cell population doubling time (PDT) (in hours) was calculated according to the established formula:

$$PDT = T \times \frac{\log 2}{\log \left(\frac{I_1}{I_2} \right)}$$

Where I₁, I₂ are the absorbance reading and T is the duration of the 2 time points within the exponential phase of cell proliferation.

4.2.5 Cell viability and morphology

Cell survival in 2D and 3D cultures were monitored via live/dead staining and performing manual cell counts using a viability stain. For live/dead staining, viable and dead cells were stained at a concentration of 4 µM Calcein-AM (Invitrogen) and 8 µM propidium iodide (PI; Sigma Aldrich) respectively. Cell mixture was incubated at 37°C for 15 mins. Images were taken with Axiovert 200M fluorescence microscope (Carl Zeiss) using FITC and Rhodamine channels. For a manual cell count, the Ca-alginate hydrogel beads were

dissolved in a dissolution buffer to retrieve all the hematopoietic cells. The bead dissolution buffer contains 50 mM tri-sodium citrate dehydrate, 77 mM NaCl and 10 mM HEPES (Sigma Aldrich). Cells were washed, stained in Trypan blue solution, and visualized under the microscope using a hemacytometer.

For a morphological analysis and hematological identification of the K562 cell population, cultured cells were washed, cytopun and stained in Hemacolor® (Merck Chemicals), a rapid Wright-Giemsa based staining solution kit, air-dried and visualized under the microscope.

4.2.6 Flow cytometry

Surface expression of different lineage-specific markers on K562 cultured cells were analyzed by Epics-Altra (Beckman Coulter) flow cytometer, equipped with a 488 nm Argon laser. At each passage, $0.5-1.0 \times 10^6$ cultured cells were harvested and incubated with directly labeled anti-human CD34, CD38 (common stem cell markers); GPA, CD71 (erythroid); CD13, CD16b (granulocytic); and CD41b and CD42b (megakaryocytic) (BD Bioscience). CD34, GPA, CD42b and CD16 were pre-conjugated with fluorescein isothiocyanate (FITC); CD38, CD71, CD41 and CD13 were pre-conjugated with phycoerythrin (PE). Staining buffer contains 2% FBS and 0.1% sodium azide (Sigma Aldrich). Matched isotype controls were used for gating and analysis purposes.

4.3 Results

4.3.1 *Cell proliferation and viability*

It is noted from light microscope observations that cells cultured in 3D tend to take shape and orientation according to the pores or wedges of the matrix, with greater tendencies in clumping together to form tight aggregates within the hydrogel (Figure 4-2). Boundaries between cells are harder to distinguish due to tight cell-cell interactions maintained in a 3D architecture. Clusters of K562 cells in 3D alginate range from 60-100 μm in diameter at day 5 and rapidly grew up to 2-3 times bigger at day 11 when they occupy all the available spaces. On the other hand, cells in 2D appear smaller ($\sim 20 \mu\text{m}$) compared to those in 3D ($\sim 35 \mu\text{m}$) and tend to be loosely stacked on top of each other.

Figure 4-3 shows the growth profile of K562 cells in 2D *versus* 3D. Cell proliferation in 3D hydrogel was comparable to 2D culture; the maximum growth achieved was 18-19 folds for an initial seeding density of 1×10^5 cells/ml in both culture systems. Expansion capacity of K562 cells, on the other hand, was more advantageous in the 3D hydrogel culture; as it is not dependent on the seeding density as seen in 2D culture. This feature would be beneficial in the long-term as high cell density does not affect the growth rate. At higher seeding densities ($2-5 \times 10^5$ cells/ml), better expansion was achieved in 3D hydrogels (~ 14 fold) as compared to the 2D culture (~ 6 fold). Despite the long lag phase, cells cultured in 3D hydrogels have a comparable average cell population doubling time (PDT) with 2D culture in the first 4 days. The cell PDT in 2D was 23 hours at 1×10^5 cells/ml, longer at 5×10^5 cells/ml (42 hours); while those in 3D

culture were 26 hours at both initial seeding densities. K562 cells doubling time was reported at around 30 hours *in vitro*.

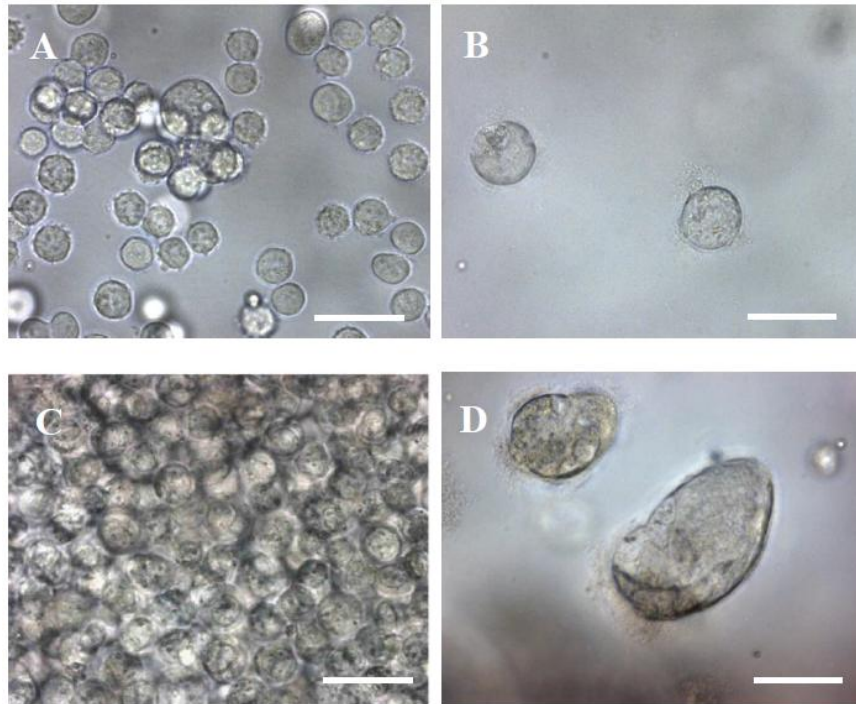


Figure 4-2 Micrographs of K562 cells in 2D vs 3D culture. Images were taken at day 3 (top row) and day 7(bottom row). (a) (c) 2D; (b) (d) 3D. Scale bar 50 μm

Table 4-1 Average population doubling time (PDT) of K562 in 2D vs 3D culture over the first 4 days of culture.

Cell density (cells/ml)	2D	3D
1E5	23	26
5E5	42	26.5

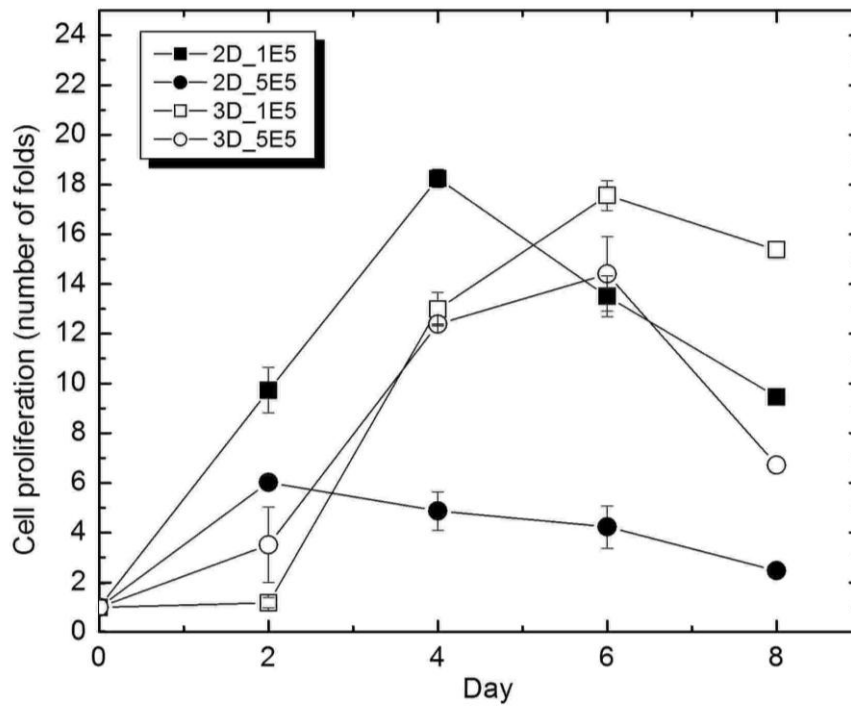


Figure 4-3 Cell proliferation in 2D TCP vs 3D alginate hydrogel cultures as measured by WST assay at different initial seeding density from 1-5 E5 cells/ml

In terms of culture adaptation, 3D cultures suffer from a longer lag phase of ~2 days as compared to the 2D culture which reflects an increase of ~6-9 folds after two days in culture. Cell viability was quite low in 3D culture for the first week (40-60%) but increased and stabilized at ~ 75% afterwards up to 2 weeks (Figure 4-4). It was observed that live cells are evenly distributed throughout the 3D hydrogel suggesting that the gel structure and composition does not limit nutrient and waste exchange throughout the matrix.

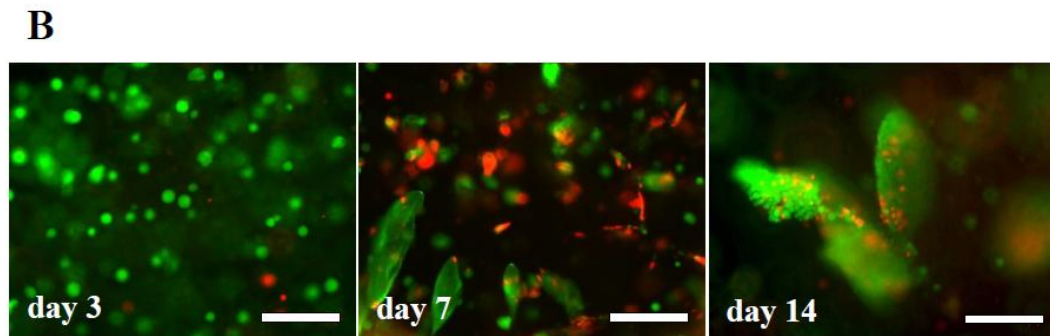
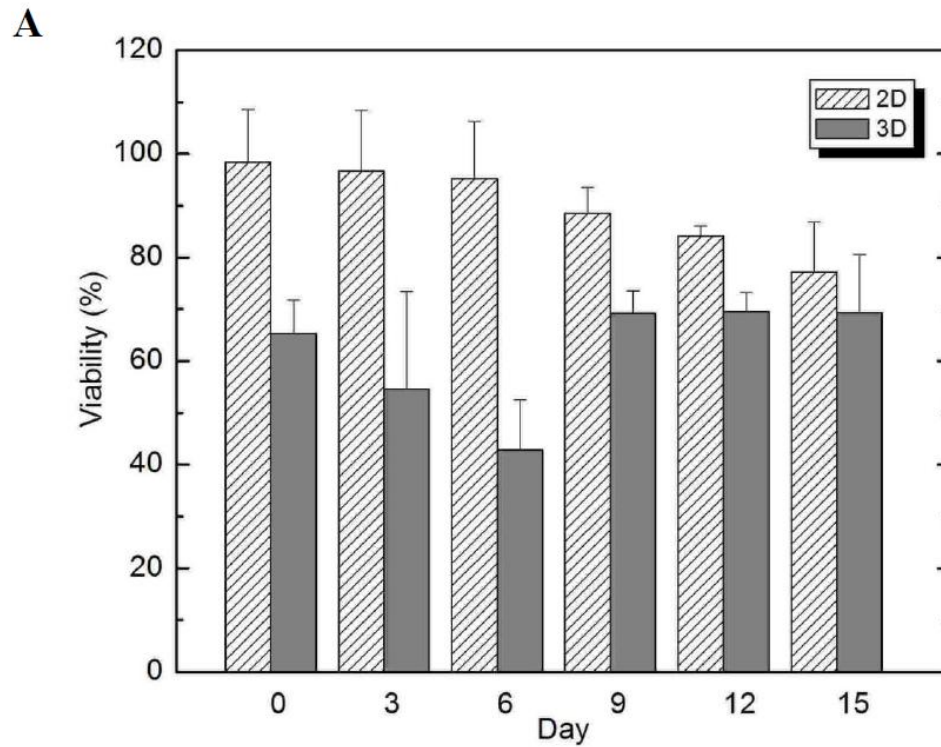


Figure 4-4 Viability of K562 cells in 2D TCP and 3D Ca-alginate hydrogel cultures as manually counted using trypan blue exclusion dye (a) and in live/dead fluorescence cell staining (b). Live cells – green, dead cells – red. Scale bar 200µm.

4.3.2 Spontaneous differentiation of K562 cells in 3D hydrogel

Typical phenotype of K562 cells cultured in 2D system expressed immature myeloblastic characteristics (98% $CD34^+CD38^-$) (Table 4-2). In contrast, culture of K562 cells in alginate hydrogel activated ~40% of the cell population to $CD38^+$; among them ~40% were $CD34^+CD38^+$ progenitor cells and ~60% were at later stage ($CD34^+CD38^+$) (Table 4-2). It is postulated that these two populations form the activating progenitor and differentiated pools in the 3D cultured cells.

Table 4-2 Expression of CD34 & CD38 markers in K562 cells in different culture systems

	$CD34^+CD38^+$	$CD34^+CD38^-$	$CD34^-CD38^+$	$CD34^-CD38^-$
2D	0.2%	0.4%	1.0%	98.5%
3D	15.9%	3.1%	23.2%	57.8%

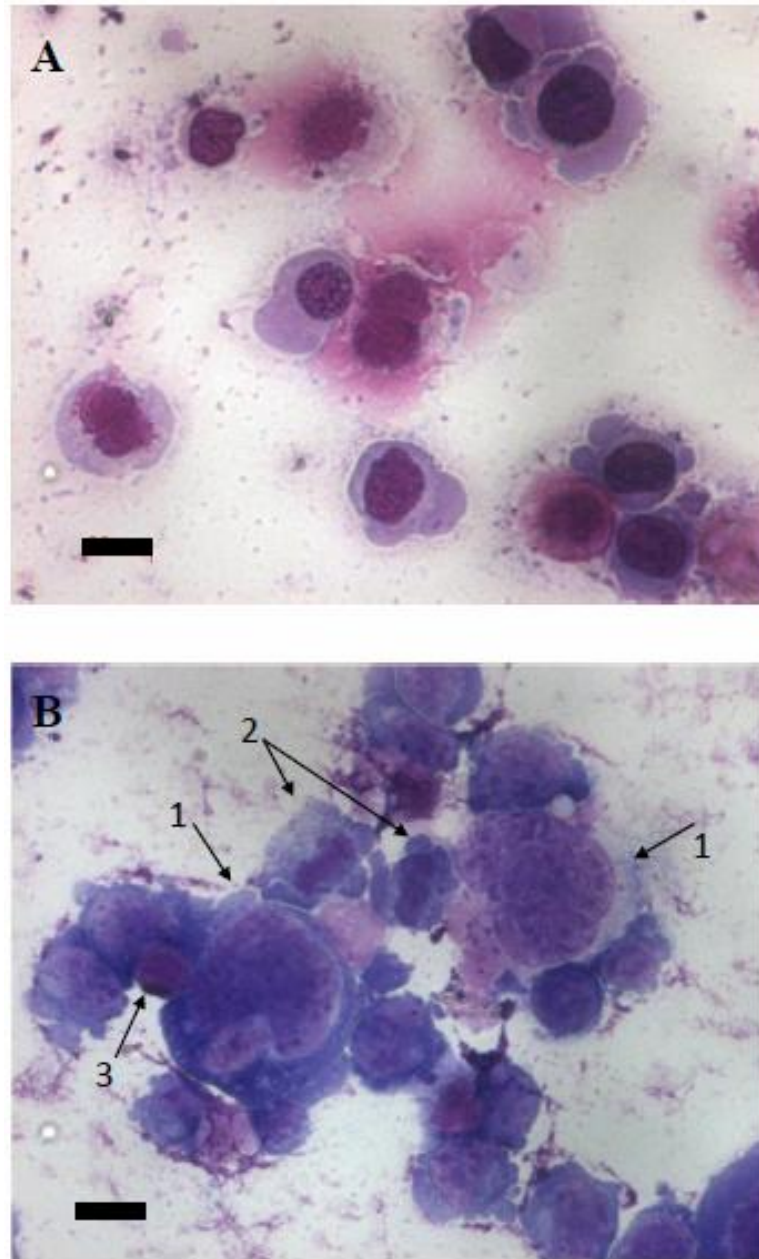


Figure 4-5 Micrographs of Wright-giemsa stained cells cultured in 2D (a) & 3D (b) at day 7. Cells cultured in 3D expressed morphology of late megakaryocytes (1), granulocytes (2) and erythrocytes (3).

Wright staining of the cells at day 9 reveals some distinguished degree of differentiation in different conditions. Cells cultured in 2D at day 9 were mostly still in primitive stages of early myeloblasts (~ 20 μm in diameter) and expressing a tendency to differentiate toward erythroid lineage with round condensed nucleus. No megakaryocytes or band cells were observed. On the other hand, K562 cells cultured in 3D appear more heterogeneous (~ 20 – 35 μm) with the presence of more mature cells of all four lineages (erythroid, megakaryocytic, granulocytic and monocytic).

4.3.3 Optimization of alginate hydrogel size

To test the effects of bead size on cell expansion, various gauge needles (21 – 30G) were used to produce different sized beads. Our results showed that the smallest sized bead (< 1.8 μm) had the greatest expansion capacity, reaching two times greater fold expansion (30-fold) than our standard beads at 2.1 μm ; this is likely due to the larger surface contact areas to volume ratio in smaller beads which may influence expansion capacity. In optimizing the components of the hydrogels, low alginate concentration (1%) produced the best result.

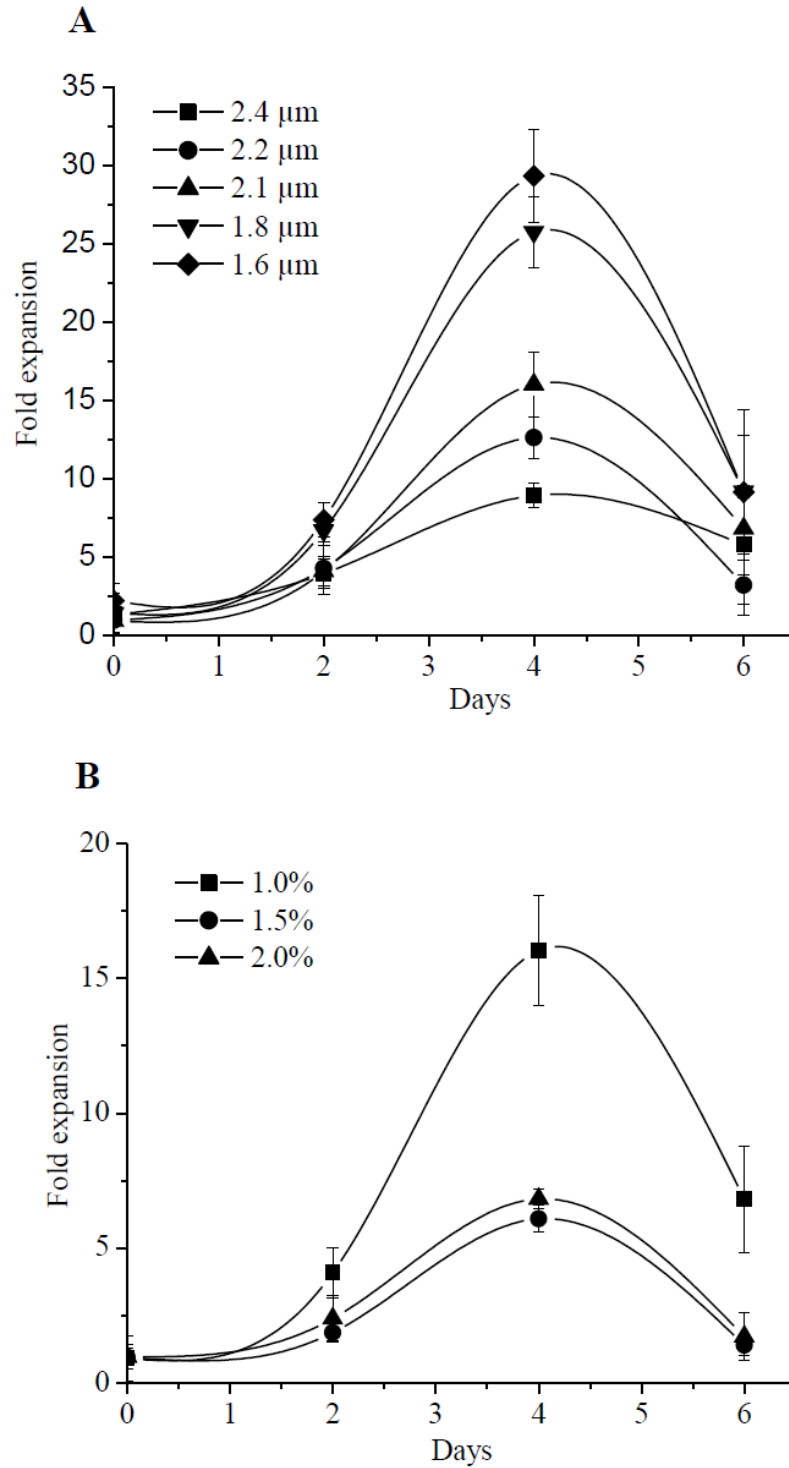


Figure 4-6 Effect of bead size (a) and alginate concentration (b) on cell expansion [148]

4.3.4 Effects of low viscosity (LV) alginate

Cell morphology, proliferation and viability of K562 cells were also assessed in culture of LV alginate crosslinked by the same concentrations of Ca^{2+} . In contrast to HV alginate (Figure 4-2), individual cells in LV alginate beads can be clearly distinguished under light microscopy at day 7 (Figure 4-7). Cells at periphery of each clump still maintain a normal rounded shape, suggesting lower mechanical stress exerted from the surrounding matrix. Clumps of cells appear ovals rather than wedges seen in HV alginate.

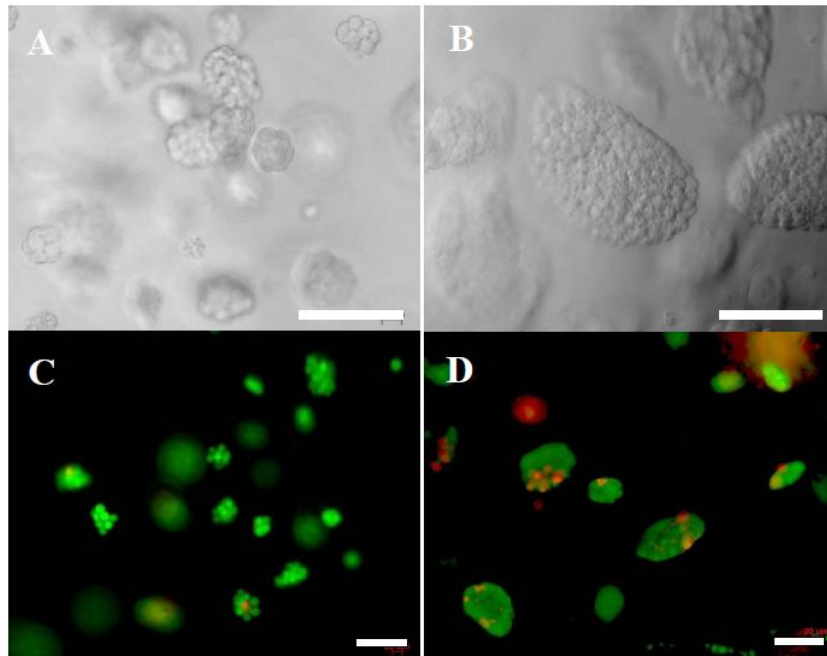


Figure 4-7 Morphology of K562 culture in alginate hydrogel at day 3 (left column) & 7 (right column). (a) (b) (c) light microscopy; (d) Live/dead cell staining. Scale bar 100 μm.

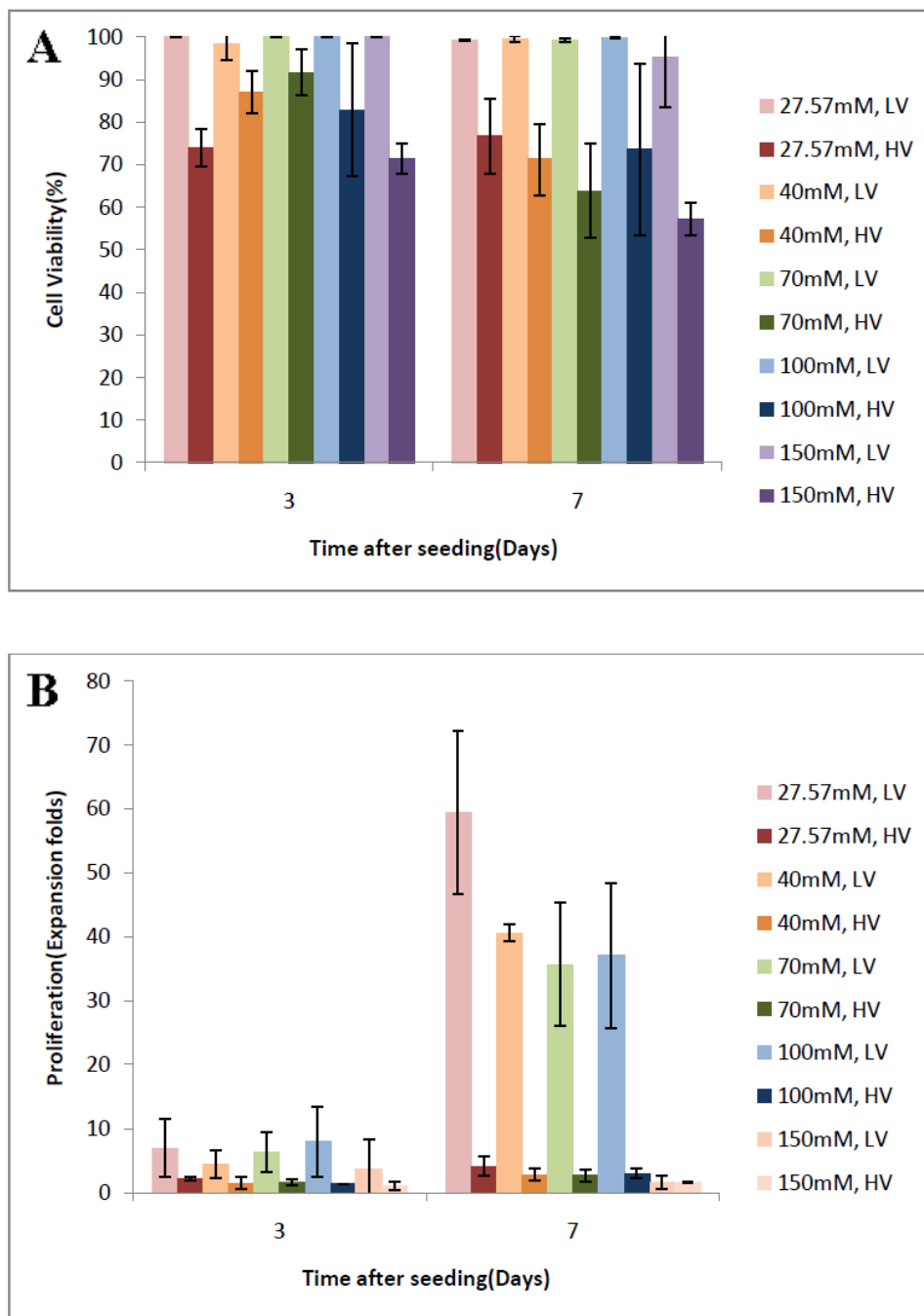


Figure 4-8 Viability (a) and proliferation (b) of K562 cells in different alginate hydrogels. Initial cell seeding density was 5×10^5 cells/ml

As predicted by the mechanical properties of the alginate hydrogel, LV alginate yields higher viability ~ 100% at most concentrations of Ca^{2+} crosslinking density through the first 7 days (Figure 4-8a). Fold expansion of cells in LV alginate achieved at day 7 was approximately 30x higher than those cultured in HV alginate (figure 4-8b), even though the estimated doubling time averaged over 7 days for LV alginate was around 30-31 hrs, which is comparable to that of cells grown in HV alginate. Cells in LV alginate appear to sustain longer cell proliferation, while cells cultured in HV alginate reached a growth plateau before day 7 (Figure 4-3). This phenomenon, together with the shorter lag time observed in LV alginate explains for the higher fold expansion of cells cultured in LV alginate at day 7. Contrary to alginate components, Ca^{2+} concentration did not seem to significantly affect the cell proliferation, except for 150mM concentration of Ca^{2+} crosslinking, which hamper the proliferation of K562 cells in both HV and LV alginates. Cell viability in high Ca^{2+} (>100mM) were also reduced, especially in HV alginate.

4.4 Discussion

In this chapter, we studied the biological response of K562 cells cultivated in Ca-alginate hydrogel. More specifically, we were interested in quantifying the overall cell survival and growth over a short-term culture (2 weeks) and drew comparisons to *in vitro* behaviors typically observed on a standard TCP culture. Through microscopic examination, we observed their time-lapsed behaviors in movement and cellular interactions in both 2D and 3D culture settings. We quantified cell proliferating capacity by obtaining cell growth curves and estimating their doubling times in each setting.

Differences in cell proliferation between 2D and 3D culture are clearly attributed from the different nature of cell microenvironments provided in each culture setting. Cells suspended freely in medium (2D culture) presented high mobility where clusters of cells are immediately formed within hours after seeding and hence, cell expansion begins rapidly. In 3D culture, cells are singly suspended inside the gel matrix and do not form direct cell-cell contact as readily due to mechanical resistance in the gel matrix. Therefore, cells cultured in 3D hydrogel tend to take a much longer time to adapt to their microenvironment, exhibiting a longer lag phase than 2D cultures. However as the cells begin to proliferate, close cell-cell interaction is facilitated in 3D culture and more space for expansion is available compared to the 2D environment. As a result, their proliferation was maximized and these cells were able to reach high growth rate with doubling time close to leukemic cells exhibited under *in vivo* condition. Growth profiles in 3D cultures appeared less dependent on the seeding density as seen in 2D culture. Greater surface-area-to-volume ratio presented in the 3D culture is another reason for longer sustenance of cellular growth observed in 3D hydrogels than in 2D TCP cultures. Healthy cell growth and sustained viability up to 2 weeks observed in 3D Ca-alginate hydrogels suggest that there are minimal restrictions to solute-waste exchange within the hydrogel matrix [134]. Diffusion coefficients of small solutes (O_2 and glucose) were calculated as high as $6 - 14 \times 10^{-6} \text{ cm}^2/\text{s}$ in 1.5% alginate [134].

Despite the limitation in maintaining good cell viability during the first week, Ca-alginate hydrogel presents subtle mechanical cues to the regulation of cell behaviors in a representative 3D manner. Cells cultured in 3D alginate system exhibited an expansion of the progenitor pool ($CD34^+$) which is in agreement with those found in the bone marrow

from CML patients [149]. As with the differentiated pool, the cell phenotype showed high proportion of granulocytic and megakaryocytic series [149] which is also similar to that expressed in 3D culture. These observations are in contrast to the typical cell behaviors observed in 2D TCP cultures as the latter skews differentiation of K562 cells toward the erythroid lineage. Cellular behaviors observed in 3D hydrogel cultures show greater resemblance to observations *in vivo* and supports the idea that 2D culture is likely to misrepresent the subtle mechanical signals thus affecting leukemic cell proliferation and differentiation.

In optimizing the hydrogel bead preparation, our data indicated that greater expansion capacity can be achieved using smaller sized beads by maximizing the cell-surface contact to volume ratio, increasing the efficiency of fluid exchange. Moreover, such culture systems are much more practical for cultivating cells in bioreactors allowing greater ease for scale-up. Concentration of alginate should be kept at low amount (1%) to provide more rooms for cell expansion.

We observed that LV alginates were more favorable for cell survival and proliferation than HV alginates. Rounded morphology of the cells is still maintained in 3D hydrogel of LV alginate compared to those in HV alginate, implying lower mechanical stress and lesser confinement of cells in LV alginate hydrogels. As a result, clumps of cells cultured in LV alginate appear more even and in oval shape. On the contrary, with a stiffer matrix in HV alginate hydrogels, cell expansion is more restricted, and the clusters tend to elongate along the bead radii. Clusters of K562 cells therefore appeared wedge-shaped in HV alginate hydrogels.

Low viscosity alginate (yielding matrix of 4-6KPa stiffness) revealed an evidential increase in cell proliferation compared to HV alginate. At this time, it is still not known to us whether the improved cell survival and growth in LV alginate is triggered by molecular signals from mechanotransduction or simply a space-advantage of the LV alginate matrix. It seems from the study that softer structure with matrix stiffness close to the native adipose tissue is more favorable for leukemic cell proliferation while increased matrix stiffness causes cell apoptosis/differentiation/de-differentiation. The underlying mechanism remains unclear. Nevertheless, by introducing tunable mechanical signals, Ca-alginate presents potentials in mimicking different niches within the native bone marrow environment.

4.5 Conclusion

Ca-alginate hydrogel was shown as an effective platform to support cell proliferation and differentiation of K562 cells as those observed *in vivo*. Cell proliferation rate was maximized, achieving average doubling time of 26 hours regardless of initial cell seeding density. Population phenotype also exhibited heterogeneity, representing characteristics of all four myeloid lineages. In optimizing the hydrogel preparation, we found that small beads (<2 μ m in diameter) made of 1% alginate and the use of LV alginate is more advantageous to the cell proliferation. However, utilizing HV alginate might be desirable to investigate the role of mechanotransduction in erythroleukemic cells, which was shown to potentially play an indispensable part in controlling the cell proliferation and differentiation. For studies on cell-ECM interactions, it is therefore imperative to develop

a realistic 3D scaffold that introduces appropriate mechanical signals as what are present in the native bone marrow environment.

Chapter 5

Role of cell-ECM interactions

Incorporation of proteins within the Ca-alginate hydrogel makes it possible to recreate special ‘niches’ mimicking the bone marrow microenvironments. This chapter explores the effects of soluble proteins entrapped in hydrogel matrix in the regulation of erythroleukemic cell behaviors *in vitro*. The proliferation and differentiation of K562 cells will be investigated in more details with comparison to a 2D control system.

5.1 Introduction

We know that ECM plays an active role in directing cellular activities and that the cell surface contains receptors that respond to extracellular signals. As soon as ligand–receptor interaction is established, the biochemical machinery involved in the control of gene expression begins. The understanding of cell differentiation and functions therefore begins from a thorough knowledge of cell–cell and cell–extracellular matrix (ECM) communication mechanisms.

There are at least two main pathways by which the ECM can affect cell behavior. One is via the mobilization of growth or differentiation factors, which modulates cell proliferation and controls cell phenotype [150]. The other is via receptor-ligand binding in cell-ECM interactions, which directly modulate cell functions as the receptor-mediated signaling pathways become activated.

The identification of cell binding sites within extracellular molecules is thus a key step toward identifying the mechanisms of cell-ECM interactions. These molecules consist of non-integrin and integrin receptors. As soon as ECM molecules bind to their specific receptors, cytoplasmic domain changes its morphology, leading to changes of the cytoskeleton at focal adhesion sites. This attachment occurs rapidly (within minutes) as a result of increased avidity rather than increased expression [151]. Finally, an assembly of focal contact proteins occurs with other intercellular components, such as phosphorylated proteins. These changes promote cytoskeleton rearrangement, which in turn determine differential interactions of chromatin and nuclear matrix at the nuclear level.

This chapter explores cell-ECM interactions in a replicated *in vitro* 3D bone marrow environment, specifically we were interested in looking at interactions with whole native soluble proteins and how they affect cellular behaviors in 3D. From that, we provide more insights into the regulatory affect of ECM to the proliferation and differentiation of leukemic cells.

5.2 Materials and Methods

5.2.1 *Experimental design*

In this study, we aim to look at the effects of three ECM proteins (FN, LN and Col I) to the cell behaviors in terms of cell proliferation and differentiation. Therefore, cell proliferation will be quantitatively measured by a metabolic assay. The differentiation behaviors of the cells will be traced by morphological changes presented in Wright-giemsa stained cells and the expression of the cell surface markers. Markers of different blood cell lineages including GPA, CD71 (erythroid specific), CD13 (common myeloid), CD14 (monocyte), CD 41 (megakaryocyte), and CD16 (neutrophil) will be quantitatively measured by flow cytometry and visualized by fluorescence microscopy.

5.2.2 *Materials*

Sodium-alginate, CaCl_2 and phosphate buffered salt (PBS) powder were all purchased from Sigma Aldrich. A 0.10 M CaCl_2 solution was prepared by dissolving CaCl_2 powder in ultrapure water with 0.01% Tween-20 and 10mM HEPES. Alginate solutions were prepared by dissolving 1.1% Na-alginate in PBS and then adding 2% gelatin solution (Sigma Aldrich) at ratio 19:1 to obtain mixture of 1% alginate and 0.1% gelatin. Hydrogels containing ECM proteins were prepared by adding each protein into the cell-alginate mixture prior to the gelation step. All ECM proteins namely collagen-I, fibronectin, and laminin (Sigma Aldrich) were diluted to a working concentration of 0.1%.

5.2.3 Cell encapsulation

Cells were resuspended in 1 ml of alginate-gelatin mixture at concentrations of $1-5 \times 10^5$ cells/ml. Assays of 96-well plates were prepared by adding 100 μ l CaCl_2 solution to each well and the cell-alginate mixture was dropped from the height of 3 cm through a 25G needle into wells containing CaCl_2 solution. Cell-encapsulated gels were solidified within 5 mins after contact with CaCl_2 forming spherical beads of 2.1 mm in diameter, one bead per well. The cell-encapsulated beads were then carefully washed thrice with sterile PBS before cell culture. All the above reagents were sterilized by autoclaving and/or filtering through 0.2 μ m membrane prior to use.

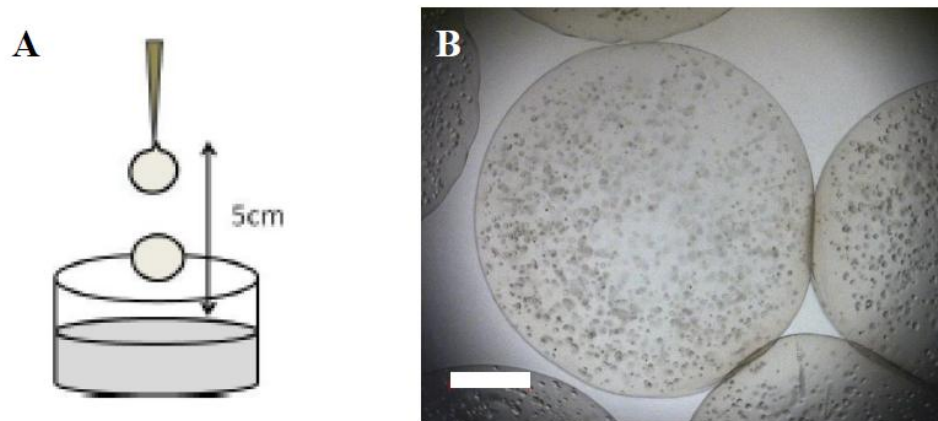


Figure 5-1 Process of making alginate hydrogel. (a) Cell-suspended alginate solution was dropped from the height from 5cm to the CaCl_2 bath in the preparation of Ca-alginate hydrogel, (b) micrograph of the hydrogel bead. Scale bar 500 μ m.

5.2.4 *Cell culture*

Human leukemic K562 cells (ATCC) were cultured in a 75 cm² tissue culture polystyrene (TCP) with Iscove's Modified Dulbecco's Medium (IMDM; Invitrogen) supplemented with 10% fetal bovine serum (FBS; Hyclone) and 1.5g/l sodium bicarbonate (Sigma Aldrich) according to ATCC formulation. Encapsulated cells for the 3D culture were cultured in 96-well plates containing the same media as stated for the 2D TCP culture. Cells were cultivated at 37°C in a fully humidified 5% CO₂ incubator for up to 2 weeks. Cell cultures were monitored daily on the light microscope and a change of media was performed every two days.

5.2.5 *Cell proliferation assay*

Assays were performed in 96-well plates, containing K562 cells cultured either in 2D plates or 3D hydrogels. Cell proliferation was quantitatively assessed by a highly stable WST assay (Cell Counting Kit-8; Dojindo), which uses tetrazolium salt WST-8 (2-(2-methoxy-4-nitrophenyl)-3-(4-nitrophenyl)-5-(2,3-disulfophenyl)-2H-tetrazolium, monosodium salt). WST-8 is bio-reduced by cellular dehydrogenases to an orange formazan product that is soluble in tissue culture medium. Assay plates were incubated for 2h at 37°C and 5% CO₂. Absorbance was measured at 450 nm. A standard curve was constructed by plotting absorbance of known cell numbers for calculating the number of viable cells in assay.

5.2.6 *Cell morphology*

For a morphological analysis and hematological identification of the K562 cell population, cultured cells were washed, cytopun and stained in Hemacolor® (Merck Chemicals), a rapid Wright-Giemsa based staining solution kit, air-dried and visualized

under the microscope. The bead dissolution buffer contains 50 mM tri-sodium citrate dehydrate, 77 mM NaCl and 10 mM HEPES (Sigma Aldrich).

5.2.7 Flow cytometry

Surface expression of different lineage-specific markers on K562 cultured cells were analyzed by Epics-Altra (Beckman Coulter) flow cytometer, equipped with a 488 nm Argon laser. At each passage, $0.5-1.0 \times 10^6$ cultured cells were harvested and incubated with directly labeled anti-human CD34, CD38 (common stem cell markers); GPA, CD71 (erythroid); CD13, CD16b (granulocytic); and CD41b and CD42b (megakaryocytic) (BD Bioscience). CD34, GPA, CD42b and CD16 were pre-conjugated with fluorescein isothiocyanate (FITC); CD38, CD71, CD41 and CD13 were pre-conjugated with phycoerythrin (PE). Staining buffer contains 2% FBS and 0.1% sodium azide (Sigma Aldrich). Matched isotype controls were used for gating and analysis.

5.3 Results

5.3.1 Enhanced proliferation of cells cultured in 3D with fibronectin and laminin

K562 cells exhibited different behaviors in the presence of common ECM proteins such as Col, FN and LN. Firstly, higher expansion was found in 3D versus 2D for cultures incorporated with FN or LN (Figure 5-2); suggesting that there is an enhanced cell-ECM interaction in 3D with FN and LN that could have induced cell proliferation. Presence of LN enhanced cell proliferation by ~100% greatest at day 9 while that achieved in presence of FN was ~50% as compared to their control 3D protein-free cultures (Figure 5-

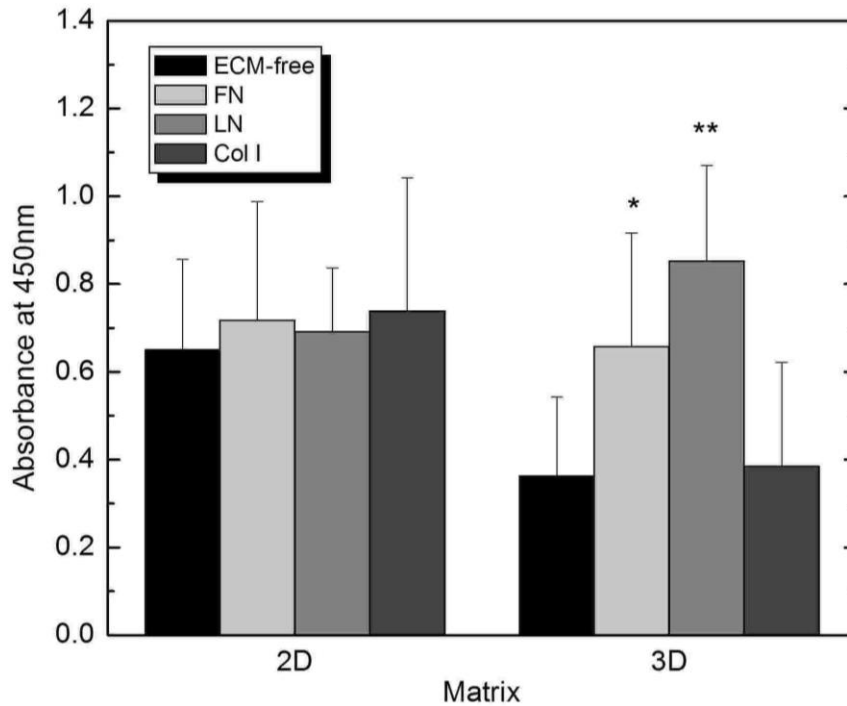


Figure 5-2 Cell proliferation in 2D TCP vs 3D alginate hydrogel cultures as measured by WST assay (a) at different initial seeding density from 1-5E5 cells/ml; (b) with added ECM proteins of 10 µg/ml at day 9 (FN – fibronectin, LN – laminin, Col I – collagen type I); data are represented in absolute absorbance and compared with the ECM-free control sample (* $p_value < 0.01$, ** $p_value < 0.001$); initial seeding densities were 2E5 cells/ml for both 2D and 3D cultures. Note that when started with the same initial seeding density, the actual cell number in 2D culture at day 0 was approximately 20 times as high as in 3D culture.

2). No changes in cell proliferation were observed in substrates containing Col-I for both 2D and 3D systems (Figure 5-2).

5.3.2 *Cell-ECM interactions exhibit a dose-response relationship*

Figure 5-3 shows the quantitative effects of FN, LN and Col-1 to cell proliferation of K562 compared with ECM-free control. It is shown that FN&LN exerted similar effects on K562 cells, i.e. reduce cellular activity between day 5 – 7 but enhance cellular activity at day 9. No significant changes were observed in Col culture except for day 9 with concentration of 5 µg/ml. The most effective concentration for all three ECM proteins was 5 – 10µg/ml.

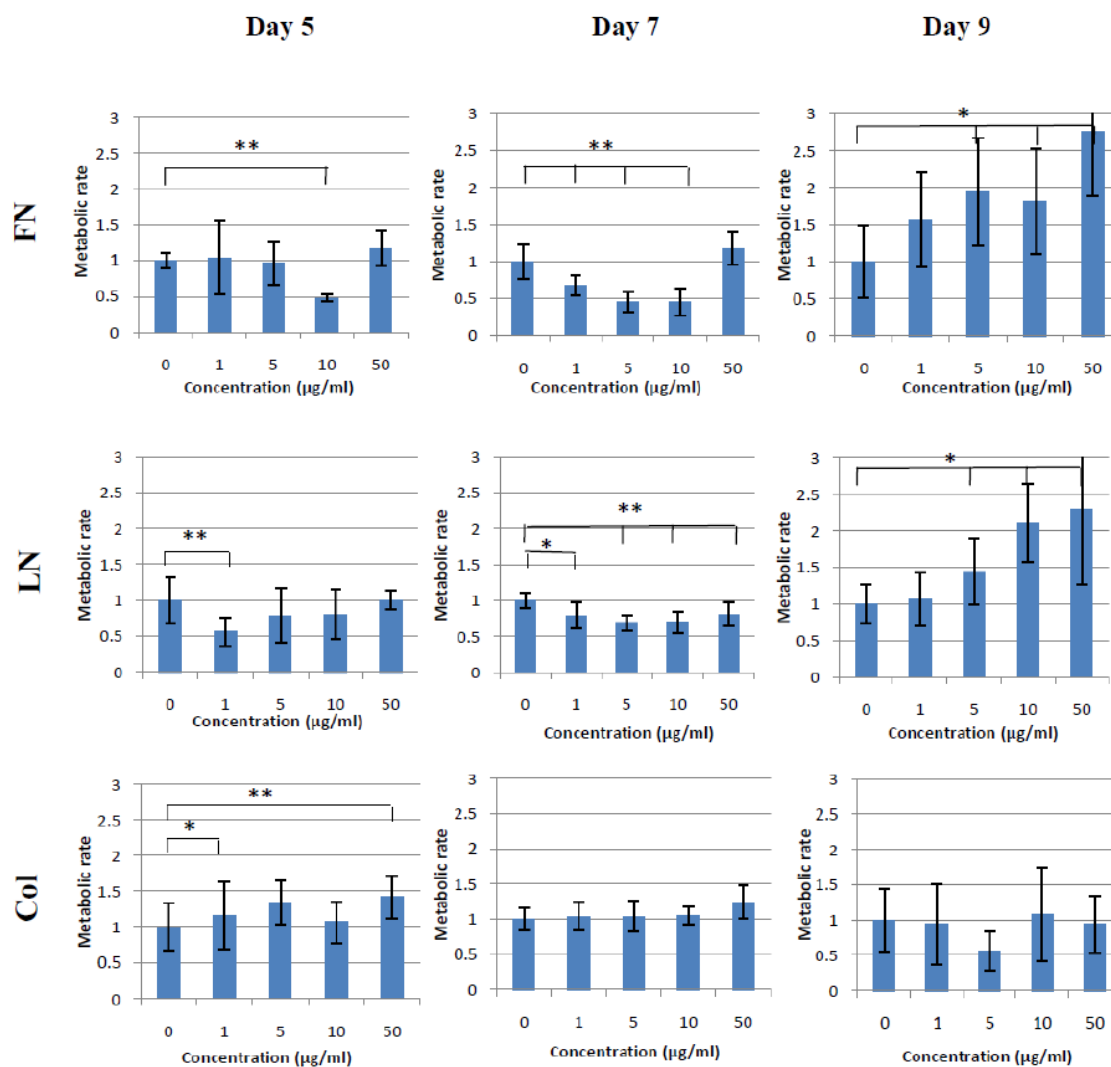


Figure 5-3 Metabolic rate of K562 cells in different ECM cultures: fibronectin (FN – top), laminin (LN – middle) & collagen (Col - bottom). Data are normalized and compared with control of ECM-free culture. *p_value < 0.05, **p_value < 0.01

5.3.3 *Effects of ECM proteins on cell maturation*

To trace K562 cell differentiation, flow cytometry was performed for surface markers of different hematopoietic lineages (GPA/CD71 for erythroid, CD13/CD16 for granulocytic, CD14 for monocytic and CD41/CD42 for megakaryocytic lineages). In the control 2D flask culture, 70% of cells expressed GPA⁺, 90% CD71⁺, <20% CD16⁺, 20% CD41b⁺ but few cells expressed markers of late granulocytes CD13⁺ and megakaryocytes CD42b⁺ (Figure 5-4d). Among the whole population, which consists mainly of erythrocytic progenitors in 2D, 27% of the erythroid cells were early GPA⁻CD71⁺ and 65% were immature GPA⁺CD71⁺ (Figure 5-4a). In contrast, culture of K562 in alginate hydrogel induced the spontaneous differentiation of K562 cells to both granulocytic and megakaryocytic lineages (Figure 5-4d) while a loss of late erythroid marker (GPA) appeared evident. Increased proliferation of early erythroid progenitors was still observed in 3D cultures and the GPA⁻CD71⁺ counts were higher (~63% population) compared to the freshly thawed K562 cells (Figure 5-4a); however, a small fraction differentiated to mature erythrocytes (~8% population of GPA⁺CD71⁻ compared to 4% in 2D culture). No expression of monocytic CD14⁺ in both 2D and 3D cultures (data not shown).

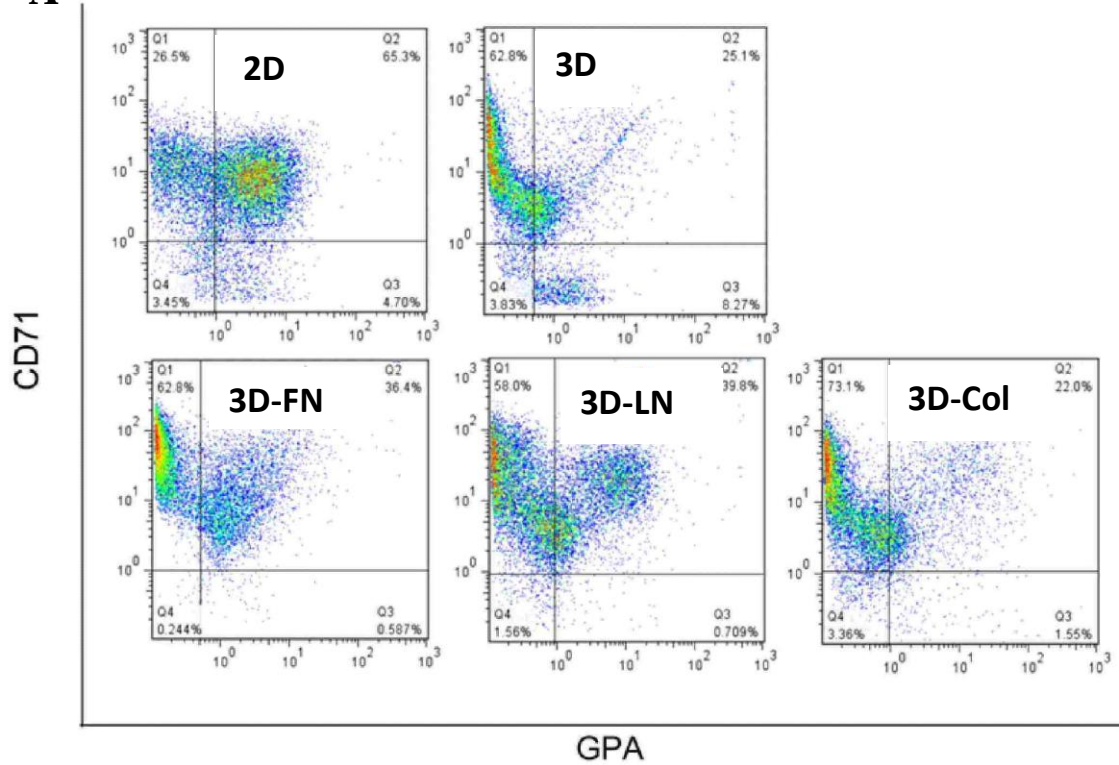
The addition of FN, LN or Col-I further induced the differentiation of K562 cells to specific lineages while they were inhibited in others (Figure 5-4). As with FN and LN, the most prolific lineage was of megakaryocytic (60% matured CD41⁺ megakaryocytes compared to 20% in protein-free samples). Differentiation of K562 cells toward erythrocytic and granulocytic lineages was evident but mostly early progenitors were present; no matured GPA⁺CD71⁻ erythrocytes and CD16⁺CD13⁻ granulocytes were found in these culture samples (compared to 6-8% in 3D culture alone). Col-I, on the other hand,

maintained the immature granulocyte phenotype of K562 as in 3D protein-free culture while no differentiation toward the megakaryocytic and erythroid lineages was observed. No matured GPA^+CD71^- erythrocytes and $CD16^+CD13^-$ granulocytes were found in Col culture either.

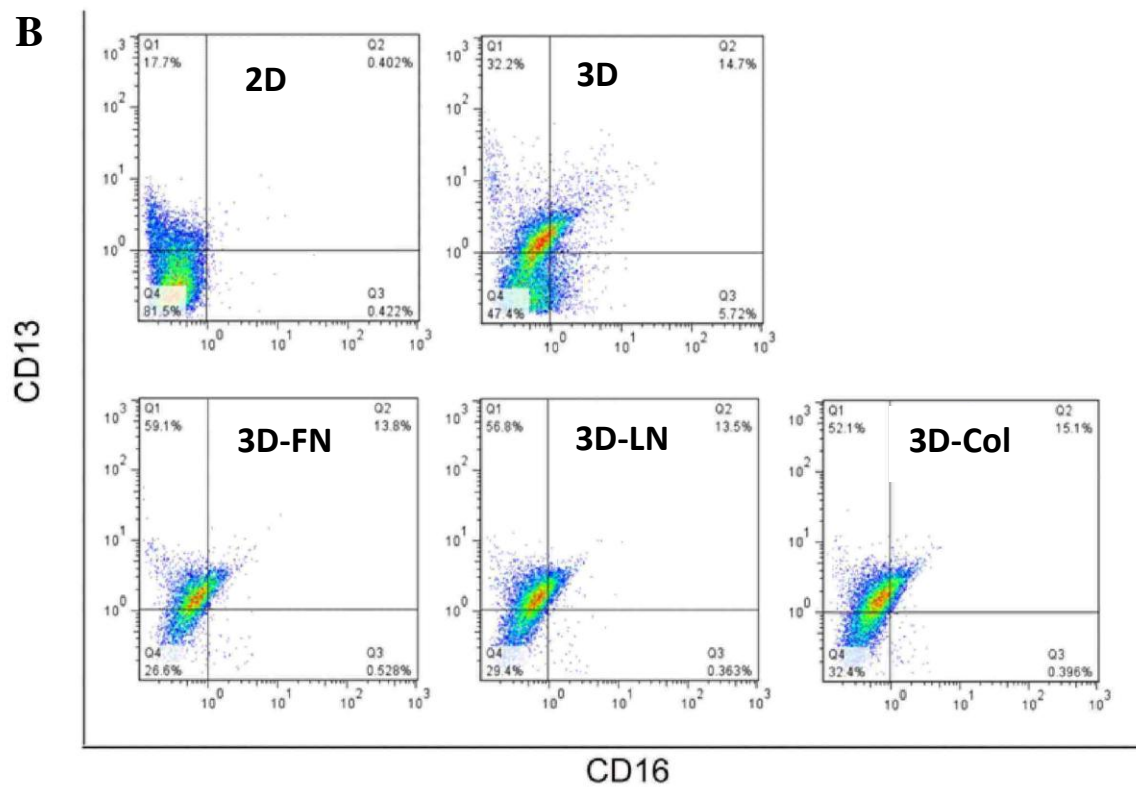
Wright-Giemsa staining of K562 cells confirmed the unique phenotypic characteristics of the cells cultured in different conditions (Figure 5-5). Mature neutrophils were found in presence of collagen. FN and LN appeared to have a greater tendency to induce K562 to the megakaryocytic lineage. Morphological observations concur with our flow cytometry data.

We also monitored the expression of surface integrins responsible for the cell adhesion to ECM (CD49b for Col-I, CD49e for FN and CD49f for LN). Figure 5-6 shows the percentage of positive cells with these surface markers within K562 population cultured in 2D and 3D structure, with/without ECM proteins. It was found that integrin $\alpha5\beta1$ (CD49e) did not significantly change over time. Day 9 marks a significant decrease in CD49b ($\alpha2\beta1$) & CD49f ($\alpha6\beta1$) in all 3D cultures. Interestingly, FN shows the same trend with LN, which is in agreement with the metabolic profile of K562 while Col and ECM-free cultures share the same pattern. Integrin expression does not appear to be correlated to cell-ECM interactions but may be indicative of cell differentiation. Decreased expression of certain integrins would be the indication of cell maturation, as cells are released from their current niche and undergo migration to another.

A



B



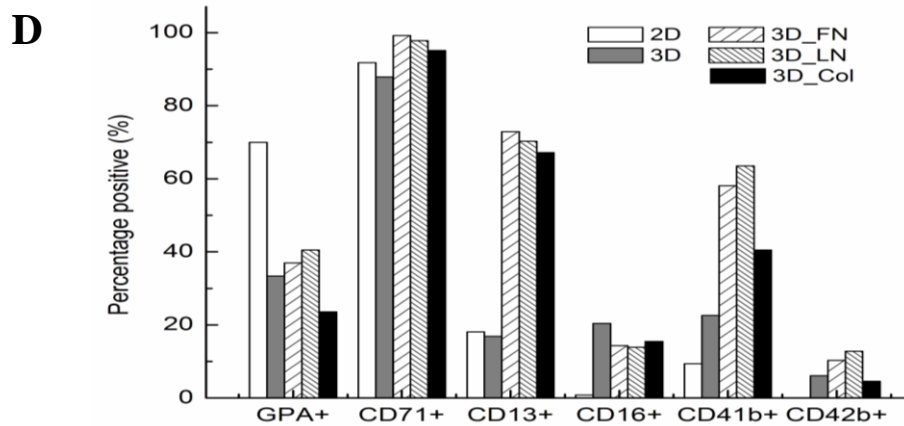
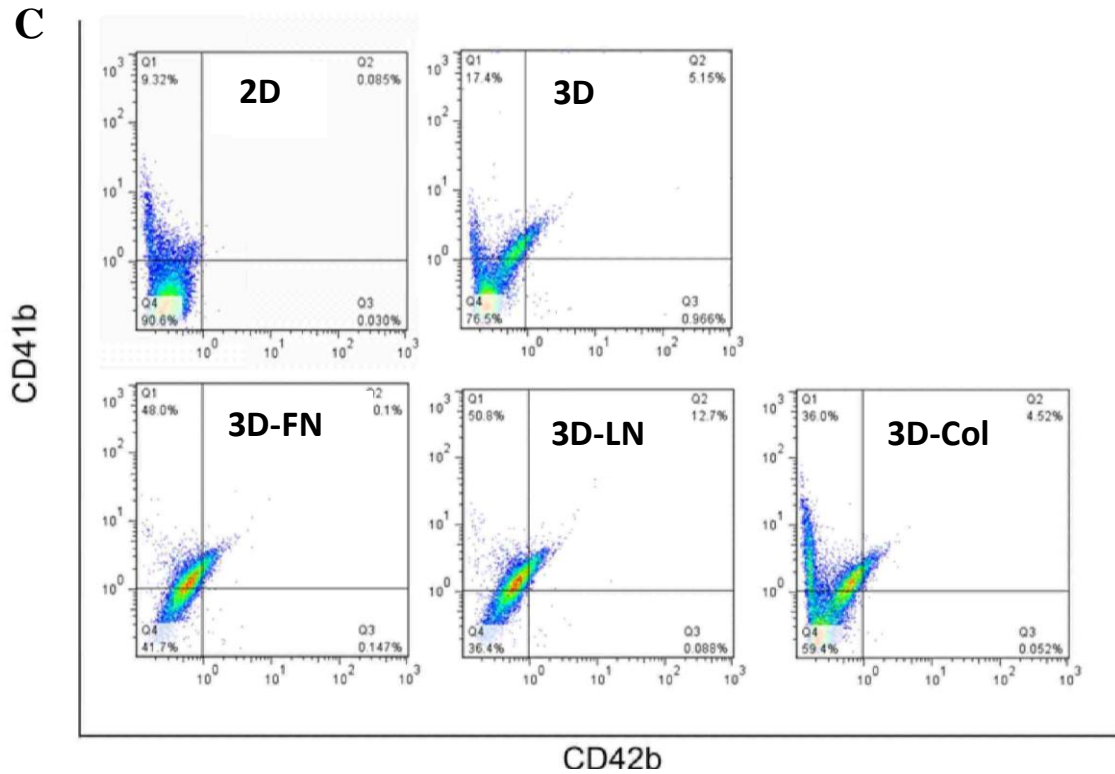


Figure 5-4 Results of Fluorescence-Activated Cell-Sorting analysis of lineage-specific marker expression. K562 cells were grown up to day 14 in 2D vs 3D cultures with/without ECM proteins. Markers of (a) erythroid, (b) granulocytic and (c) megakaryocytic lineages. (d) Summary of percentage of positive cells expressing specific-lineage markers. Gating was done based on corresponding same isotype controls.

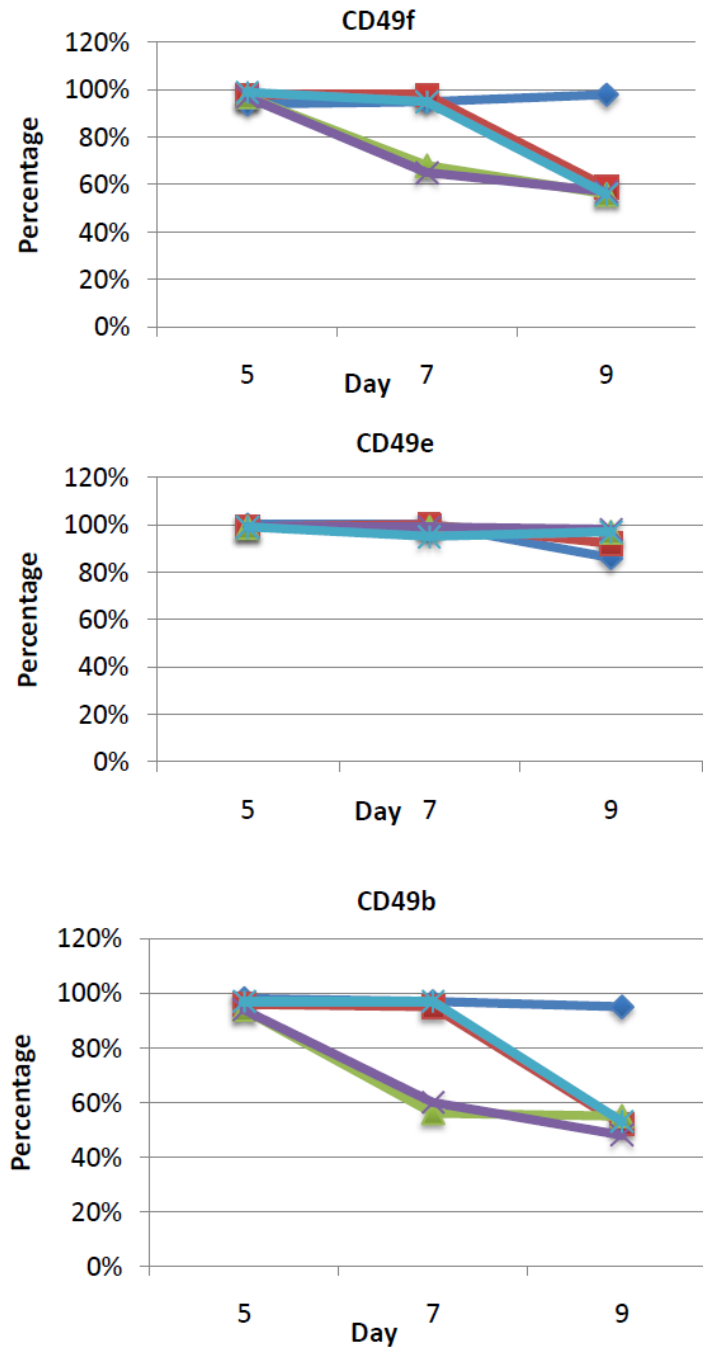


Figure 5-5 K562 expression of $\beta 1$ integrins over time as analyzed by FACS. Data are represented by percentage of cells expressing positive degree of integrins with respect to corresponding isotype controls. 2D —, 3D —, FN —, LN —, Col —

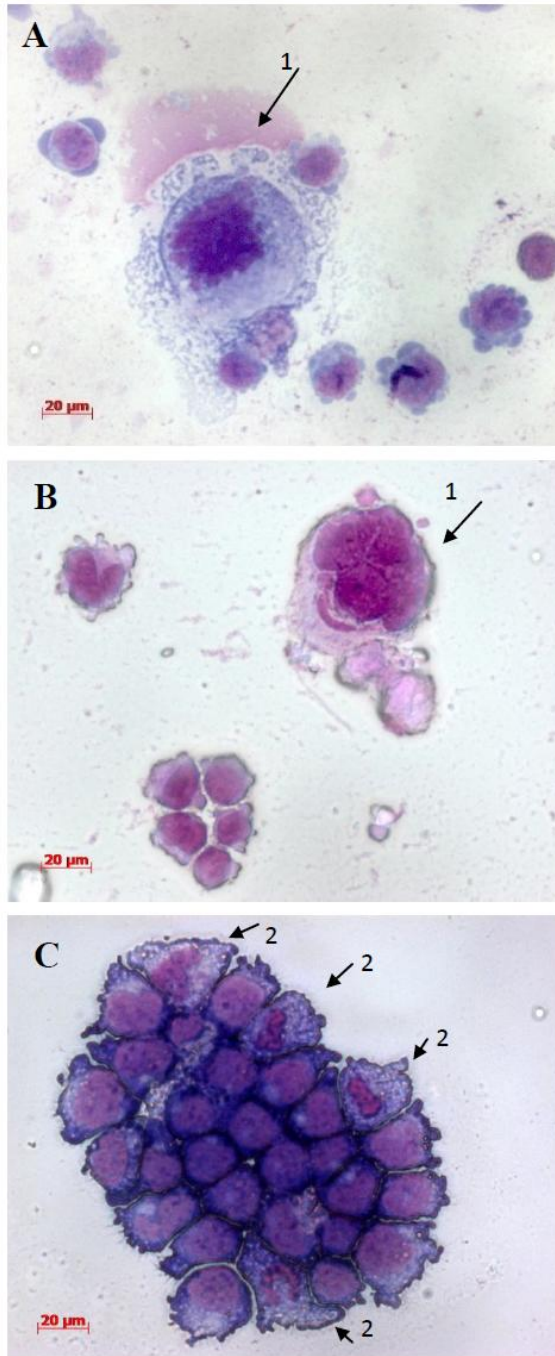


Figure 5-6 Micrographs of Wright-giemsa stained K562 cells cultured with different ECM proteins [148]. Pictures were taken after 7 days culture.(a) FN, (b) LN, (c) Col I. (1) megakaryocyte, (2) neutrophilic band cells.

5.4 Discussion

Covalently-conjugated proteins and peptides on various scaffolds including those of alginate hydrogels [152, 153] were extensively used to study specific cell-ECM interactions. These studies furnish the understanding of specific protein/peptide sequences and their active role in cell-ECM interactions. However, in this study, we are interested in the interaction of free unmodified proteins in a 3D *in vitro* environment. Proteins entrapped in the matrix are present in soluble form, thus exhibiting its natural conformation which is believed to expose more binding sites for cells. Proteins in 2D cultures physically adsorb onto the surfaces of TCP but the presence of other proteins can induce desorption of proteins from these surfaces. On the other hand, in 3D alginate system, diffusional coefficient of high MW protein in 1.5% alginate is low, in the range of $5-7 \times 10^{-8} \text{ cm}^2/\text{s}$ and does not change over 90 days [154]. With a small pore size of $<5 \mu\text{m}$ on the gel surface, it is postulated that entrapped proteins would stay inside the matrix for long-term culture.

As a general observation, interaction of leukemic cells with ECM proteins appeared more enhanced in 3D hydrogel than 2D cultures. Based on our argument of greater receptor presentation and prolonged entrapment, K562 cells cultured in FN and LN indeed showed better growth in 3D than in 2D cultures as a consequence of enhanced cell-ECM interaction. The impact of FN and LN was not significant in the first 7 days but appeared more profoundly afterwards with protein concentrations of higher than $5 \mu\text{g}/\text{ml}$. These leukemic cell behaviors resemble the trends found in its normal counterpart, where interaction with FN and LN enhance proliferation of more primitive CD34^+ HSC

population [76, 77, 86-88]. Observations on the effects of Col on leukemic cells are so far consistent with those observed in normal hematopoietic cell behaviors, which showed no significant effects on cell proliferation.

The multipotential nature of K562 cells to differentiate toward erythroid, megakaryocytic and granulocytic lineages in the presence of various inducing agents has been extensively studied *in vitro* [31, 33, 155]. So far no one has considered quantifying the effects of ECM proteins on leukemic/hematopoietic cell differentiation and this may likely be due to the fact that no such impact has been significant in 2D TCP cultures, as we have shown here. Yet when we begin to culture these cells in a 3D matrix, spontaneous differentiation of K562 cells was observed both in the presence or absence of ECM proteins. Here we take a closer look at the impact of each ECM protein on myeloleukemic cell differentiation potential under a 3D microenvironment, FN and LN were able to induce the leukemic cells to differentiate toward megakaryocytic lineage, which most probably involve the activation of ERK/MAPK pathway as other megakaryocytic-inducing factors do [135, 156]. For Col-I, culture in 3D did not enhance leukemic cell growth, just as normal HSCs [91]. However, it is for the first time documented here that the presence of Col-I is able to induce K562 cells to differentiate toward some granulocytic lineages such as neutrophilic band cells, and observed only in 3D cultures. In the absence of any ECM protein, spontaneous differentiation of K562 cells was also observed. We suggest that a possible role in mechanotransduction on cell differentiation could occur, but further studies will be required to verify this hypothesis. The 3D Ca-alginate hydrogel system presents an opportunity to study the contribution of

cell-cell and cell-ECM interactions in a more realistic *in vivo* mimicking microenvironment

Findings on the cell-ECM protein interactions provided interesting information to leukemic cell behaviors. Researchers have found an abnormal trafficking of primitive CML progenitors towards the basement membrane component LN [127, 129], which is now shown to be favorable to the cell proliferation in 3D. Mechanisms of these interactions remain unclear; nevertheless, the mechanotransduction theory on cell-ECM interactions revealed that FN and LN both shared common MAPK/JNK1 pathway [157] which can transduce signals for differentiation and inhibition of apoptosis in the hematopoietic system [138, 158]. This may explain for the analogous increased proliferation and skewed differentiation of K562 cells in cultured with FN and LN. This study has provided strong evidences in the high dependency of leukemic cells to both the biochemical and mechanical aspects of its surrounding microenvironment.

5.5 Conclusion

The 3D Ca-alginate hydrogel system showed more supportive hematopoietic activity for K562 cells over traditional 2D TCP in terms of cell growth and differentiation. Enhanced cell-ECM interactions achieved in the 3D hydrogel appear to play a role in cell fate decisions, altering proliferation and differentiation of the erythroleukemic population. For example, cell interactions with FN and LN enhance cell proliferation and trigger its maturation to megakaryocytes; Col-I seems to skew the cell differentiation to granulocytic lineage but does not have a significant effect on cell proliferation. Each component in the ECM thus project distinct roles in directing stem cell fate; however, the interactions seem

independent from the expression of integrin molecules. Integrins appear to be activated during differentiation process, and it is predicted to be more important in regulating cell migration *in vivo*. Future studies might focus on the molecular pathways that modulate the whole development process. After all, Ca-alginate hydrogel present many opportunities in creating inductive environment for cell proliferation and differentiation. Hence, the use of this system will pave the way for studying 3D cell interactions of both hematopoietic and leukemic stem cells in the future.

Chapter 6

Conclusions

In this thesis, we reported the initial use of Ca-alginate hydrogel as a 3D cell culture model for studying leukemogenesis *in vitro*. We interrogated the mechanical properties of different alginate hydrogels, ability of the hydrogel in supporting the cell development, and 3D reconstruction of ECM matrix to emulate cell-ECM interactions in the bone marrow. Here, we summarize important findings implicated from the entire study.

6.1 Mechanical properties of Ca-alginate hydrogel

Ca-alginate hydrogel offer many opportunities for recapitulating the native bone marrow environment. Structurally, it resumes the space-filling function of adipose tissue within the bone marrow that few materials can do. Within the hydrogel, high number of wedges or pores present provides individual niches specifying special signals for the encapsulated cells. It was shown in the study that the hydrogel architecture and mechanical strength is tunable by modifying the constitutive components consist of alginate. The alginate molecular structure such as M:G ratio and MW weight of the monomers will determine the crosslinking capability and hence the elastic modulus of the resulting hydrogel. On the

other hand, by altering Ca^{2+} ion concentrations, cross-linking density is finely tuned while surface topography changes accordingly. These matrix characteristics highly affect the subtle behaviors of erythroleukemic cells, most probably by the mechanotransduction pathway. Nevertheless, defined characteristics of the natural bone marrow environment have yet to be elucidated; hence experimental models would mainly rely on the behavioral characteristics of the cells.

6.2 Three-dimensional Ca-alginate as a platform for cell development

It was shown from this study that alginate hydrogels are superior in supporting cell proliferation and differentiation of erythroleukemic cells than a 2D culture. However, LV alginate hydrogel yielded better cell survival and expansion than that from HV alginate. The cause of cell death in HV alginate hydrogel during the first week of culture is currently not known, but could be due to unfavorable conditions or mechanical stress from the alginate hydrogel. While Ca^{2+} crosslinking concentration did not significantly affect cell proliferation, proliferation and spontaneous differentiation of cells were promoted in HV alginate hydrogel. These observations suggest the role of mechanotransduction in controlling hematopoietic cell fate. Scaffolds, which introduce appropriate mechanical signals, are therefore imperative in recreating the natural environment in hematopoiesis.

6.3 Study of cell-ECM interactions

As ECM was shown to be crucial for the maturation of the erythroleukemic cells just as in normal hematopoiesis, findings suggested that the abnormal components of ECM inside

the bone marrow might facilitate their aberrant behaviors. Cell expansion in our 3D bone marrow mimicry appeared to be limited within the progenitor pool and did not change in the presence of ECM proteins. On the other hand, FN and LN can induce further differentiation to megakaryocyte, and to a lesser extent to granulocytes and erythroblasts while Col-I directed cells more toward neutrophilic lineage. An imbalance of these proteins can therefore result in the arrest of immature hematopoietic cells at different stages of differentiation. This study emphasized that the regulatory role of cell-ECM interactions to cell proliferation and differentiation in leukemogenesis must be made in an appropriate culture environment as no observations were made in 2D cultures. However, we do not know whether it is practical to use ECM to suppress the leukemogenesis *in vivo*. The observations expose a possibility of reconstructing the bone marrow niche for improving prognosis of leukemia. Further studies are required to unravel the complex interplay and contributions of cell-ECM interactions.

6.4 Limitation

One of the major limitations of this study is the inability to measure the amount of proteins retained within the matrix as well as those that have actual interactions with the cells due to the interference of other proteins present in the culture medium. There is evidence that free proteins are readily released from the matrix without cells up to 80% within the first 24 hours [159] while in another study, diffusion coefficient of large protein IgG (155KD) was found to be $\sim 6 \times 10^{-7} \text{ cm}^2/\text{s}$ and remain unchanged during 60 day period [160]. Nevertheless, it is evidential in this study that cell interactions with matrix proteins presented in the alginate hydrogel do affect cell behaviors; such interactions may

serve to retain ECM proteins within the hydrogel matrix. However, the actual amount of those proteins remains unknown. Quantification of these interactions is therefore limited, making it difficult to depict the differences and similarities between our model and the *in vivo* environment.

6.5 Future work

As studying the leukemic cell behaviors in an inductive *in vitro* Ca-alginate system, questions regarding the underlying mechanisms become relevant. Future work would therefore be focus on the quantification of proteins which are retained in the matrix and interact with encapsulated cells. Results from these findings might be useful in comparison with other established studies on cell interactions with modified/covalently conjugated protein sequence. This information will provide us with more insight into the roles of specific protein segments to the cell growth and differentiation.

On the other hand, our model can be used to study cell-ECM interactions on other leukemic cell lines. Cell physiology characteristics such as cell cycle, molecular differential pathways might also be investigated in complement to the growth/differentiation behavior patterns of the involving cell lines. The knowledge obtained would unravel a more thorough understanding of the regulatory role of ECM on leukemia development in general.

6.6 Final Conclusions

This study proposed a model from Ca-alginate hydrogel as a platform for supporting hematopoiesis *in vitro*. Our results and observations affirm controversial questions laid

upon behavioral characteristics of leukemic cells in relation to a 3D microenvironment and mechano biology. It has also, for the first time, revealed how cell-ECM interactions of free soluble proteins with leukemic cells affected cellular function in a 3D matrix. This pioneering work draws focus to us on the underlying mechanism of mechanotransduction and cell-ECM communication to intracellular pathways that modulate leukemic cell proliferation and differentiation. It further supports our hypothesis in that cellular interactions and ECM presentation in 3D differs from that in 2D thus having profound effects atypical of those observed *in vitro* on flask cultures. Despite the fact that hematopoietic and leukemic cells are inherently non-adherent or suspension in nature, cellular interactions modulated by their physical and biochemical environment are still just as critical in cell fate decisions. The study of apoptosis in this case would also be equally relevant to unveil the nature of cell behaviors in Ca-alginate hydrogel. Finally, by utilizing the proposed 3D hydrogel model, we can engineer bone marrow like niches that would enable us to study leukemic/hematopoietic cell behaviors in their most natural environment.

References

1. Hann, I., M. Bodger, and A. Hoffbrand, *Development of pluripotent hematopoietic progenitor cells in the human fetus*. Blood, 1983. **62**(1): p. 118-123.
2. Kohli-Kumar, M., et al., *Haemopoietic stem/progenitor cell transplant in Fanconi anaemia using HLA-matched sibling umbilical cord blood cells*. British Journal of Haematology, 1993. **85**(2): p. 419-422.
3. Vowels, M.R., et al., *Correction of X-Linked Lymphoproliferative Disease by Transplantation of Cord-Blood Stem Cells*. New England Journal of Medicine, 1993. **329**(22): p. 1623-1625.
4. Wagner, J., et al., *Transplantation of umbilical cord blood after myeloablative therapy: analysis of engraftment [see comments]*. Blood, 1992. **79**(7): p. 1874-1881.
5. Pahwa, R.N., et al., *Successful hematopoietic reconstitution with transplantation of erythrocyte-depleted allogeneic human umbilical cord blood cells in a child with leukemia* Proc Natl Acad Sci USE, 1994. **91**: p. 4485-4488.
6. Issaragrisil, S., et al., *Transplantation of Cord-Blood Stem Cells into a Patient with Severe Thalassemia*. New England Journal of Medicine, 1995. **332**(6): p. 367-369.
7. NA, K., et al., *Umbilical cord blood infusion in a patient for correction of Wiskott-Aldrich syndrome*. Blood Cells, 1994. **20**: p. 245-248.
8. Ogawa, M., *Differentiation and proliferation of hematopoietic stem cells*. Blood, 1993. **81**(11): p. 2844-2853.

9. Bonnet, D., *Normal and leukaemic stem cells*. British Journal of Haematology, 2005. **130**: p. 469-479.
10. Robb, L., A.G. Elefanty, and C.G. Begley, *Transcriptional Control of Hematopoiesis*, in *Ex Vivo Cell Therapy*, S. Klaus and N. Robert, Editors. 1999, Academic Press: San Diego. p. 5-26.
11. Robb, L., et al., *Absence of yolk sac hematopoiesis from mice with a targeted disruption of the scl gene*. Proceedings of the National Academy of Sciences of the United States of America, 1995. **92**(15): p. 7075-7079.
12. Shivdasani, R.A. and S.H. Orkin, *The transcriptional control of hematopoiesis [see comments]*. Blood, 1996. **87**(10): p. 4025-4039.
13. Owen, M., *Marrow stromal stem cells*. J Cell Sci Suppl, 1988. **10**: p. 63-76.
14. Angela, C., et al., *Leukemic Cells Create Bone Marrow Niches That Disrupt the Behavior of Normal Hematopoietic Progenitor Cells*. Science, 2008. **322**(5909): p. 1861-1865.
15. Migliaccio, G., et al., *Human embryonic hemopoiesis. Kinetics of progenitors and precursors underlying the yolk sac---liver transition*. J Clin Invest, 1986. **78**(1): p. 51-60.
16. Fleischman, R.A., R.P. Custer, and B. Mintz, *Totipotent hematopoietic stem cells: Normal self-renewal and differentiation after transplantation between mouse fetuses*. Cell, 1982. **30**(2): p. 351-359.
17. Jordan, C.T., J.P. McKearn, and I.R. Lemischka, *Cellular and developmental properties of fetal hematopoietic stem cells*. Cell, 1990. **61**(6): p. 953-963.

18. Spangrude, G., S. Heimfeld, and I. Weissman, *Purification and characterization of mouse hematopoietic stem cells*. Science, 1988. **241**(4861): p. 58-62.
19. Morrison, S.J. and I.L. Weissman, *The long-term repopulating subset of hematopoietic stem cells is deterministic and isolatable by phenotype*. Immunity, 1994. **1**(8): p. 661-673.
20. Osawa, M., et al., *Long-Term Lymphohematopoietic Reconstitution by a Single CD34-Low/Negative Hematopoietic Stem Cell*. Science, 1996. **273**(5272): p. 242-245.
21. Randall, T., et al., *Expression of murine CD38 defines a population of long-term reconstituting hematopoietic stem cells*. Blood, 1996. **87**(10): p. 4057-4067.
22. Dexter, T., *Regulation of hemopoietic cell growth and development: experimental and clinical studies*. Leukemia, 1989. **3**(7): p. 469-474.
23. Damiano, J.S., et al., *Cell Adhesion Mediated Drug Resistance (CAM-DR): Role of Integrins and Resistance to Apoptosis in Human Myeloma Cell Lines*. Blood, 1999. **93**(5): p. 1658-1667.
24. Colmone, A., et al., *Leukemic Cells Create Bone Marrow Niches That Disrupt the Behavior of Normal Hematopoietic Progenitor Cells*. Science, 2008. **322**(5909): p. 1861-1865.
25. Reya, T., et al., *Stem cells, cancer, and cancer stem cells*. Nature, 2001. **414**(6859): p. 105-111.
26. Passegué, E., E.F. Wagner, and I.L. Weissman, *JunB Deficiency Leads to a Myeloproliferative Disorder Arising from Hematopoietic Stem Cells*. Cell, 2004. **119**(3): p. 431-443.

27. Moore, M.A.S. and D. Metcalf, *Cytogenetic analysis of human acute and chronic myeloid leukemic cells cloned in agar culture*. International Journal of Cancer, 1973. **11**(1): p. 143-152.
28. Minden, M., R. Buick, and E. McCulloch, *Separation of blast cell and T-lymphocyte progenitors in the blood of patients with acute myeloblastic leukemia*. Blood, 1979. **54**(1): p. 186-195.
29. Sutherland, H., A. Blair, and R. Zapf, *Characterization of a hierarchy in human acute myeloid leukemia progenitor cells*. Blood, 1996. **87**(11): p. 4754-4761.
30. Lozzio, C. and B. Lozzio, *Human chronic myelogenous leukemia cell-line with positive Philadelphia chromosome*. Blood, 1975. **45**(3): p. 321-334.
31. Tetteroo, P.A.T., et al., *Megakaryoblastic differentiation of proerythroblastic K562 cell-line cells*. Leukemia Research, 1984. **8**(2): p. 197-206.
32. Lozzio, B.B., et al., *A multipotential leukemia cell line (K-562) of human origin*. Proceedings of the Society for Experimental Biology and Medicine. Society for Experimental Biology and Medicine (New York, N.Y.), 1981. **166**(4): p. 546-50.
33. Leary, J.F., et al., *Multipotent human hematopoietic cell line K562: Lineage-specific constitutive and inducible antigens*. Leukemia Research, 1987. **11**(9): p. 807-815.
34. Tabilio, A., et al., *Myeloid and Megakaryocytic Properties of K-562 Cell Lines*. Cancer Research, 1983. **43**(10): p. 4569-4574.
35. Alder, S., A. Ciampi, and E.A. McCulloch, *A kinetic and clonal analysis of heterogeneity in K562 cells*. Journal of Cellular Physiology, 1984. **118**(2): p. 186-192.

36. Sutherland, J.A., et al., *Differentiation of K562 Leukemia Cells Along Erythroid, Macrophage, and Megakaryocyte Lineages*. Journal of Immunotherapy, 1986. **5**(3): p. 250-262.
37. Castaigne, S., et al., *All-trans retinoic acid as a differentiation therapy for acute promyelocytic leukemia. I. Clinical results [see comments]*. Blood, 1990. **76**(9): p. 1704-1709.
38. Toffoli, G., et al., *In K562 leukemia cells treated with doxorubicin and hemin, a decrease in c-myc mRNA expression correlates with loss of self-renewal capability but not with erythroid differentiation*. Leukemia Research, 1989. **13**(4): p. 279-287.
39. Goliaei, B., M. Rafiei, and Z. Soheili, *Effects of hyperthermia on the differentiation and growth of K562 erythroleukemic cell line*. Leukemia Research, 2004. **28**: p. 1323-1328.
40. Chenais, B., et al., *Time-course of butyric acid-induced differentiation in human K562 leukemic cell line : Rapid increase in γ -globin, porphobilinogen deaminase and NF-E2 mRNA levels*. Leukemia, 1997. **11**: p. 1575-1579.
41. Alitalo, R., *Induced differentiation of K562 leukemia cells: A model for studies of gene expression in early megakaryoblasts*. Leukemia Research, 1990. **14**(6): p. 501-507, 509-514.
42. Schofield, R., *The relationship between the spleen colony-forming cell and the haemopoietic stem cell*. Blood Cells, 1978. **4**: p. 7-25.
43. Kopp, H.-G., et al., *The Bone Marrow Vascular Niche: Home of HSC Differentiation and Mobilization*. Physiology, 2005. **20**: p. 349-356.

44. Arai, F. and T. Suda, *Maintenance of Quiescent Hematopoietic Stem Cells in the Osteoblastic Niche*. Annals of the New York Academy of Sciences, 2007. **1106**: p. 41-53.
45. Abboud, C.N. and L.M. A, *Structure of the marrow and the hemopoietic microenvironment*. Hematology, ed. B. E, et al. 2001, New York: McGraw-Hill.
46. Dao, M.A., et al., *Adhesion to Fibronectin Maintains Regenerative Capacity During Ex Vivo Culture and Transduction of Human Hematopoietic Stem and Progenitor Cells*. Blood, 1998. **92**(12): p. 4612-4621.
47. Campbell, A.D., M.W. Long, and M.S. Wicha, *Haemonectin, a bone marrow adhesion protein specific for cells of granulocyte lineage*. Nature, 1987. **329**(6141): p. 744-746.
48. Weinstein, R., et al., *Dual role of fibronectin in hematopoietic differentiation*. Blood, 1989. **73**(1): p. 111-116.
49. Bentley, S.A., *Close range cell:cell interaction required for stem cell maintenance in continuous bone marrow culture*. Exp Hematol, 1981. **9**(3): p. 308-312.
50. Spooncer, E., et al., *Self-renewal and differentiation of interleukin-3-dependent multipotent stem cells are modulated by stromal cells and serum factors*. Differentiation, 1986. **31**(2): p. 111-118.
51. Lichtman, M.A., *The ultrastructure of the hemopoietic environment of the marrow: a review*. Exp Hematol, 1981. **9**(4): p. 391-410.
52. De Bruyn, P.P.H., S. Michelson, and R.P. Becker, *Endocytosis, transfer tubules, and lysosomal activity in myeloid sinusoidal endothelium*. Journal of Ultrastructure Research, 1975. **53**(2): p. 133-151.

53. Weiss, L., *Transmural Cellular Passage in Vascular Sinuses of Rat Bone Marrow*. Blood, 1970. **36**(2): p. 189-208.
54. Hunt, P., et al., *A single bone marrow-derived stromal cell type supports the in vitro growth of early lymphoid and myeloid cells*. Cell, 1987. **48**(6): p. 997-1007.
55. Brockbank, K., et al., *Hemopoiesis on purified bone-marrow-derived reticular fibroblast in vitro*. Exp Hematol, 1986. **14**(5): p. 186-194.
56. Ikebuchi, K., et al., *Interleukin 6 enhancement of interleukin 3-dependent proliferation of multipotential hemopoietic progenitors*.
57. Kodama, H.-A., et al., *A new preadipose cell line derived from newborn mouse calvaria can promote the proliferation of pluripotent hemopoietic stem cells in vitro*. Journal of Cellular Physiology, 1982. **112**(1): p. 89-95.
58. Rich, I., *The macrophage as a production site for hematopoietic regulator molecules: sensing and responding to normal and pathophysiological signals*. Anticancer Res, 1988. **8**(5A): p. 1015-1040.
59. Riley, R.S., *Bone Marrow Interpretation*. 2006, Virginia Commonwealth University.
60. McAdams, T.A., et al., *Ex vivo expansion of primitive hematopoietic cells for cellular therapies: An overview*. Cytotechnology, 1995. **18**(1): p. 133-146.
61. Quesenberry, P., *Stroma-dependent hematolymphopoietic stem cells*. Curr Top Microbiol Immunol, 1992. **177**: p. 151-166.
62. Kittler, E., et al., *Biologic significance of constitutive and subliminal growth factor production by bone marrow stroma*. Blood, 1992. **79**(12): p. 3168-3178.

63. Roberts, R., et al., *Heparan sulphate bound growth factors: a mechanism for stromal cell mediated haemopoiesis*. Nature, 1988. **332**(6162): p. 376-378.
64. Gordon, M.Y., et al., *Compartmentalization of a haematopoietic growth factor (GM-CSF) by glycosaminoglycans in the bone marrow microenvironment*. Nature, 1987. **326**(6111): p. 403-405.
65. Rapraeger, A.C., A. Krufka, and B.B. Olwin, *Requirement of heparan sulfate for bFGF-mediated fibroblast growth and myoblast differentiation*. Science, 1991. **252**(5013): p. 1705-1708.
66. Graham, G.J., et al., *Identification and characterization of an inhibitor of haemopoietic stem cell proliferation*. Nature, 1990. **344**(6265): p. 442-444.
67. Broxmeyer, H., et al., *Enhancing and suppressing effects of recombinant murine macrophage inflammatory proteins on colony formation in vitro by bone marrow myeloid progenitor cells*. Blood, 1990. **76**(6): p. 1110-1116.
68. Eaves, C., et al., *Mechanisms that regulate the cell cycle status of very primitive hematopoietic cells in long-term human marrow cultures. II. Analysis of positive and negative regulators produced by stromal cells within the adherent layer*. Blood, 1991. **78**(1): p. 110-117.
69. Sing, G., et al., *Transforming growth factor beta selectively inhibits normal and leukemic human bone marrow cell growth in vitro*. Blood, 1988. **72**(5): p. 1504-1511.
70. Nilsson, S.K., et al., *Immunofluorescence characterization of key extracellular matrix proteins in murine bone marrow in situ*. The journal of histochemistry & Cytochemistry, 1998. **46**(3): p. 371-377.

71. Juliano, R., *Membrane receptors for extracellular matrix macromolecules: relationship to cell adhesion and tumor metastasis*. Biochim Biophys Acta, 1987. **907**(3): p. 261-278.
72. Yuchen Gu, et al., *Characterization of Bone Marrow Laminins and Identification of α 5-Containing Laminins as Adhesive Proteins for Multipotent Hematopoietic FDCP-Mix Cells*. Blood, 1999. **93**(8): p. 2533-2542.
73. Patel, V.P. and H.F. Lodish, *A fibronectin matrix is required for differentiation of murine erythroleukemia cells into reticulocytes*. The Journal of Cell Biology, 1987. **105**(6): p. 3105-3118.
74. Patel, V.P. and H.F. Lodish, *Loss of adhesion of murine erythroleukemia cells to fibronectin during erythroid differentiation*. Science, 1984. **224**(4652): p. 996-998.
75. Patel, V.P., et al., *Mammalian reticulocytes lose adhesion to fibronectin during maturation to erythrocytes*. Proceedings of the National Academy of Sciences of the United States of America, 1985. **82**(2): p. 440-444.
76. Ravi, B., D.W. Andrea, and A.M. Heidi, *Contact with fibronectin enhances preservation of normal but not chronic myelogenous leukemia primitive hematopoietic progenitors*. Experimental hematology, 2002. **30**(4): p. 324-332.
77. Jianga, X.-S., et al., *Surface-immobilization of adhesion peptides on substrate for ex vivo expansion of cryopreserved umbilical cord blood CD34⁺ cells*. Biomaterials, 2006. **27**: p. 2723-2732.
78. Franke, K., et al., *Engineered matrix coatings to modulate the adhesion of CD133⁺ human hematopoietic progenitor cells*. Biomaterials, 2007. **28**(5): p. 836-843.

79. Kerst, J.M., J.B. Sanders, and I.C.M. Slaper-Cortenbach, *$\alpha 4\beta 1$ and $\alpha 5\beta 1$ are differentially expressed during myelopoiesis and mediate the adherence of human CD34+ cells to fibronectin in an activation-dependent way.* Blood, 1993. **81**: p. 344-351.
80. Simmons, P., et al., *Vascular cell adhesion molecule-1 expressed by bone marrow stromal cells mediates the binding of hematopoietic progenitor cells.* Blood, 1992. **80**: p. 388-395.
81. Teixido, J., et al., *Role of $\beta 1$ and $\beta 2$ integrins in the adhesion of human CD34^{hi} stem cells to bone marrow stroma.* J Clin Invest, 1992. **90**: p. 358-367.
82. Williams, D., M. Rios, and C. Stephens, *Fibronectin and VLA-4 in hematopoietic stem cell microenvironment interactions* Nature, 1991. **352**: p. 438-441.
83. Catherine, V., M.J. B., and M. PB, *Differentiation of primitive human multipotent hematopoietic progenitors into single lineage clonogenic progenitors is accompanied by alterations in their interaction with fibronectin.* J Exp Med, 1991. **174**: p. 693-703.
84. Huygen, S., et al., *Adhesion of synchronized human hematopoietic progenitor cells to fibronectin and vascular cell adhesion molecule-1 fluctuates reversibly during cell cycle transit in ex vivo culture.* Blood, 2002. **100**(8): p. 2744-2752.
85. Olivier, G., et al., *Cell cycle activation of hematopoietic progenitor cells increases very late antigen-5-mediated adhesion to fibronectin.* Experimental hematology, 2001. **29**(4): p. 515-524.
86. Gu, Y.-C., et al., *Laminin isoform-specific promotion of adhesion and migration of human bone marrow progenitor cells.* Blood, 2003. **101**(3): p. 877-885.

87. Ulrich Siler, et al., *Characterization and functional analysis of laminin isoforms in human bone marrow*. Blood, 2000. **96**(13): p. 4194-4203.
88. Kikkawa, Y., et al., *Integrin binding specificity of laminin-10/11: laminin-10/11 are recognized by $\alpha 3\beta 1$, $\alpha 6\beta 1$ and $\alpha 6\beta 4$ integrins*. Journal of Cell Science, 2000. **113**: p. 869-876.
89. Qian, H., et al., *Distinct roles of integrins $\alpha 6$ and $\alpha 4$ in fetal liver hematopoietic stem and progenitor cell homing*. Cell Research, 2008. **18**.
90. Vivek, R. and M.V. Catherine, *Expression and function of cell adhesion molecules on fetal liver, cord blood and bone marrow hematopoietic progenitors: Implications for anatomical localization and developmental stage specific regulation of hematopoiesis*. Experimental hematology, 1999. **27**(2): p. 302-312.
91. Koenigsman, M., et al., *Myeloid and erythroid progenitor cells from normal bone marrow adhere to collagen type I*. Blood, 1992. **79**(3): p. 657-665.
92. Molla, A. and M.R. Block, *Adherence of human erythroleukemia cells inhibits proliferation without inducing differentiation*. Cell growth & differentiation, 2000. **11**: p. 83-90.
93. Sugahara, H., et al., *Induction of programmed cell death in human hematopoietic cell lines by fibronectin via its interaction with very late antigen 5*. The Journal of Experimental Medicine, 1994. **179**(6): p. 1757-1766.
94. Verfaillie, C.M., J.B. McCarthy, and P.B. McGlave, *Mechanisms underlying abnormal trafficking of malignant progenitors in chronic myelogenous leukemia. Decreased adhesion to stroma and fibronectin but increased adhesion to the*

- basement membrane components laminin and collagen type IV. J Clin Invest, 1992. 90: p. 1232-1241.*
95. Catherine, V., M.J. B, and M.P. B, *Mechanisms underpying abnormal trafficking of maglinant progenitors in chronic myelogenous leukemia: decreased adhesion to stroma and fibronectin but increased adhesion to the basement membrane components laminin and collagen type IV. J Clin Invest, 1992. 90: p. 1232-1239.*
 96. Gordon, M., et al., *Altered adhesive interactions with marrow stroma of hematopoietic progenitor cells in chronic myelogenous leukemia. Nature, 1987. 328: p. 342-344.*
 97. Vijayan, V.K., S.H. Advani, and S.M. Zingde, *Chronic myeloid leukemic granulocytes exhibit decreased adhesion to fibronectin. Leukemia Research, 1994. 18(12): p. 877-879.*
 98. Thomas, X., et al., *Differential adhesiveness between blood and marrow leukemic cells having similar pattern of VLA adhesion molecule expression. Leukemia Research, 1998. 22: p. 953-960.*
 99. Catherine, V., et al., *Role of bone marrow matrix in normal and abnormal hematopoiesis. Critical reviews in oncology/hematology, 1993. 16: p. 201-224.*
 100. Bhatia, R., et al., *Interferon- α restores normal {idhesion of chronic myelogenous leukemia hematopoietic progenitors to bone marrow stroma by correcting impaired fll integrin receptor function. J. clin. Invest, 1994. 94: p. 384-391.*
 101. Molla, A., et al., *Beta 1 integrins mediate adherent phenotype of human erythroblastic cell lines after phorbol 12-myristate 13-acetate induction.*

102. Spessotto, P., et al., *Preferential locomotion of leukemic cells towards laminin isoforms 8 and 10*. Matrix Biol, 2003. **22**(4): p. 351-361.
103. Soligo, D., et al., *Expression of integrins in human bone marrow*. British Journal of Haematology, 1990. **76**(3): p. 323-332.
104. Liesveld, J., et al., *Adhesive interactions of normal and leukemic human CD34+ myeloid progenitors: role of marrow stromal, fibroblast, and cytomatrix components*. Exp Hematol, 1991. **19**(1): p. 63-70.
105. Liesveld, J., et al., *Expression of integrins and examination of their adhesive function in normal and leukemic hematopoietic cells*. Blood, 1993. **81**(1): p. 112-121.
106. Montuori, N., et al., *Expression of the 67-kDa Laminin Receptor in Acute Myeloid Leukemia Cells Mediates Adhesion to Laminin and Is Frequently Associated with Monocytic Differentiation*. Clinical Cancer Research, 1999. **5**(6): p. 1465-1472.
107. Virla, M.B., et al., *The molecular basis for the cytokine-induced defect in homing and engraftment of hematopoietic stem cells*. Experimental hematology, 2001. **29**(11): p. 1326-1335.
108. Petrides, P.E. and K.H. Dittmann, *How do normal and leukemic white blood cells egress from the bone marrow?* Blut, 1990. **61**: p. 3-13.
109. Tarekegn Geberhiwot, et al., *Erythromegakaryocytic Cells Synthesize Laminin-8 (α4β1γ1)*. Experimental Cell Research, 2000. **254**(189-195).
110. FUJITA, A., et al., *Hematopoiesis in Regenerated Bone Marrow Within Hydroxyapatite Scaffold*. Pediatric Research, 2010. **68**(1): p. 35-40
10.1203/PDR.0b013e3181e1cfce.

111. Di Maggio, N., et al., *Toward modeling the bone marrow niche using scaffold-based 3D culture systems*. Biomaterials, 2011. **32**(2): p. 321-329.
112. Conrad, V., et al., *Expansion and differentiation of haemopoietic progenitor cells on endothelialized hydroxyapatite under static conditions*. British Journal of Haematology, 1999. **105**(1): p. 40-49.
113. Li, Y., et al., *Human Cord Cell Hematopoiesis in Three-Dimensional Nonwoven Fibrous Matrices: In Vitro Simulation of the Marrow Microenvironment*. Journal of Hematotherapy & Stem Cell Research, 2001. **10**(3): p. 355-368.
114. Feng, Q., et al., *Expansion of engrafting human hematopoietic stem/progenitor cells in three-dimensional scaffolds with surface-immobilized fibronectin*. Journal of Biomedical Materials Research Part A, 2006. **78A**(4): p. 781-791.
115. Thevenot, P.T., et al., *The effect of incorporation of SDF-1[alpha] into PLGA scaffolds on stem cell recruitment and the inflammatory response*. Biomaterials, 2010. **31**(14): p. 3997-4008.
116. Bladergroen, B.A., et al., *In Vivo Recruitment of Hematopoietic Cells Using Stromal Cell-Derived Factor 1 Alpha-Loaded Heparinized Three-Dimensional Collagen Scaffolds*. Tissue Engineering Part A, 2009. **15**(7): p. 1591-1599.
117. TY, W., B. JK, and W. JH, *Multilineal hematopoiesis in a three-dimensional murine long-term bone marrow culture*. Experimental hematology, 1995. **23**(1): p. 26-32.
118. Mantalaris, A., et al., *Engineering a Human Bone Marrow Model: A Case Study on ex Vivo Erythropoiesis*. Biotechnology Progress, 2008. **14**(1): p. 126-133.

119. Rajyalakshmi, A., K. Balasubramanian, and S. Mishra, *An in vitro adhesion pattern study of hematopoietic stem cells on porous Titanium and bioceramics scaffolds* Trends in Biomaterials and Artificial Organs, 2010. **24**(2): p. 116-122.
120. Oswald, J., et al., *Gene-Expression Profiling of CD34+ Hematopoietic Cells Expanded in a Collagen I Matrix*. STEM CELLS, 2006. **24**(3): p. 494-500.
121. Kurth, I., et al., *Hematopoietic stem and progenitor cells in adhesive microcavities*. Integrative Biology, 2009. **1**(5-6): p. 427-434.
122. Moiola, E.K., et al., *Synergistic Actions of Hematopoietic and Mesenchymal Stem/Progenitor Cells in Vascularizing Bioengineered Tissues*. PLoS ONE, 2008. **3**(12): p. e3922.
123. Chua, K.-N., et al., *Surface-aminated electrospun nanofibers enhance adhesion and expansion of human umbilical cord blood hematopoietic stem/progenitor cells*. Biomaterials, 2006. **27**(36): p. 6043-6051.
124. Ma, K., et al., *Electrospun nanofiber scaffolds for rapid and rich capture of bone marrow-derived hematopoietic stem cells*. Biomaterials, 2008. **29**(13): p. 2096-2103.
125. Chua, K.-N., et al., *Functional nanofiber scaffolds with different spacers modulate adhesion and expansion of cryopreserved umbilical cord blood hematopoietic stem/progenitor cells*. Experimental Hematology, 2007. **35**(5): p. 771-781.
126. Lu, J., et al., *A Novel Technology for Hematopoietic Stem Cell Expansion Using Combination of Nanofiber and Growth Factors* Recent Patents on Nanotechnology, 2010. **4**(2): p. 125-134.

127. Caicedo-Carvajal, C.E., et al., *Cancer Tissue Engineering: A Novel 3D Polystyrene Scaffold for In Vitro Isolation and Amplification of Lymphoma Cancer Cells from Heterogeneous Cell Mixtures*. Journal of Tissue Engineering, 2011. **2011**.
128. Vaiselbuh, S.R., et al., *Ectopic Human Mesenchymal Stem Cell-Coated Scaffolds in NOD/SCID Mice: An In Vivo Model of the Leukemia Niche*. Tissue Engineering Part C: Methods, 2010. **16**(6): p. 1523-1531.
129. Blanco, T.M., et al., *The development of a three-dimensional scaffold for ex vivo biomimicry of human acute myeloid leukaemia*. Biomaterials, 2010. **31**(8): p. 2243-2251.
130. Yamamoto, M., et al., *Generation of stable co-cultures of vascular cells in a honeycomb alginate scaffold*. Tissue engineering, 2010. **16**: p. 299-309.
131. Dean, S.K., et al., *Differentiation of Encapsulated Embryonic Stem Cells After Transplantation*. Transplantation, 2006. **82**(9): p. 1175-1184
10.1097/01.tp.0000239518.23354.64.
132. Maguire, T., et al., *Alginate-PLL microencapsulation: Effect on the differentiation of embryonic stem cells into hepatocytes*. Biotechnology and Bioengineering, 2006. **93**(3): p. 581-591.
133. Chang, J.-C., S.-h. Hsu, and D.C. Chen, *The promotion of chondrogenesis in adipose-derived adult stem cells by an RGD-chimeric protein in 3D alginate culture*. Biomaterials, 2009. **30**(31): p. 6265-6275.

134. Rebecca, L.H., A.H. David, and G.T. Frank, *Transport characterization of hydrogel matrices for cell encapsulation*. Biotechnol. Bioeng., 1996. **50**: p. 365-373.
135. Whalen, A., et al., *Megakaryocytic differentiation induced by constitutive activation of mitogen-activated protein kinase kinase*. Mol. Cell. Biol., 1997. **17**(4): p. 1947-1958.
136. Rebecca, L.H., A.H. David, and G.T. Frank, *Transport characterization of hydrogel matrices for cell encapsulation*. Biotechnology and Bioengineering, 1996. **50**: p. 365-373.
137. Saha, K., et al., *Designing synthetic materials to control stem cell phenotype*. Current Opinion in Chemical Biology, 2007. **11**(4): p. 381-387.
138. Zhang, W. and H.T. Liu, *MAPK signal pathways in the regulation of cell proliferation in mammalian cells*. Cell Res, 2002. **12**(1): p. 9-18.
139. A, S., et al., *Measuring the elastic modulus of ex vivo small tissue samples*. Phys Med Biol, 2003. **48**(14): p. 2183-98.
140. Dzieman, A.J., *A Provisional Casualty Criteria for Fragments and Projectiles*, in *Edgewood Arsenal Maryland Report*. 1960, U.S. Army, Edgewood, MD.
141. Enderle, J., S.M. Blanchard, and J. Bronzino, *Introduction to Biomedical Engineering*. Biomedical Engineering. 2005.
142. Mørch, Y.A., I. Donati, and B.L. Strand, *Effect of Ca²⁺, Ba²⁺, and Sr²⁺ on Alginate Microbeads*. Biomacromolecules, 2006. **7**(5): p. 1471-1480.

143. Bajpai, S.K. and S. Sharma, *Investigation of swelling/degradation behaviour of alginate beads crosslinked with Ca²⁺ and Ba²⁺ ions*. Reactive and Functional Polymers, 2004. **59**(2): p. 129-140.
144. LT, S. and T. AD, *Aligned arrays of biodegradable poly(epsilon- caprolactone) nanowires and nanofibers by template synthesis*. Nano Lett., 2007. **7**: p. 1463-1468.
145. Beyec, J.L., et al., *Cell shape regulates global histone acetylation in human mammary epithelial cells*. Exp. Cell Res., 2007. **313**(14): p. 3066-3075.
146. Chen, C.S., et al., *Geometric control of cell life and death*. Science, 1997. **276**(5317): p. 1425-1428.
147. Koefler, H. and D. Golde, *Human myeloid leukemia cell lines: a review*. Blood, 1980. **56**(3): p. 344-350.
148. Thao, V.T.T., H. Kaur, and M. Lim. *Toward a Bone Marrow Niche: Culture of Hematopoietic Cells in Two-dimensional Versus Three-dimensional Microenvironments*. in *First International Symposium on Biomedical Engineering*. 2011: Research Publishing.
149. He, L., et al., *Synergistic effects of electrospun PLLA fiber dimension and pattern on neonatal mouse cerebellum C17.2 stem cells*. Acta Biomaterialia, 2010. **6**(8): p. 2960-2969.
150. GOSPODAROWICZ, D. and J.-P. TAUBER, *Growth Factors and the Extracellular Matrix*. Endocrine Reviews, 1980. **1**(3): p. 201-227.

151. Lawrence, M.B. and T.A. Springer, *Leukocytes roll on a selectin at physiologic flow rates: Distinction from and prerequisite for adhesion through integrins*. Cell, 1991. **65**(5): p. 859-873.
152. Kim, B.-S. and D.J. Mooney, *Development of biocompatible synthetic extracellular matrices for tissue engineering*. Trends in Biotechnology, 1998. **16**(5): p. 224-230.
153. Rowley, J.A., G. Madlambayan, and D.J. Mooney, *Alginate hydrogels as synthetic extracellular matrix materials*. Biomaterials, 1999. **20**(1): p. 45-53.
154. Wang, G., et al., *Electrospun PLGA–silk fibroin–collagen nanofibrous scaffolds for nerve tissue engineering*. In Vitro Cellular & Developmental Biology - Animal, 2011. **47**(3): p. 234-240.
155. Villeval, J.L., et al., *Erythroid properties of K562 cells: Effect of hemin, butyrate and TPA induction*. Experimental Cell Research, 1983. **146**(2): p. 428-435.
156. Meshkini, A. and R. Yazdanparast, *Involvement of ERK/MAPK pathway in megakaryocytic differentiation of K562 cells induced by 3-hydrogenkwadaphnin*. Toxicology in Vitro, 2008. **22**(6): p. 1503-1510.
157. Christopherson, G.T., H. Song, and H.-Q. Mao, *The influence of fiber diameter of electrospun substrates on neural stem cell differentiation and proliferation*. Biomaterials, 2009. **30**(4): p. 556-564.
158. Wagner, E.F. and A.R. Nebreda, *Signal integration by JNK and p38 MAPK pathways in cancer development*. Nat Rev Cancer, 2009. **9**(8): p. 537-549.
159. Gombotz, W.R. and S. Wee, *Protein release from alginate matrices*. Advanced Drug Delivery Reviews, 1998. **31**(3): p. 267-285.

160. Shoichet, M.S., et al., *Stability of hydrogels used in cell encapsulation: An in vitro comparison of alginate and agarose*. Biotechnology and Bioengineering, 1996. **50**(4): p. 374-381.